Structure and dynamics in binary mixtures with limited miscibility

Investigation of aqueous solutions of methyl-substituted pyridines

László Almásy

Doctoral Thesis

Paris 2002

Acknowledgements

This thesis has been completed in cooperation between the University Eötvös Lóránd in Budapest, and the University Pierre and Marie Curie (Paris-6). The effective work has been carried out in two host institutes: the Institute for Solid State Physics and Optics of the Hungarian Academy of Sciences, and the Laboratoire Léon Brillouin, a common laboratory of the French research agencies CEA and CNRS. During my stay in France I profited of a scholarship provided by the French Government.

I would like to express my gratidute first of all to my thesis supervisors Marie-Claire Bellissent-Funel and László Cser for their continuous support in the development of this research, they were also my first teachers who introduced me to the various fields of the neutron scattering.

This work could never have been written without my senior collegue Gábor Jancsó, who initiated the topic and also the development of the method we have used in this research.

I am grateful for the very few, but always very valuable and stimulating discussions to José Teixeira.

I would like to thank to a multitude of my young collegues: for many discussions and common thinking on questions of neutron scattering, in particular to Misha Avdeev and Pál Jóvári, for useful advices to Ingo Köper and Jean-Marc Zanotti, and for the very friendly atmosphere in the two laboratories to Eszter, Adél, Daniela, Sandra, Julia, Bouchra, Fabrice, and Marie-Sousai.

I thank very much the support of my family – Éva, Gábor, Mari, and my Mother, during the many months I spent far away from them.

I would like also to thank for the perfect work and friendly support of the ladies who dealt with administrative tasks: Edit, Chantal Marais and Chantal Pomeau, Christelle Abraham and Cloude Rousse, Sandrine Besson, Erika Boros and Hajnalka Fekete.

Contents

Introduction

Liquid mixtures exhibit various phenomena which cannot be found in pure substances. The most interesting of these are perhaps the new types of phase equilibria which arise from the extra degrees of freedom introduced by the possibility of varying the proportions of the components. In some mixtures there are such regions in the phase space, in which the mixture demixes into two parts, which have different compositions and are in equilibrium with each other. Such systems are said to be partially miscible. In some partially miscible systems the phase diagram is more complicated: the immiscibility region is completely surrounded by a miscible region, or even more than one immiscible region can exist. Such systems are called mixtures with reentrant miscibility, or reentrant mixtures.

Many attempts have been made to explain the physical mechanisms which lead to partial miscibility but so far only thermodynamic models have been able to explain some types of phase diagrams with immiscibility regions. By this classical tool however the microscopic driving mechanism of the phase separation is not seen. Experimental information on the structure and dynamics on atomic scale in mixtures approaching phase separation is still missing.

The aqueous solutions of methyl-substituted pyridines constitute an interesting and widely studied family of such mixtures. The pyridine molecule is polar, has a hydrogen bond acceptor part and a large hydrophobic part. In the methyl-substituted pyridines the methyl group enlarges the hydrophobic part, but also affects the hydrogen bonding ability by redistribution of the electron charge in the ring. By varying the position of the methyl substituent, the strength of the methylpyridine – water hydrogen bond can be changed.

The physical and chemical properties of most of the aqueous solutions of the methyl-substituted pyridines have been studied in details, so these mixtures can serve as model systems for studying various aspects of the mixing behavior.

The investigations collected in the present work intended to get an insight into the structure and dynamics of aqueous solutions of methyl-substituted pyridines at microscopic level. We used for this purpose various experimental techniques – small-angle neutron scattering, quasielastic neutron scattering, and nuclear magnetic resonance. Theese tools are sensitive to the structural arrangement of the atoms and molecules and to their motions. By comparing the experimental results obtained on different

methylpyridine solutions with their miscibility behavior and molecular structures (available from literature data), we expected to obtain information regarding the relations between macroscopic and microscopic properties of the system, thus connecting the different physical aspects of the studied phenomena.

Experimental tools

The primary aim of the present studies was to investigate the behavior of the mixtures on atomic level, that is to measure their structure and dynamics. The knowledge of the structure is essential for revealing the nature of the intermolecular interactions. Diffraction techniques probe the structure in a direct way: there exists an equivocal mapping of the structure to the measured diffraction pattern. This allows one to develop structural models of the investigated systems, which are in the best possible agreement with the measurements.

The knowledge of the dynamics at the level of movements of individual atoms, atomic groups or molecules can also help a lot in understanding the behavior of the intermolecular interactions. There exist several experimental methods that are also sensitive to the microscopic dynamic behavior, such as NMR or different electromagnetic relaxation techniques. Neutron scattering allows one to look into the molecular motions directly by following the variation of the position of the scattering particles.

Small-angle neutron scattering By small-angle neutron scattering (SANS) one can investigate the static (time-averaged) structure of liquid solutions on mesoscopic scale. It can furnish information about the way of aggregation of molecules. Geometrical quantities related to the interaction between molecules and their aggregates thus can be obtained.

Quasielastic neutron scattering In a quasielastic neutron scattering (QENS) experiment the movements of the nuclei are followed by measuring the energy and impulse exchange of the nuclei with a neutron. The typical time scale covered in the experiment makes it possible to study the diffusive and rotational motions of molecules in liquid state. Due to the high incoherent scattering cross-section of the proton the QENS is an effective tool to probe motion of molecules containing hydrogen atoms.

NMR The nuclear magnetic resonance technique measures the spin relaxation process of an artificially excited nucleus. The relaxation rate depends on the surrounding of the nucleus, so in an NMR experiment information can be obtained about the structure and dynamics of the local arrangement of the probed nuclei.

Part I.

Liquid mixtures

1. Phenomena of partial miscibility

Partial miscibility can be found in various kinds of multicomponent systems: mixtures of gases, liquid and solid alloys, liquid crystals, polymer blends and liquid solutions (see e.g. [1]). Partial miscibility is often called *phase splitting*. The possibility of such behavior can be deduced from the phase rule of Gibbs: A system of one component with one phase has two degrees of freedom (temperature and pressure, for example). A two-component system with one phase has three degrees of freedom, temperature, pressure and composition. This results in the possibility of forming two coexistent phases at a given temperature and pressure, in which the compositions are different. The compositions of the two phases are related to each other because the total amount of the components in the system is fixed.

Aqueous solutions of several organic liquids (e.g. alcohols, heterocyclic compounds, tetrahydrofurane, acetonitrile) exhibit two regions in the phase diagram in concentration-temperature coordinates. Varying thermodynamic parameters, like temperature or pressure, a phase transition takes place: the mixture becomes non-homogeneous, microregions form which contain the two components in different proportions.

Due to their different densities and the gravity they separate and form "upper phase" and "lower phase" in the cuvette. Prior to phase separation, usually at one or two degrees below the separation temperature, the liquid turns to be opaque. This is due to the scattering of the visible light on the inhomogeneities with sizes comparable to the wavelength of the light. This is an indication that the demixing is preceeded by microscopic fluctuations of composition.

The demixing tendency in such systems can be observed already in the one - phase region. Many experimentally measurable properties have strong extrema at some intermediate concentration, and these extrema become stronger as the system is approaching the phase-separation line of the phase diagram. The presence of small-angle scattering, and the observation of the critical opalescence also indicate that in the homogeneous region the mixtures are not homogeneous at microscopical scales. In other words, aggregates, or at least regions with different compositions are present in the solutions.

The mechanism leading to phase separation undoubtably should be searched in the interactions between the similar and different molecules. Studying of the structure and the dynamics of the liquid at this level requires experimental techniques sensitive to interatomic and intermolecular interactions.

1.1. Thermodynamic models

Thermodynamic approach is very useful for understanding the behavior of liquids and liquid mixtures. The thermodynamic criteria of splitting in multicomponent mixtures are well understood. A binary system is stable (macroscopically homogeneous) if the following equation holds:

$$\frac{\partial^2 G^E}{\partial x_1^2} > -\frac{RT}{x_1 x_2} \tag{1.1}$$

G^E is the excess Gibbs free energy of mixing, x_1 and x_2 are the mole fractions of the components. The excess Gibbs free energy can be formally written as a function of concentration and of one or several parameters, which can be temperature and pressure dependent. Their temperature dependence may have a form, leading to the *reentrant miscibility*, when the system is miscible at low and high temperatures and shows a closed immiscibility loop in between. The form of the excess free energy function and the parameters should be related to quantities characterizing the microscopic interaction between the components, which can be very complex for real systems.

For understanding the behavior of the system, it is useful to start with some model of interactions between the molecules. One of the simplest models is the Bragg-Williams model, we shall look how it can relate the macroscopic phase behavior of a mixture to microscopic, interparticle interactions.

Bragg-Williams theory

The Bragg-Williams theory, called also the theory of regular solutions [2], is based on a lattice model, where each site can accommodate one molecule irrespective of type and size. All lattice positions are supposed to be occupied, and the following basic assumptions are used:

1. The mixture is random.
2. The number of neighbors is constant.
3. The interaction is limited to neighbors.

Introducing only pairwise interaction energies, independent of concentration and temperature, some useful results can be simply derived. The important quantity to calculate is the excess Gibbs free energy, or free energy of mixing: $G^E = \Delta E - T\Delta S$. The requirement for two liquids to be miscible is that $G^E < 0$. A demixing into two parts with different compositons will occur if the $G^E(x)$ has two minima at different compositions, thus it has a maximum in between.

For one mole of the regular solution the free energy of mixing can be written:

$$G^E/RT = \chi x_1 x_2 + x_1 \ln x_1 + x_2 \ln x_2 \tag{1.2}$$

where x_1 and x_2 are the mole fractions of the components, $\chi = wz/kT$, z is the number of neighbors, and w is the average interaction energy per one molecule:

$w = w_{12} - w_{11}/2 - w_{22}/2$. w_{ij} are the pairwise interaction energies. The interaction energy parameter w is positive when the interaction between the non-similar species is more attractive than the interactions between the similar species. The second derivative of the free energy of mixing becomes zero when the parameter χ reaches the value of 2. At $\chi > 2$ a phase separation takes place.

According to this simplified model a binary mixture must undergo a phase separation when lowering the temperature if the attractive interaction between the nonsimilar species is much stronger than the (non-repulsive) interaction between the similar species. This phenomenon is indeed observed in many liquid mixtures, the temperature of phase separation is the upper critical solution temperature (UCST).

In real systems one may sometimes find that phase separation takes place with increasing the temperature; this goes outside the Bragg-Williams model. We discuss such behavior in the next sections.

1.2. Models based on simplified intermolecular interaction

There are some statistical mechanical theories which can explain the appearance of reentrant phase behavior in binary mixtures. These theories are based on lattice models, therefore they can only give a hint on the particular interaction, responsible for the phase separation. Usually, a particularly important parameter in these models is the strength of the hydrogen bond that forms between unlike molecules.

Hirschfelder in 1937 suggested that phase separation that occurs while temperature is increasing can be related to the formation of a directional bond between two nonsimilar molecules [3]. The presence of such bonded pairs is favourable energetically, but destroys the randomness of the distribution of the species. The configurational entropy is lowered due to forming stable pairs, and also the entropy related to the rotational degrees of freedom is lowered. A hydrogen bond is a typical example for such bonding interaction.

This idea of the strong directional bonds has been incorporated in lattice models, and resulted in the appearance of closed immiscibility regions in the simulated binary mixtures. Due to the increasing complexity of the models, now lattice gas models with directional bonds can reproduce many closed loops observed in real systems using only a few adjustable parameters [1].

Further development would be to go from lattice models to continuous models, and to give a statistical mechanical description of the phase separation in which the potentials resemble the real continuous intermolecular potentials.

A step in this direction was made recently by Pápai and Jancsó [4]. They calculated by theoretical methods the strength of the hydrogen bond between a water molecule and

different methylpyridine molecules, aiming to relate the geometry and the energy of this interaction with the miscibility behavior of the different methylpyridine solutions.

Another, recently proposed model [5] deals with interactions between a water and a methylpyridine molecule, and assume the possibility of forming one or two H-bonds simultaneously between the two molecules. We describe this model in the section 1.4.

1.3. Computer simulations

At the present time the computer simulations of realistic ensembles of molecules are a useful and continuously developing tool to get the liquid structure at atomic level. However, Monte Carlo simulations or molecular dynamics simulations seem to be hardly applied to mixtures with high degree of non-ideality. The intermolecular potentials are usually determined empirically, in order to fit the properties of the pure components, and the cross interaction potentials between the sites of the non-similar species are defined using some averaging forms. In result, while the interactions between the similar molecules are often modeled on a satisfactory level, the peculiarities of the interactions between the non-similar molecules can be easily lost, and the excluded volume effects may dominate the behavior of the simulated liquid mixture. Another technical difficulty is the required large size of the simulation box, where the composition fluctuations and phase separation could be eventually observed. Such size is probably too big for the present computer power. As it is known from small-angle scattering experiments performed on liquid mixtures with limited miscibility, long-range correlations in the composition with dimensions above 20 Å are often present. If the simulation box size does not exceed substantially these lengths, then the regions with low and high solute concentrations cannot evolve during the simulation, thus even the intermolecular arrangement at the level of the closest neighbors looses its correctness.

Only in some recent simulation works the demixing tendency was observed in liquid mixtures (pyridine - water [6], urea - water [7]). The accuracy of these simulations (system size and time of simulations) have not made it possible to obtain quantitative estimates of the aggregation or dimerization of the solute molecules, though such studies might be promising in the future.

1.4. A possible mechanism of reentrant phase transition

We close this chapter by describing in more detail a model of the reentrant miscibility in aqueous solutions of methylpyridine, proposed recently by Brovchenko and Oleinikova [5, 8].

Suppose that in the solution, the methylpyridine (MP) can connect to a water molecule forming two types of hydrogen bonds: one to the N atom, the second one to the π electron cloud of the pyridine ring. In the solution there are three populations of the MP molecules: forming one H-bond with a water molecule (via the N atom), forming two bonds or having no bonds at all.

If an MP is connected to a water molecule only by a single bond, then this water is able to form other H-bonds with other water molecules, thus the MP molecule will be connected to a group of water molecules. At high methylpyridine concentrations there is not enough water to form such shells around each MP molecules. Those MP molecules, which cannot be surrounded by a water shell, will therefore aggregate. The MP molecules surrounded by water shells will form the solvent-rich phase, with some characteristic average composition.

In the other two cases, when the MP forms two or zero H-bonds with a water molecule, no stable water shell can be formed around the MP, so the mixture does not exhibit phase separation. The probability of the average number of H-bonds between the MP and the water depends on the strength of the bonds and on the temperature.

This model can reproduce the temperature behavior of the phase separation. The proportion of the numbers of MP molecules belonging to the three populations changes with temperature. Raising the temperature more MP molecules will appear having less (one or zero) H-bonds. In this way at some intermediate temperatures there is a maximum of MP molecules having only one H-bond, and if this number is sufficiently high then a phase separation can take place. Further increase of the temperature diminishes the number of MP molecules with a single H-bond, thus the mixture becomes miscible again.

In summary, the previous theoretical studies could explain more or less accurately the phenomena of partial miscibility, including also the reentrant-type of phase behavior. However they deal always with rather crude models. In fact, there is not yet direct experimental information about the mechanism of the molecular interactions in unmixing solutions. Moreover, it is not yet known, whether it is possible to obtain such direct information by experimental methods, that is why any experimental information, related with these phenomena can be useful. This is the aim of our studies: to study liquid mixtures in a such state, where the system is close to the demixing and its behavior shows up features characteristic for the phase separation.

In the next chapters we describe those theoretical and experimental tools we have used, and summarize some results of previous studies on aqueous solutions of methylpyridines.

2. Aqueous solutions of methyl-substituted pyridines

2.1. Pyridine and methyl-substituted pyridines

Pyridine is one of the simplest aromatic heterocyclic molecules. Its dipole moment can lead to dipole-dipole intermolecular interaction, and the hydrogen bond acceptor ability of the molecule gives rise to various phenomena in solutions where such interactions are possible, for example in water.

In methylpyridines (called also *picolines*) one methyl group is attached to the pyridine ring, in ortho, metha or para position to the nitrogen atom. The molecules are called respectively 2-methylpyridine (2MP), 3-methylpyridine (3MP) or 4-methylpyridine (4MP). The dimethylpyridines (called also *lutidines*) have two methyl substituents. Pyridine, picolines and lutidines are liquids with freezing points between +10 and −50°C and boiling points above +120°C. The molecular geometries of many of them have been determined by X-ray diffraction and were calculated with using approximations of different levels in quantum chemical methods (e.g. [4]). The liquid state structure of pyridine has been investigated by neutron [10] and X-ray diffraction [10, 11], and by MD simulations [11, 12]. These studies suggested that the structure of the liquid is determined mainly by steric effects (excluded volume packing), and a weak alignment of the neighboring molecules is caused by the dipole moment of the pyridine. Pure liquid methyl-substituted pyridines have not yet been investigated by scattering techniques. Some authors say that the association of the pyridine bases can occur as a result of N $\cdots$ π interactions between the free electron pair on the nitrogen of one molecule with the aromatic ring π electrons of another molecule [13].

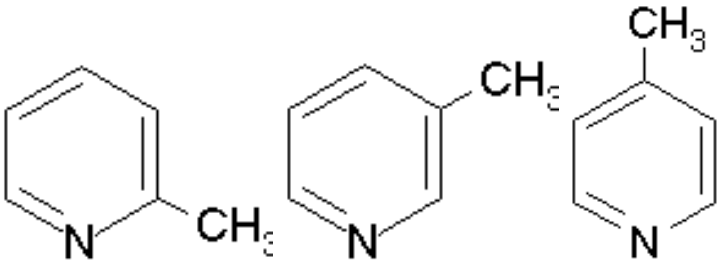

Figure 2.1.: *Molecular structures of 2-methylpyridine, 3-methylpyridine and 4-methylpyridine.*

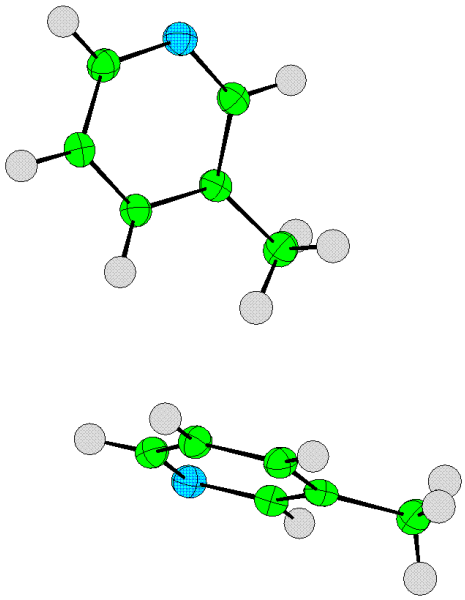

Figure 2.2.: *Position of two neighboring 3MP molecules in the crystal. The proton of the methyl group on the upper molecule looks towards the center of the pyridine ring of the molecule below.*

2.1.1. Crystal structure of methylpyridines

The crystal structures of 2MP and 3MP and four dimethylpyridines were determined by Davies and Bond in 2001-2002 using single-crystal X-ray diffraction [14, 15, 16, 17, 18, 19]. The structure of pyridine and 4-methylpyridine are known since longer time [20, 21]. The difficulties connected with the preparation of single crystals at low temperature were probably the main reason why these simple molecular crystal structures were determined relatively late.

Not being aware of studies of Davies and Bond, we have also started experiments on measuring the crystalline structures of methylpyridines by X-ray diffraction. Single crystal of 3MP has been grown and its structure has been determined by A. Cousson at the LLB[*not published*]. An interesting feature was observed: the closest approach between two neighboring molecules has such form, that a proton of the methyl group looks directly to the center of the pyridine ring of the neighboring molecule (figure 2.2).

2-methylpyridine has been crystallised and measured by I. Vorontsov in Moscow. The crystal structure can be described as follows [23]: " Interesting peculiarity of the crystal packing of [2MP] is the C – H $\cdots$ π intermolecular contact with short H $\cdots$ X distance 2.64Å, which can bring about the packing motif of [2MP] (X is the center of the aromatic ring, C is a carbon atom of the ring)." The crystal structure is shown in Fig. 2.3.

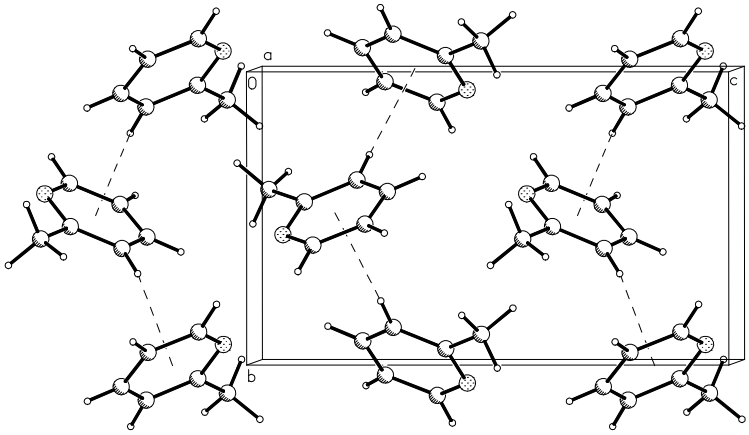

Figure 2.3.: *Crystal packing of 2MP. Dashed lines represent C – H $\cdots$ π contacts between H atoms and centers of the pyridine rings [23].*

The distances of these contacts are short enough to consider them as possible week C – H $\cdots$ π bonds, which might play some role in the forming of the crystal structure. The existence of similar contacts have attracted considerable attention in the last years, as analysis of many structures of molecular crystals and crystal structures of solid solutions showed up the presence of such close contacts [25].

The same structure can be described in different ways, accenting on those features which are considered to be important for one or another reason. For example, describing the crystal structures of 2MP and 3MP, Bond and Davies did not mention at all C – H $\cdots$ π contacts. Instead, they were apparently looking for C – H $\cdots$ N contacts, and indeed they have found one or two such contacts between neighboring 2MP molecules, and noted that "there are no apparent directional C – H $\cdots$ N interactions" in the 3MP crystal [14, 15].

Although quantum chemical calculations have not yet been performed looking for possible energy minima in these contacts, these experimental findings may indicate the existence of some kind of interaction between the proton and the π-electron cloud of the ring, or between the proton and a neighboring H-bond acceptor nitrogen. If these interactions have energy minima (or sufficiently low energies), then it may happen that they can facilitate direct aggregation of methylpyridines (i. e. formation of contact-pairs) in the liquid state or in solutions.

2.1.2. Crystal hydrates

Besides the crystal structures of the pure methylpyridines, the possible existence of low-temperature clathrate hydrates in methylpyridine solutions can be also interesting. There is a common opinion that structure of many aqueous solutions of hydrophobic molecules at some characteristic concentration resembles the structure of a low-temperature crystalline state, in which the solute molecule is surrounded by a shell of water molecules [26]. The stability of such a structure in the liquid state can explain the behavior of the compressibility with variation of temperature and composition. In many aqueous solutions of alcohols at certain concentrations the compressibility does not change with temperature, suggesting therefore a rather stable structure of the solution.

Up to now only crystalline pyridine trihydrate [20] and 4-methylpyridine trihydrate [21] have been observed experimentally. In pyridine trihydrate all water molecules form hydrogen bonds with each other, and one hydrogen bond connects the N atom of pyridine with a water molecule. This composition does not fall in the family of clathrate hydrates (usually one solute molecule for about 20 - 30 water molecules), so these structures cannot be considered as models of hydrate-like liquid structure.

We have also tried to find crystalline structures by cooling mixtures of water and 3-methylpyridine of different compositions, but all the samples froze in a glassy state, no crystalline peaks were observed by X-ray diffraction. One reason for that could be the relatively small amount of sample (we used glass capillaries of 1 mm inner diameter). Due to the high viscosity of the solution at low temperature, the probability of the onset of the crystallization process is much lower, and in a small volume it could easily happen that too much time would be required for the crystallization process to start. Similar difficulties were experienced when we tried to crystallize pure 2,4-dimethylpyridine in capillary near its freezing point: no crystallization could be achieved. Thermal analysis showed however that in a sample volume of the DSC apparatus (about 3 mm^3) the crystallization process took place. 3MP – water mixtures of different concentrations gave similar crystallization/melting peaks, and also glass transition has been was observed in all samples at about 165 K, showing that only a part of the solution crystallizes.

2.2. Phase diagram of the mixtures

Deviations from the ideal mixing can be identified in many thermodynamic quantities, like the mixing enthalpy, entropy, molar volume, compressibility or others, but the most striking phenomena is probably the appearance of an immiscible region in the phase diagram. An extensive thermodynamic study of aqueous solutions of methylpyridines has been carried out in 1952 – 1957 by Andon, Cox and Herington [27, 28, 29, 30]. Closed loop phase diagrams have been observed in heavy water solutions of 2-methylpyridine and 3-methylpyridine, and in mixtures of lutidines both with water and heavy water. The phase diagrams of heavy water solutions of 2-methylpyridine and 3-methylpyridine

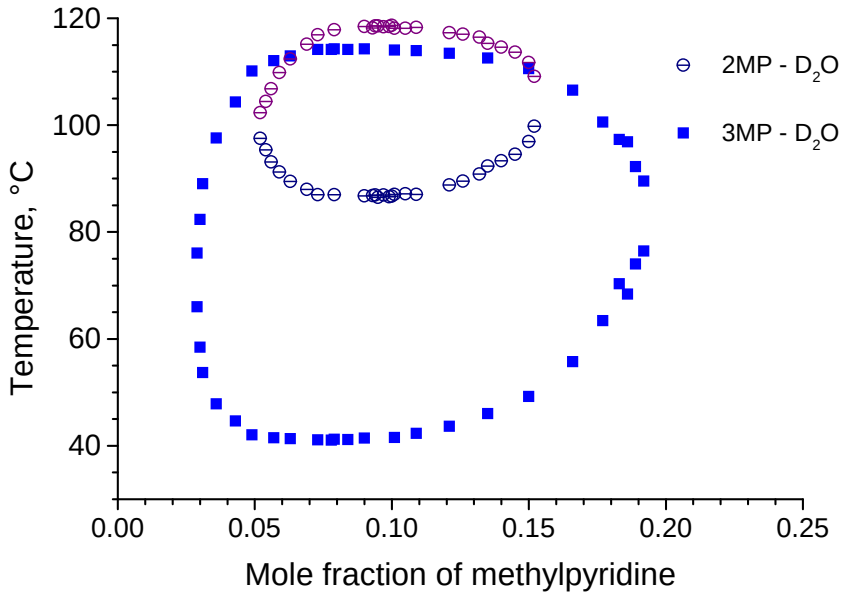

Figure 2.4.: *Phase diagram of heavy water mixtures of 2MP and 3MP at normal pressure [31]. The mixtures are macroscopically homogeneous outside the closed loop and demix into two phases within the loop.*

are shown in Figure 2.4, as determined in a more recent work [31]. All monomethyl-substituted pyridines mix with light water at all proportions. Both water and heavy water solutions of dimethyl-substituted pyridines have large immiscibility regions.

A simple factor explaining the appearance of an immiscibility region by changing water to heavy water can be the difference in the strength of the hydrogen bonds. The deuterium bonds are known to be stronger than the hydrogen bonds. If the phase separation process is dominated by the repulsion of the hydrophobic molecule by the hydrogen-bonded water network, the more strong water-water interaction in the heavy water can enhance the demixing process.

2.3. Light scattering studies

Light scattering is sensitive to large inhomogeneities in the solutions, caused by fluctuations in composition, or micro – phase separation. Aqueous solutions of pyridine and methylpyridines were studied by the method of depolarized light scattering [32]. Intensive light scattering was observed in all solutions with maximum at concentrations near 10 mol% for pyridine, and between 7 and 9 mol% for the picoline solutions. The temperature of the maximum intensity was about 60°C for pyridine, 70°C for 4MP and 80°C for 3MP. To explain the observations, the authors suggested that at those concentrations and temperatures the solutions are close to a hidden immiscibility region. Such

hidden immiscibility region can be made to appear by changing some thermodynamic parameter. The easiest way is to add an increasing amount of heavy water, as it was demonstrated by Cox et. al. [28], or to change the pressure, or to add a small amount of a simple salt [33].

2.4. Vapor pressure studies

The mixing processes can be characterized by changes in energy and entropy. For determination of the excess enthalpies and excess Gibbs energies calorimetric and vapor pressure measurements are usually performed. Vapor pressures in methylpyridine solutions were measured by several authors, at different temperatures and in different composition intervals. From vapor pressure data the activity coefficients and the excess Gibbs free energies can be calculated.

Yushkova et. al. measured vapor pressures in very dilute aqueous solutions of methyl-substituted pyridines [34, 35]. They calculated various excess functions and the activity coefficients of the components. In all studied systems (water + 3MP, 4MP, 2,6DMP) a strong increase of the activity coefficient around $x_{MP} = 0.003$ was observed. The explanation of the volatility maxima at low solute concentrations were explained by probable forming of solute associates (at very low concentrations). The differences in the behavior of the different methylpyridines were attributed to size effects: the 4MP has the smallest "diameter" that allows it to enter into the hydrogen-bonded water network without breaking many water-water hydrogen bonds.

Unfortunately the concentrations studied in this work were rather small, they covered range between 0.0002 and 0.02 mole fraction of methylpyridines. Because of this choice the measured and calculated quantities had relatively large uncertainties, and the results were not always reproducible. It is not possible to compare their results with other literature data, and unfortunately we could not use them in combination with our small-angle neutron scattering results. The lowest concentration for which we could measure small-angle scattering was about 0.005 mole fraction of methylpyridine in heavy water.

In 1978 Abe, Nakanishi and Touhara measured the densities and vapor pressures of aqueous solutions of pyridine, the three methylpyridines and 2,6-dimethylpyridine at 25 and 35°C over the whole concentration range [36]. They calculated various excess functions (enthalpy, Gibbs free energy, entropy), and the absolute values of all the excess functions were found to increase in the order: pyridine < methylpyridine < dimethylpyridine. The concentration dependence of the excess functions shows a rather symmetric shape centered near the mole fraction 0.5. The most important feature (as pointed out by the authors) was the larger absolute value of the excess entropy compared to the excess enthalpy. This indicates that the interactions in the mixtures are essentially entropy-controlled processes.

We found the data of Abe et. al. [36] to be the most accurate and used them in our calculations of the partial molar volumes and the derivatives of the excess free energy.

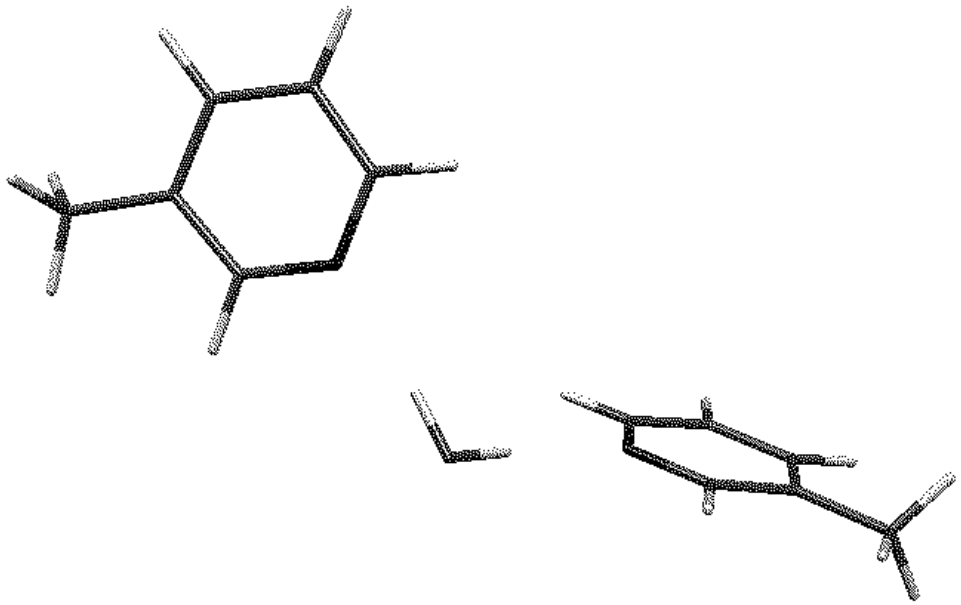

Figure 2.5.: *Optimum configuration of one 3MP and one water molecule as found in quantum chemical calculations [4]. The second 3MP is placed in a similar position connected to the second hydrogen of the water molecule.*

2.5. Ultrasound speed measurements

The speed of ultrasound has been measured in many solutions of methylpyridine with water and heavy water by Marczak et. al. [37, 38, 39, 40, 41, 42]. In all mixtures similar behavior was observed: the adiabatic compressibility changes with temperature in such a way, that the compressibility isotherms cross each other within a narrow concentration interval in the vicinity of methylpyridine mole fraction close to 0.04. The presence of these so-called isosbestic points were explained by the maximum of the rigidity of the liquid at that concentration. The authors suggested [42], that this rigidity (insensitivity to temperature change) may be caused by strong hydrogen-bonded network of water, and the solute molecules are placed in cages surrounded by water molecules, similarly as in crystal hydrates.

2.6. Quantum chemical studies

Recently Pápai and Jancsó performed quantum chemical calculations on pyridine – water and methyl-substituted pyridine – water complexes [4]. Their aim was to compare the H-bonding energies and the optimal configurations for several methylpyridine isomers. They found that: 1. the methyl substitution stabilizes the hydrogen bond (the energy minimum is deeper). 2. The association energies corresponding to the N $\cdots$

H – O hydrogen bonding progressively increase in the pyridine – methylpyridine – dimethylpyridine series. 3. The ordering of the association energies within the families of monomethyl-substituted pyridines or the dimethylpyridines however does not correlate with the trend in the miscibility properties, obtained by comparing the phase diagrams. This can suggest that the differences in the miscibility behavior of the methyl-substituted pyridines cannot be simply related to the strength of the hydrogen bond that they form with the water molecule. So the properties of the liquid mixtures should be affected also by the interaction of the hydrophobic part of the solute molecule with the surrounding water, that is called in general hydrophobic hydration.

The deep energy minima of the O – H $\cdots$ N hydrogen bonds formed between a water molecule and a methylpyridine molecule suggest that in aqueous solutions many of the MP molecules can be attached to a water molecule. The second hydrogen of such bound water molecule can also bond to another MP molecule, thus forming a "solvent-separated dimer" of methylpyridines. Such a hypothetical structure is depicted in Figure 2.5.

3. Structure of liquid mixtures

In this chapter, we report on the various methods that contribute to obtaining information about the structure of liquids.

Probably the most complete way of defining the structure of liquids is to give all information about the positions of all particles in the sample, or at least in such a big subregion that can be regarded to be characteristic of the whole system. Such an aim is not achievable obviously, so one must simplify the question: what are those characteristic features of the structure, which can be hopefully extracted using experimental or theoretical methods.

The level of such questions evolved during the years due to the development of the science. For example, in the XIX century, the most concrete and useful information was that the chemical species consist of an assembly of atoms. One could answer the question, which atoms can form pairs, how many of them can be bonded about a certain kind of atom. Later, the development of thermodynamics allowed to answer questions about the average behavior of the large systems of particles, the crystallography opened the possibility to tell precisely where the atoms are in the crystalline lattice.

The liquid state is probably the most complicated from the point of the microscopic structure. It is characterised by a short range order. Presently in practice it is impossible to determine precisely all the positions of a large number of molecules.

The most frequently used description of a liquid or amorphous structure is that using the partial radial distribution functions $g_{ij}(r)$, which give the probability of finding an atom of type i at a given distance from another atom of type j. They can be used to give the number of the neighbors in the first or second coordination shell of a given type of atom. The expression

$$dN = 4\pi r^2 \rho_j g_{ij}(r) dr \tag{3.1}$$

gives the average number of molecules of type j, located at a distance between r and $r + dr$ from a molecule of type i. ρ_j is the bulk number density of molecules of type j in the sample. Knowing all *pdf*s for all pairs of types of atoms gives a very useful description of the liquid structure. The advantage of this method is that the *pdf*s can often be measured with high precision by scattering methods, and also can be extracted directly from numerical simulations.

Another difficulty is that when constructing the *pdf* from an atomic configuration, we sum up all possible positions of the given atoms and molecules, so the resulting pair distribution functions represent only some average structure. By this way some features

of the structure might be hidden by the smearing, and cannot be recovered from these smeared *pdf*s by the conventional methods. Sometimes the 'average' structure, which is usually obtained by considering the number of neighboring atoms in the coordination shells might happen to be not relevant at all.

Such situation can occur for instance in non-homogeneous systems. The simplest example is a two-phase liquid where the two phases having different internal structures are somehow distributed in the system. (In case of mixtures they can have also different composition). It is not yet known how to describe such systems better than by using average pair distribution functions.

3.1. Molecular liquid mixtures – pair distribution functions of molecules

The classical way to characterise the structure of a molecular liquid mixture is to describe it in terms of partial pair distribution functions (*pdf*) of all atoms. The knowledge of all partial *pdf*s gives a rather good structural description of a mixture, at the exception of the orientational correlations and of the possible non-uniform distribution. However in practice it is hardly possible to measure all *pdf*s, especially if the mixture components are molecules containing more than two or three atoms.

The problem can be simplified by considering the pair distribution functions of the molecules, which can be defined so that the reference point is placed at some fixed point within the molecule, e. g. its centre of gravity. Then in a two-component mixture we have only three 'molecular' *pdf*s. In some favourable cases the molecules can contain one specific atom, on which isotopic substitution can be made and from three different neutron diffraction measurements the *pdf*s of these atoms (and therefore of the molecules) can be determined. Similar result can be obtained by combining neutron and X-ray measurements, or using anomalous X-ray scattering.

An advantage of considering the molecular distribution functions in liquids or liquid mixtures is that they are related to thermodynamic quantities. In principle there is a straightforward connection between the *pdf*s and the internal energy of the liquid or liquid mixture, however it is of little practical use as calculations of the energy would require the knowledge of the *pdf*s over the infinite r-range [9].

It can be shown using statistical thermodynamic considerations, that integrals of the *pdf*s over the entire r-range can be also related to some macroscopic properties of the liquids. This approach was elaborated by Bhatia and Thornton [43] and Kirkwood and Buff [44], and has been proved to be very useful in the analysis of experimental data obtained from small-angle neutron or X-ray scattering (works of Nishikawa *et.al.*, [45, 46, 47]). We shall present this method in the section 3.3.

3.2. Molecular liquid mixtures – counting the associated molecules

One may use another, more simple way to describe a non-crystalline atomic or molecular mixture. If the atoms or molecules interact in a way to forming pairs or aggregates of molecules, a rather useful measure can be introduced, by counting the relative proportion of pairs and all kinds of aggregates. This method can be further developed by using virial coefficients, which measure the deviation of the system from the ideal, non-interacting behavior.

Phase separation in a binary mixture is closely related to the preferential association of similar species. Therefore a mixture in the macroscopically homogeneous region, but close to the phase separation boundary must contain associated particles of the same species. So, from structural point of view, one can look for the existence of such associated molecules. An often used experimental method to detect such associated molecules is to measure their vibrational spectra by infrared or Raman spectroscopy. Another possibility can be to see the molecular aggregates directly by small-angle scattering.

This latter approach was realised in a series of SANS studies by D'Arrigo et. al. on aqueous alcohol solutions [48, 49], and by Cser et. al. on aqueous solutions of tetramethylurea [50, 51]. From the experimentally measured static structure factor Cser et. al. determined the proportions of monomers and dimers present in the solution. From this the second virial coefficient of the solute molecule interaction could be calculated.

In principle this type of analysis can be extended to take into account association of higher order. However, experimentally, it is not possible to obtain interaction parameters higher than triplets. Another limitation of this approach is that it can deal only with dilute solutions because of the definition of the second virial coefficient, and also because of the experimental difficulties connected to the interparticle interference in solutions of higher concentrations.

3.3. The Kirkwood-Buff integrals

The structure of a two-component system can be expressed in a good approximation by the three pair distribution functions (*pdf*s). If they are known over a sufficiently wide range of distances, we can construct an integral quantity for each of the *pdf*s:

$$G_{ij} = \int_0^\infty (g_{ij}(r) - 1) 4\pi r^2 dr \tag{3.2}$$

where $g_{ij}(r)$ are the pair distribution functions between the species i and j, and r is the distance between them. The G_{ij} quantities are called Kirkwood-Buff integrals (KBIs), they give a measure of the excess of molecules j around a central molecule i. The Kirkwood-Buff integrals are usually interpreted by considering the meaning of $\rho_i G_{ij}$, where ρ_i is the number density of the species i. The quantity $\rho_i g_{ij}(r) 4\pi r^2 dr$ measures

the average number of i molecules in a spherical shell of width dr at distance r from the centre of the j molecule. $\rho_i 4\pi r^2 dr$ would be the average of this quantity, if the distribution of the molecules in the liquid would be fully random (like in ideal gas). Thus the quantity $\rho_i G_{ij}$ is the measure of the deviation from the random distribution – the excess or the deficiency of the total number of molecules i in the entire surrounding of molecule j.

The usefulness of studying the KBIs is in their relation to simple thermodynamic quantities, which can be measured in the liquid or liquid mixture.

If we want to see the non-randomness in the distribution of the two species, caused by the intermolecular interactions, we need to compare the KBI values with those calculated for some reference systems. For that the so-called excess numbers of molecules around a central one are introduced:

$$\Delta n_{ij} = \rho_i (G_{ij} - G_{ij}^{ref}) \tag{3.3}$$

where Δn_{ij} is the excess (or deficit) number of molecules of type i around a central molecule j. The KBIs have nonzero values for ideal mixtures and the quantities G^{ref} are the corresponding KBIs of a properly chosen reference state [52]. They will be given in section 3.3.3.

For a one-component system the KBIs are also defined in a similar way, the single KBI in the liquid measures the non-random packing of the molecules and is related to the isothermal compressibility.

Thus the KBIs can measure the clustering of molecules in the mixture, they can provide information on the solute-solute, solute-solvent, and solvent-solvent interactions. In the solution theory of Kirkwood and Buff these integrals are calculated from thermodynamic data only. There are no approximations in the theory, and it is valid for the whole concentration range. These features make the method of Kirkwood and Buff often more useful than other approaches, e. g. those dealing with virial coefficients.

3.3.1. Direct determination of KB integrals

The Kirkwood-Buff integrals can be calculated according to their definition, using the pair distribution functions of the centers of molecules, obtained, for example, from computer simulations. However several difficulties arise: the integration should be made up to infinity, therefore sufficiently large simulation boxes must be used. Even if the box size is sufficiently large, it is rather time consuming to obtain reasonable statistical accuracy, and to allow the development of the fluctuations, which occur in a real mixture.

In a recent work [53], the behavior of water – trifluorethanol mixture was studied by molecular dynamics simulation, and the Kirkwood-Buff integrals were also computed. The obtained KBIs did not show any agreement with those calculated from thermodynamic data, though the latter can be considered to be sufficiently precise. One reason

of the disagreement can be the limiting size of the simulation box. The $(g_{ij}(r) - 1)$ in Eq. 3.2 goes to zero at large distances, but the multiplication by r^2 enhances even the smallest oscillations and can affect strongly the integrals. Certainly there must exist some limiting large distance beyond which the impact of the oscillations to the calculated KBIs disappears. This size can be checked by analyzing the dependence of the KBIs on the upper integration limit in Eq. 3.2. Such analysis showed for pure water [54] that oscillations of $r^2(g(r) - 1)$ decay for r higher than 15Å. The integration unfortunately could not be extended to longer distances because of the limited range of the available $g(r)$ data.

Another reason for the discrepancy between the calculated and the measured KBIs can be the uncertainties in the intermolecular interaction potentials.

A somewhat different method was used by Misawa and Yoshida [55]: the initial configuration in the simulation box has been constructed artificially, using the experimentally determined KB integrals. The two species (water and propanol) were modeled by spheres of appropriate diameters. After constructing the initial distribution the spheres were replaced by the molecules and the solution was allowed to equilibrate by a MD simulation. The resulting total structure factor could be compared to the experimental wide-angle neutron structure factor. This type of molecular dynamics or Monte Carlo simulations might be promising for systems having large composition fluctuations. The starting configuration already containing inhomogeneities is in any case more realistic than a fully random distribution usually used. It can be further investigated, whether the inhomogeneous solute-solvent distribution is conserved over long simulation times, and what kind of molecule-molecule arrangements develop in the solute-rich and the solvent-rich regions.

Another possibility is to work with model systems, for example spheres of different diameters or having different interaction potentials, and looking for the phase behavior and the concentration fluctuations. A few such simulation studies have been carried out so far, some of them in two-dimensions [56], however they are far yet from being able to describe real systems.

3.3.2. Calculation of Kirkwood-Buff integrals using zero-angle scattering

The fluctuations in the concentration and the particle number can be expressed by certain thermodynamic data and of the value of coherent scattering at zero angle of neutrons or X-rays. The method is based on the Bhatia-Thornton formalism [43], and was extensively used by Nishikawa [45] for studies of several aqueous alcohol solutions by small-angle X-ray scattering. We adopted the relations proposed by Nishikawa for the case of neutron scattering [57].

The coherent scattering intensity at zero angle of a two-component mixture can be

expressed as a weighted sum of the fluctuation terms [43]:

$$I_{coh}(0)/\rho = \bar{b}^2 S_{NN}(0) + (b_1 - b_2)^2 S_{CC}(0) + 2\bar{b}(b_1 - b_2) S_{NC}(0) \tag{3.4}$$

where ρ is the number density of the molecules, b_1 and b_2 are the sums of the coherent scattering lengths of the nuclei forming the two types of molecules. *Throughout this work, component* 1 *will always represent the solute, and component* 2 *the water.* For example, in pyridine - heavy water mixture:

$$b_1 = 5b_C + 5b_H + b_N = 2.39 * 10^{-12} cm$$

$$b_2 = 2b_D + b_O = 1.914 * 10^{-12} cm$$

$\bar{b}$ is defined as: $\bar{b} = x_1 b_1 + (1 - x_1) b_2$. $I_{coh}(0)$ in Equation 3.4 is given in units of cm^{-1}, used in small-angle neutron scattering.

The fluctuation terms are defined as follows:
$S_{NN}(0) =< (\Delta N)^2 > /N$ - fluctuation in the number of molecules,
$S_{CC}(0) = N < (\Delta x_1)^2 >$ - fluctuation in the concentration of molecules of type 1,
$S_{NC}(0) =< \Delta N \Delta x_1 >$ - correlation between the two fluctuations.

The fluctuations are defined in a hypothetical volume, which is small compared to the whole system but much larger than the sizes of the inhomogeneities, i. e. the range at which the molecules are correlated in their position.
$S_{NN}(0)$ and $S_{NC}(0)$ are related to $S_{CC}(0)$:

$$S_{NN}(0) = \rho k_B T \kappa_T + \delta^2 S_{CC}(0) \tag{3.5}$$

$$S_{NC}(0) = -\delta S_{CC}(0) \tag{3.6}$$

where κ_T is the isothermal compressibility, δ is the dilatation factor defined as $\delta = (\bar{V}_1 - \bar{V}_2)/V_{mol}$. $\bar{V}_1$ and $\bar{V}_2$ are the partial molar volumes of the components, V_{mol} is the molar volume of the mixture. Combining equations 3.4, 3.5 and 3.6, $S_{CC}(0)$ can be calculated using the following equation:

$$I_{coh}(0) = \rho^2 k_B T \kappa_T \bar{b}^2 + \rho[\bar{b}\delta - (b_1 - b_2)]^2 S_{CC}(0) \tag{3.7}$$

From $S_{CC}(0)$ the $S_{NN}(0)$ and $S_{NC}(0)$ are calculated. Thus, using the $I_{coh}(0)$ value from a single diffraction experiment (without isotopic substitution), it is possible to obtain structural information on the solution.

KBIs from the fluctuation terms

The Kirkwood-Buff integrals can be expressed as linear combinations of the fluctuation terms [59]:

$$G_{11} = \frac{1}{\rho}\left(S_{NN}(0) + \frac{2}{x_1}S_{NC}(0) + \frac{1}{x_1^2}S_{CC}(0) - \frac{x_2}{x_1} - 1\right) \tag{3.8}$$

$$G_{22} = \frac{1}{\rho}\left(S_{NN}(0) - \frac{2}{x_2}S_{NC}(0) + \frac{1}{x_2^2}S_{CC}(0) - \frac{x_1}{x_2} - 1\right) \tag{3.9}$$

$$G_{12} = \frac{1}{\rho}\left(S_{NN}(0) + \frac{x_2 - x_1}{x_1 x_2}S_{NC}(0) - \frac{1}{x_1^2}S_{CC}(0)\right) \tag{3.10}$$

Thus the Kirkwood-Buff integrals can be calculated from the measured forward scattering intensity, Eq. 3.7. It is to be noted that the three integrals do not bear independent information: knowing one integral the other two can be calculated by using the partial molar volumes and the compressibility. Neverthless for analyzing the solvent and the solute distribution (and clustering) it is convenient to use all the three KBIs.

3.3.3. Calculation of Kirkwood-Buff integrals from thermodynamic data

In the theory of Kirkwod and Buff the KBIs can be calculated from the following thermodynamic data [58]: the isothermal compressibility κ_T, the molar volume of the mixture V_{mol}, the partial molar volumes $\bar{V}_i$ and $\bar{V}_j$, and a quantity D, related to the Gibbs free energy of mixing.

$$G_{ij} = G_{ji} = RT\kappa_T - \frac{\bar{V}_i\bar{V}_j}{DV_{mol}} \tag{3.11}$$

$$G_{ii} = G_{ij} + \frac{1}{x_i}\left(\frac{\bar{V}_j}{D} - V_{mol}\right),\ i \neq j \tag{3.12}$$

x_i, x_j are the mole fractions of the components. The partial molar volumes $\bar{V}_i$ are defined by

$$\bar{V}_i = \left(\frac{\partial V_{mol}}{\partial n_i}\right)_{T,P,n_j} \tag{3.13}$$

where n_i and n_j are the number of moles of the components in the solution.

The function D is expressed by the second derivative of the excess Gibbs free energy:

$$D = 1 + x_i x_j \left(\frac{\partial^2 G^E/RT}{\partial x_i^2}\right)_{T,P} \tag{3.14}$$

Reference system

There are several possibilities to choose a proper reference state with which the KBIs can be compared. Matteoli and Lepori [58] used the ideal solution as the reference state. In ideal solution the excess Gibbs free energy of mixing is zero, the molar quantities change linearly with the composition, the partial molar volumes are equal to the molar volumes of the pure components. The Kirkwood-Buff integrals then have the following form:

$$G_{ij}^{id} = RT\kappa_T^{id} - \frac{V_i^0 V_j^0}{V_{mol}^{id}} \tag{3.15}$$

where κ_T^{id} and V_{mol}^{id} are the isothermal compressibility and the molar volume of an ideal solution, respectively. V_i^0 and V_j^0 are the molar volumes of the pure components.

Shulgin and Ruckenstein proposed a slightly different form [59] of the KB integrals of the reference state. The excess Gibbs free energy in their reference mixture is still zero, but the compressibility and the volumes in the Eq. 3.15 are replaced by the experimental compressibility, partial molar volumes and the molar volume of the mixture. For systems that deviate only weakly from the ideal mixing, it is necessary to consider these corrections. For mixtures with very strong non-ideal mixing behavior, the choice of the reference state is not substantial, as other sources of errors have much higher impact on the calculated KBIs.

Approximations

Analysis of the errors in KBIs caused by using approximate or inconsistent thermodynamic data was discussed in several papers [54, 58]. They showed that the largest error can arise from the excess free energy term. Slightly incorrect experimental data on vapor pressures can lead to non-predictable errors in the second derivative of the excess free energy.

Sometimes all data required to calculate the KBIs in a particular system are not available. For example, the values of isothermal compressibility of the mixtures, κ_T, as a function of the composition are often not known. However, since their contribution to G_{ij} is quite small, linearly interpolated values between the compressibilities of the pure components as a function of volume fraction can be safely used, or even the values of the adiabatic compressibility κ_S, available from ultrasound speed measurements can be employed [62]. The partial molar volumes are usually easy to determine from measured densities. But even if there are no data for the partial molar volumes, they can be replaced by the molar volumes of the pure components. The error introduced by this simplification is not so high, the partial molar volumes are similar to the molar volumes usually within 10%.

3.3.4. KBIs from light scattering

The intensity of the Rayleigh scattering gives another possibility to calculate the fluctuation terms and the Kirkwood-Buff integrals. This approach has been used for studies of aqueous and non-aqueous mixtures and proved to be quite precise, the experimental uncertainties in the published studies were less than 10% [63, 64]. One of the required quantities in this method is the refractive index as a function of the concentration. This implies an important criterion for the applicability of the method: the refractive indices of the two components must differ substantially, because the concentration derivative of the refractivity of the solution is used to calculate the concentration fluctuations. This can be easily obtained in those cases where the refractivities of the two components are not close to each other, and the refractivity of the solution varies smoothly with the composition. There exist some interesting mixtures with pronounced non-ideal mixing, in which this latter criterion is not met. For example, in water – acetonitrile mixtures strong concentration fluctuations have been observed by small-angle X-ray scattering [65]. The refraction index in this mixture varies with the composition in a very strange, non-monotonic way [66], so the determination of the derivative of the refractivity requires very precise measurements, and can lead to high errors when calculating the fluctuations and the Kirkwood-Buff integrals.

The aqueous solutions of methylpyridines can probably be easily studied by this technique. The difference of the refractive indexes of water and of methylpyridines is sufficiently high, ($n_{H_2O} = 1.333$; $n_{MP} \approx 1.50$) and the refractivity of the solution changes monotonically with the concentration. In our studies we did not try to perform such measurements. However, the application of this technique for methylpyridine solutions can give results as good as those obtained by neutron scattering. Moreover, it should be possible to reveal the structural and solvation differences in water and in heavy water solutions, as they can be measured with equal precision.

Part II.

Experimental methods

4. Neutron scattering, basic relations

In a neutron scattering experiment a collimated neutron beam hits the sample, scatters on it and diffuses in different directions. Neutron detectors are placed around the sample at given positions thus the scattering angle is determined. In inelastic scattering measurement the energy of the scattered neutron is also registered, this can be achieved by measuring its velocity or wavelength. Measuring the angle and the energy of the scattered neutron, information can be obtained regarding the structural arrangement and the dynamics of the nuclei constituting the sample.

4.1. Elastic and inelastic scattering

The neutrons scattered on nuclei, being spherical waves, interfere with each other. Therefore the intensity away from the sample varies with the angle between the direction of scattered neutron and the initial beam. The useful quantity related to the scattering angle is the momentum exchange:

$$\hbar q = \frac{4\pi\hbar}{\lambda}\sin(\theta/2) \tag{4.1}$$

where θ is the scattering angle, λ is the wavelength of the neutron, and q is the amplitude of the scattering vector.

Elastic scattering

If there is no energy exchange between the neutron and the nucleus, the intensity $I(q)$ scattered from an assembly of nuclei is proportional to the coherent differential cross section $\frac{d\sigma}{d\Omega}(\mathbf{q})$, defined as:

$$I(\mathbf{q}) \sim \frac{d\sigma}{d\Omega}(\mathbf{q}) = \langle\sum_{m,n}^{N} b_m b_n \exp(i\mathbf{q}(\mathbf{r}_n - \mathbf{r}_m))\rangle \tag{4.2}$$

b_m are the scattering amplitudes of the nuclei, $\bar{b}$ is their arithmetical mean over all N nuclei in the sample. One can define the structure factor $S(\mathbf{q})$:

$$S(\mathbf{q}) = \frac{1}{N\bar{b}^2}\frac{d\sigma}{d\Omega}(\mathbf{q}) \tag{4.3}$$

The double sum in Eq. 4.2 can be replaced by an integral, and averaged over all directions. Then the structure factor can be expressed as a Fourier transform of the pair distribution function $g(r)$:

$$S(q) - 1 = \frac{4\pi\rho}{q} \int_0^\infty r(g(r) - 1) \sin(qr) dr \tag{4.4}$$

If there are more than one type of atoms, partial pair distribution functions $g_{\alpha,\beta}(r)$ are used and a similar equation can be written for the partial structure factors $S_{\alpha\beta}(q)$.

Inelastic scattering

In the scattering process the scattered neutron can exchange energy with the system:

$$E = \hbar\omega = E_i - E_f = \frac{\hbar^2}{2m}(k_i^2 - k_f^2) \tag{4.5}$$

i and f denotes the initial and the final impulse and energy of the neutron.

The formalism which relates the energy and momentum transfer of a scattered neutron to the structure and dynamics in the sample was developed by Van Hove [68]. The quantity describing the structure and the dynamics in an atomic assembly is the time-dependent correlation function:

$$G(\mathbf{r}, t) = \frac{1}{N} \int \langle \rho(\mathbf{r}', 0) \rho(\mathbf{r}' + \mathbf{r}, t) \rangle d\mathbf{r}' \tag{4.6}$$

It corresponds to the probability of finding a particle with coordinates $(\mathbf{r}, t)$, if a particle (the same or another one) was at $(\mathbf{0}, 0)$. The function which is measured in the neutron scattering experiment is the space and time Fourier transform of the time-dependent correlation function:

$$S(q, \omega) = \frac{1}{2\pi} \langle \int \int G(\mathbf{r}, t) \exp(i(\mathbf{qr} - \omega t)) d\mathbf{r} dt \rangle \tag{4.7}$$

$S(q, \omega)$ is called the dynamic structure factor, it is proportional to the scattering intensity.

When the energy of the detected neutron is not analysed, i. e. the detector counts all neutrons with the given momentum transfer, then the static structure factor is measured:

$$S(q) = \int_{-\infty}^{+\infty} S(q, \omega) d\omega = \frac{1}{N} \langle \sum_{m,n}^{N} \exp i(\mathbf{r}_n - \mathbf{r}_m) \rangle \tag{4.8}$$

4.2. Small-angle neutron scattering

The q-range covered in small-angle scattering type of measurements is usually between 0.001 and 1Å^{-1}. This is achieved by using neutrons with wavelengths between 4 and 20 angstroem. Measurements at lower angles are limited by experimental difficulties, at higher angles other features of the structure become visible, which are out of the field of small-angle scattering. Such momentum exchange permits to study the structure at length scales from one nanometer up to few hundreds of nanometers.

The q-dependence of the scattering intensity, like in other diffraction techniques, is related to the structural arrangement of the scattering centers (nuclei) by a space-Fourier transformation. The q-range covered in small-angle scattering corresponds to such length scales where the individual atoms cannot be distinguished, therefore the quantity which is measured is the distribution of the scattering length density $\rho_{sc.l.}$ in the sample. It is defined as the ratio of the sum of the scattering lengths b_i of all nuclei to the volume V they are contained in:

$$\rho_{sc.l.} = \frac{1}{V} \sum_i b_i$$

In the following we describe some quantities and formulas which will be used for the interpretation of our experimental results.

Scattering at zero angle

In liquids, gases or other disordered systems the coherent scattering at small momentum transfer originates from the presence of regions with different scattering length densities. In many cases the atoms or molecules in the sample are distributed obeying the laws of statistical mechanics, therefore the structure of the system can be described relatively simply in terms of random fluctuations in molecular density and concentration. For the simple system, monoatomic or monomolecular fluid or gas, the intensity scattered at zero angle can be written as follows:

$$I(0) = \rho\, b^2 \frac{\langle (\Delta N)^2 \rangle}{N} \tag{4.9}$$

The $I(0)$ in this equation is given in units of cm^{-1}, ρ is the number density of atoms or molecules, and b is the coherent scattering length of the atom or the sum of the scattering lengths of the atoms constituting the molecule. The last term in Eq. 4.9 is the fluctuation of the mean number of particles in an arbitrarily chosen volume, which is much smaller than the whole system but sufficiently large to fulfill the usual approximations of statistical mechanics. The fluctuations are related to the isothermal

compressibility κ_T (Section 3.3.2), thus the zero-angle limit of the scattering intensity takes the form:

$$I(0) = \rho^2 b^2 k_B T \kappa_T \tag{4.10}$$

Correlation length

Another quantity is used to characterize the spatial extension of the inhomogeneities in the sample. It is called usually correlation length. In a compressible liquid close to the critical point, or in a two-component molecular mixture the scattering length distribution can be well described by the Debye equation:

$$\langle(\rho_{sc.l.}(r) - \rho_{average})^2\rangle^{1/2} \sim \frac{1}{r} exp(-r/\xi) \tag{4.11}$$

ξ is the correlation length, which can be regarded roughly as a distance up to which the correlation between the fluctuations of the local density extends. The corresponding scattering intensity takes the form of a Lorentzian function, resulting from the Fourier transform the scattering length density distribution:

$$I(q) = \frac{I(0)}{1 + q^2\xi^2} \tag{4.12}$$

This equation is called often Ornstein-Zernike formula [69] and can be used for a graphical determination of the correlation length and of the scattering intensity at zero angle. At large values of the scattering vector the intensity decays proportionally to q^2.

4.3. Quasielastic neutron scattering

The structure factor $S(q, \omega)$ can be separated to two parts, the coherent and the incoherent structure factors. In the case of hydrogenated samples the coherent contribution can be neglected due to the dominance of the incoherent scattering from hydrogen over the scattering from other atoms.

In the incoherent quasielastic neutron scattering experiment the incoherent part of the structure factor is measured. This corresponds to the motions of the individual atoms. Due to the high incoherent cross-section of the proton, in a hydrogen-containing sample almost exclusively the proton motions are seen. The small energy transfer in a QENS measurement corresponds to energies of the translational, rotational, and vibrational motions of the atoms. As these three motions have very different time scales, the scattering function can be approximated as a convolution of the three terms associated to these motions. This is called *decoupling approximation* and is the standard way to

analyze quasielastic neutron scattering spectra. The dynamic structure factor $S(q,\omega)$ can be expressed as follows:

$$S(q,\omega) = S^{vibr}(q,\omega) \otimes S^{rot}(q,\omega) \otimes S^{trans}(q,\omega) \tag{4.13}$$

where $\hbar\omega$ is the energy transferred to the sample by a scattered neutron. $S^{vibr}(q,\omega)$, $S^{rot}(q,\omega)$ and $S^{trans}(q,\omega)$ are the contributions to the incoherent scattering intensity coming from the vibrational, rotational and translational motions of the atoms. The time scale of the motions observed by a time-of-flight spectrometer is usually between 1 and $100ps$. This is much longer than the period of thermal vibrations of a hydrogen atom. In this long-time limit, the vibrational part of the dynamic structure factor is reduced to the Debye-Waller factor, and the structure factor takes the form:

$$S(q,\omega) = e^{-q^2\langle u^2\rangle/3}\left(S^{trans}(q,\omega) \otimes S^{rot}(q,\omega)\right) \tag{4.14}$$

where $\langle u^2\rangle$ is the mean square displacement of the nuclei due to thermal vibrations.

Measurements at high energy resolution can furnish information about the slow motions in the system, these are usually the diffusive translational motions of the molecules. If the diffusion obeys the Fickian diffusion law, then the translational part of the dynamic structure factor takes the form of a Lorentzian line:

$$S^{trans}(q,\omega) \sim \frac{\Gamma(q)}{\hbar^2\omega^2 + \Gamma(q)^2} \tag{4.15}$$

where $\Gamma(q)$ is the half width at half maximum (HWHM) of the quasi-elastic line.

Diffusion models

Several models are elaborated that give a relation between the way of motion of the particles and the quasielastic line broadening.

Continuous diffusion

The continuous diffusion corresponding to Einstein's theory of Brownian motion predicts for $\Gamma(q)$ the following form:

$$\Gamma(q) = \hbar q^2 D_{trans} \tag{4.16}$$

where D_{trans} is the translational self-diffusion coefficient. It can be expressed by the mean square displacement of the particle (Einstein relation):

$$D_{trans} = \lim_{t->\infty} \frac{1}{6t} < [R_i(t) - R_i(0)]^2 > dt \tag{4.17}$$

or in terms of the velocity auto-correlation function [71]:

$$D_{trans} = \frac{1}{3}\int_0^\infty < v_i(\tau)v_i(t+\tau) > dt \tag{4.18}$$

Here the scalar product has to be formed of the velocity v_i of a particle numbered i at time τ with the velocity of the same particle at time $t+\tau$. The brackets denote the ensemble average over all species and all choices of the time origin.

The continuous diffusion model is quite a good approximation for motions over large distances, much larger than the atomic scale. It corresponds to small q, so in the usual representation of QENS data, the line broadening versus the squared momentum transfer, the curve starts with a linear part. At higher q the behavior at smaller distances becomes visible. When the distances are as small as the atomic spacing, the diffusion cannot longer be regarded as continuous, but new features appear that reflect the atomistic behavior of the motion.

Jump diffusion

The random jump-diffusion model involves the existence of two processes: a jump between two neighboring positions (sites), and oscillatory motions in a given site between two jumps, which is characterized by the residence time τ_0 [70]. This model leads to scattering laws in which the quasi-elastic broadening deviates noticeably from the q^2D_s behavior. The $\Gamma(q)$ in the jump diffusion model is given by

$$\Gamma(q) = \frac{\hbar q^2 D_s}{1 + q^2 D_s \tau_0} \tag{4.19}$$

This model may be an oversimplification for representing the short- and intermediate-time diffusion in a real system (water), but due to its simplicity, small number of parameters and remarkable agreement with the experimental quasielastic line broadening, it is widely used for characterizing the motion of water molecules [72]. Given the diffusion coefficient and the residence time, a characteristic jump distance L_{av} can be introduced:

$$L_{av} = \sqrt{6 D_s \tau_0} \tag{4.20}$$

For liquid water this jump distance was found to be 1 - 2 Å, increasing with the decrease of the temperature [72].

At low q values, which correspond to long distances, the details of the elementary jump processes are no longer observed and the jump-diffusion law is reduced to the continuous model.

Part III.

Results and analysis

5. SANS studies

5.1. SANS experiments

We performed a series of small-angle neutron scattering experiments on aqueous and non-aqueous solutions of different organic solutes at temperatures and concentrations where the mixtures are macroscopically homogeneous. The chosen systems are those for which strong non-ideal mixing behavior is expected. In this work, we present the results obtained for heavy water solutions of pyridine, three methylpyridines and two dimethylpyridines.

Three different SANS instruments have been used for the measurements: the Yellow Submarine diffractometer in Budapest, the PAXE and the PACE instruments in Saclay. The first two instruments are very similar to each other (64*64 pixels two-dimensional position sensitive multidetector; sample-detector distance variable between 1 and 5.5 m). On the PACE instrument the detector consists of 30 concentric rings, which is suitable for measurements of isotropic scattering patterns only. The technical data about the instruments can be found on the homepages of the laboratories [74, 75].

The measurements have been usually performed as follows:

A series of samples of different concentrations was prepared by weighing the appropriate amounts of methylpyridines (purchased from Sigma-Aldrich) and heavy water (99.8 - 99.9 % purity, from different companies). The quartz cuvettes of 2 mm path length were filled with solutions, and placed into an automatic sample changer that was thermostated with a precision of about 0.1 - 0.5 degrees. All samples were measured at standard temperature 25°C. Some of them have been also measured at higher temperatures, staying always in the one-phase region of the phase diagram. In Table 5.1, the experimental conditions for the measurements are summarized.

In all the measurements of aqueous solutions of methyl-substituted pyridines the scattering patterns have a similar behavior: enhanced small-angle scattering has been registered for all the solutions over a wide concentration range. The maximum intensity was found at about 8-10 mol% for all methylpyridine solutions. The measured curves are well described by the Ornstein-Zernike model (Eq. 4.12) with an additional background term (Eq. 6.1). The intensities were always higher at higher temperatures, which is attributed to the higher degree of the composition fluctuations (see the following parts with analysis and discussion of the results).

During the course of our studies, we performed experiments on different SANS instruments. It is a widespread practice to calibrate the measured SANS intensities to the

Table 5.1.: *Concentration and temperature range of SANS measurements on heavy water solutions of pyridine and methyl-substituted pyridines. The lower demixing temperatures are indicated for water and heavy water solutions of 2MP, 3MP and 2,6DMP.*

Solute	Concentrations	Temperatures	LCST in H_2O	LCST in D_2O
Pyridine	0.02 - 0.30	15°C - 55°C	no demixing	no demixing
2MP	0.005 - 0.25	25°C - 51°C	no demixing	86.5°C
3MP	0.005 - 0.80	25°C - 51°C	no demixing	38.5°C
4MP	0.005 - 0.25	25°C - 51°C	no demixing	no demixing
2,6MP	0.01 - 0.18	25°C	31°C	28.7°C

scattering of a 1 mm thick light water sample, because of the high incoherent scattering of the protons. However, it is necessary to correct for the pronounced inelastic scattering of water, and these empirical correction factors are usually different for the different instruments [77, 78]. This limits the precision of the determination of the measured absolute intensity, and also can lead to some uncertainty when comparing measurements performed on different instruments. Therefore for studying one system or a series of similar systems it is recommended to use the same SANS instrument.

In the following part we present the SANS curves measured for the different pyridine and methylpyridine solutions and the main quantities that can be used to characterize the measured scattering curves: the forward scattering intensities and the characteristic sizes of the inhomogeneities as determined using the Ornstein-Zernike model.

5.1.1. Pyridine solutions

Solutions of pyridine in heavy water have been measured on the PACE instrument at 15, 25, 40 and 55°C over the mole fraction range 0.02 - 0.25. In Figure 5.1 the spectra recorded at T = 25°C are plotted, together with the fits of the model used Eq. 6.1. The obtained values of the forward scattering intensity, of the correlation length and of the background are listed in Table 5.2. The forward scattering intensity and the correlation length have maxima around 10 mol%, indicating the region with the largest inhomogeneities.

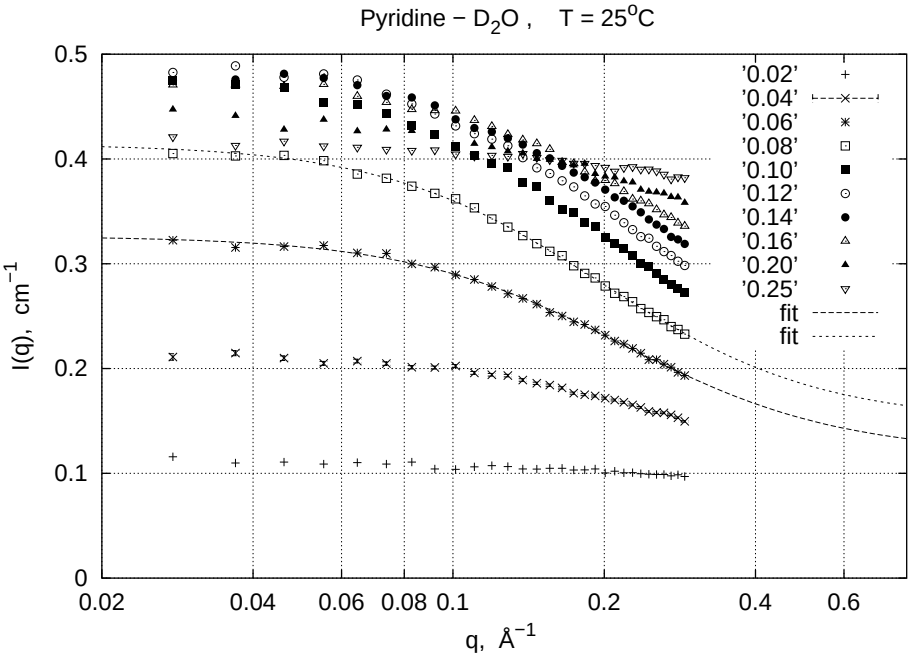

Figure 5.1.: *SANS curves of pyridine – D_2O solutions measured on the PACE diffractometer at 25°C. Mole fractions of pyridine in the solutions are indicated. The solid lines are fits to Eq. 6.1*

.

Table 5.2.: *Results of fitting the SANS curves with the Ornstein-Zernike model (Eq. 6.1) for pyridine – D_2O solutions measured at 25°C.*

Pyridine mole fraction	A / cm^{-1}	Bg / cm^{-1}	ξ / Å
0.02	0.025 ± 0.005	0.086 ± 0.005	3.6 ± 0.8
0.04	0.115 ± 0.005	0.098 ± 0.005	3.73 ± 0.18
0.06	0.207 ± 0.003	0.120 ± 0.003	4.61 ±0.11
0.08	0.265 ± 0.002	0.149 ± 0.005	5.07 ± 0.08
0.10	0.302 ± 0.003	0.176 ± 0.004	5.03 ± 0.09
0.12	0.293 ± 0.004	0.201 ± 0.005	4.84 ± 0.11
0.14	0.275 ± 0.007	0.210 ± 0.007	4.22 ± 0.14
0.16	0.237 ± 0.006	0.241 ± 0.007	4.22 ± 0.16
0.20	0.134 ± 0.008	0.304 ± 0.008	4.08 ± 0.29
0.25	0.061 ± 0.008	0.353 ± 0.009	3.59 ± 0.58

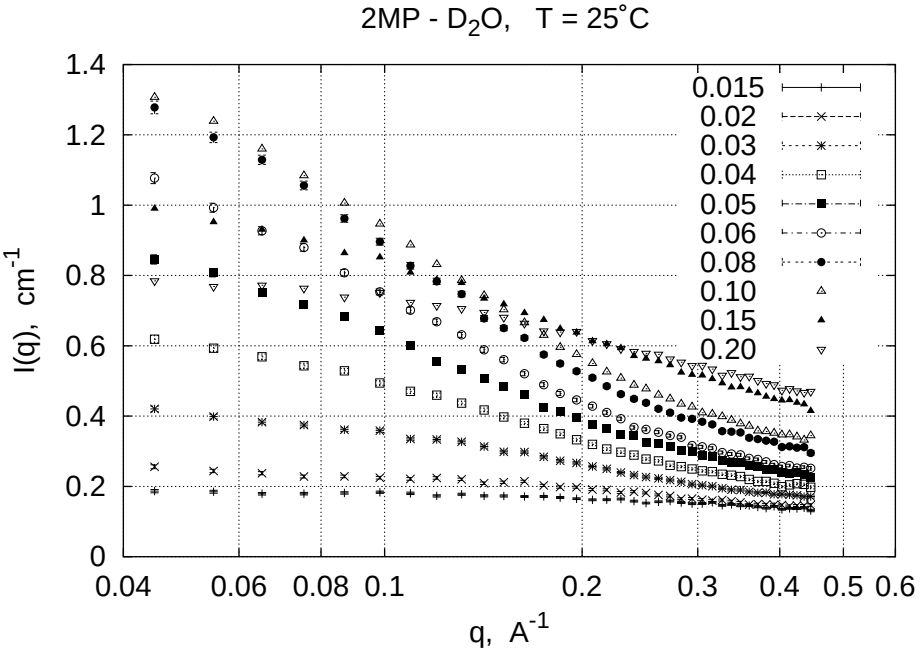

Figure 5.2.: *SANS curves of some of the 2-methylpyridine – D_2O solutions measured on the PAXE diffractometer at 25°C.*

Table 5.3.: *Results of fitting the SANS curves with the Ornstein-Zernike model (Eq.6.1) for 2-methylpyridine – D_2O solutions measured at 25°C.*

2MP mole fraction	A / cm^{-1}	Bg / cm^{-1}	ξ / Å
0.015	0.072 ± 0.005	0.088 ± 0.006	2.8 ± 0.3
0.02	0.122 ± 0.003	0.091 ± 0.004	3.9 ± 0.2
0.025	0.210 ± 0.002	0.117 ± 0.002	5.4 ± 0.1
0.03	0.256 ± 0.002	0.108 ± 0.002	5.4 ± 0.1
0.035	0.345 ± 0.002	0.128 ± 0.001	6.3 ± 0.1
0.04	0.437 ± 0.004	0.125 ± 0.002	6.6 ± 0.1
0.05	0.635 ± 0.006	0.152 ± 0.002	7.8 ± 0.1
0.06	0.843 ± 0.008	0.159 ± 0.002	8.4 ± 0.1
0.08	1.020 ± 0.01	0.204 ± 0.002	8.9 ± 0.1
0.1	1.008 ± 0.008	0.220 ± 0.002	8.3 ± 0.1
0.15	0.571 ± 0.005	0.296 ± 0.004	5.7 ± 0.1
0.2	0.373 ± 0.005	0.314 ± 0.006	4.0 ± 0.1
0.25	0.262 ± 0.05	0.304 ± 0.052	1.6 ± 0.2

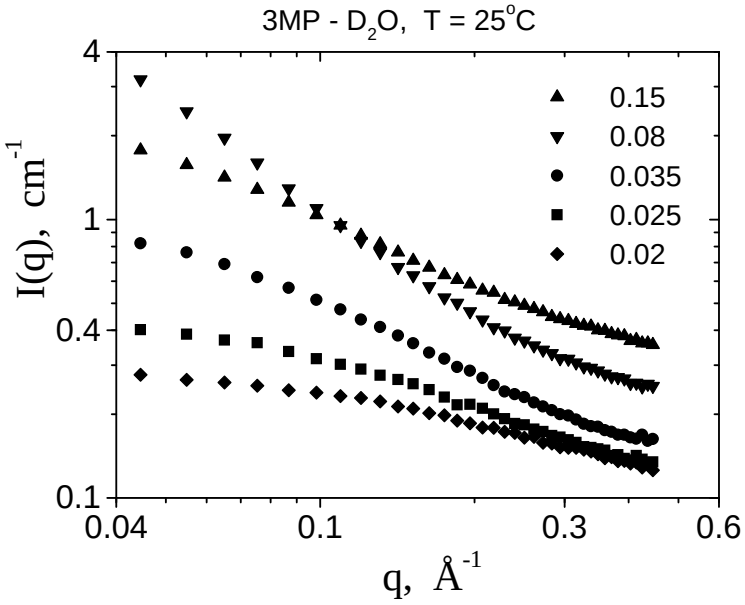

Figure 5.3.: *SANS curves of some of the 3MP – D_2O solutions measured on the PAXE diffractometer at 25°C.*

Table 5.4.: *Results of fitting the SANS curves with the Ornstein-Zernike model (Eq.6.1) for 3-methylpyridine – D_2O solutions measured at 25°C.*

3MP mole fraction	A / cm^{-1}	Bg / cm^{-1}	ξ / Å
0.005	0.024 ± 0.002	0.073 ± 0.002	3.3 ± 0.3
0.01	0.043 ± 0.004	0.087 ± 0.002	2.6 ± 0.3
0.015	0.102 ± 0.001	0.089 ± 0.002	4.1 ±0.1
0.02	0.175 ± 0.002	0.104 ± 0.001	5.4 ± 0.1
0.025	0.323 ± 0.003	0.104 ± 0.001	7.1 ± 0.1
0.03	0.524 ± 0.005	0.122 ± 0.001	8.9 ± 0.1
0.035	0.835 ± 0.010	0.123 ± 0.001	10.6 ± 0.1
0.04	1.417 ± 0.018	0.143 ± 0.001	13.6 ± 0.1
0.05	2.675 ± 0.048	0.150 ± 0.001	17.5 ± 0.2
0.06	4.578 ± 0.012	0.179 ± 0.001	22.4 ± 0.4
0.08	6.56 ± 0.020	0.203 ± 0.002	25.3 ± 0.5
0.1	6.69 ± 0.16	0.231 ± 0.002	25.4 ± 0.4
0.15	1.81 ± 0.03	0.304 ± 0.003	12.1 ± 0.2
0.25	0.198 ± 0.015	0.377 ± 0.018	2.9 ± 0.3

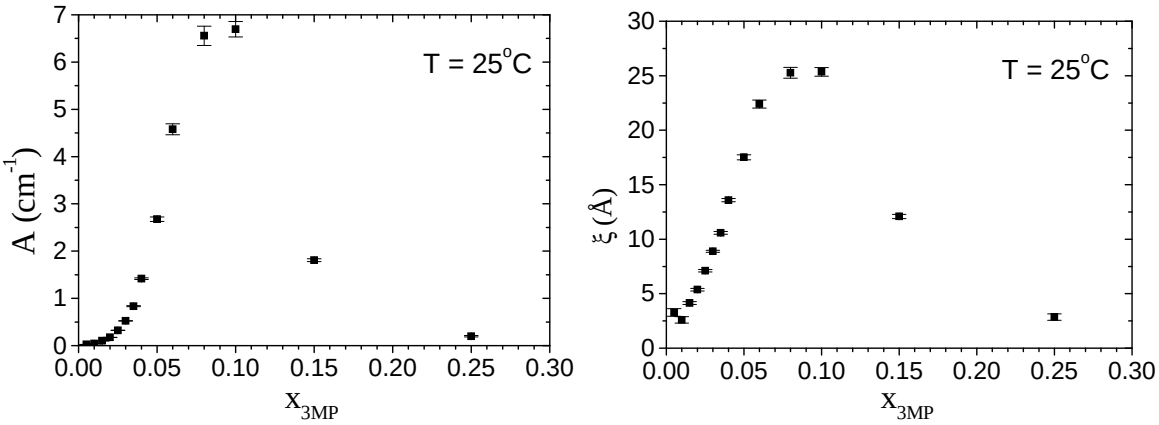

Figure 5.4.: *Forward scattering intensities and correlation lengths in 3-methylpyridine – heavy water mixtures as obtained from a fitting of the SANS curves by the Ornstein-Zernike model (Eq. 6.1).*

5.1.2. Methylpyridine solutions

Solutions of the three methylpyridines have been measured on the PAXE diffractometer during one experimental cycle. This could be important for comparing the results obtained for the three mixtures, as possible differences connected with the absolute calibration are avoided. All the three systems have been measured over a concentration range of 0.01 - 0.25 mole fraction of methylpyridine at three temperatures: 25, 31.1 and 51.5°C. At the two lower temperatures all the solutions were in the fully miscible state. The 3MP – D_2O samples of concentrations higher than 4 mol% exhibit a phase separation above 38°C, therefore only some of them have been measured at 51.5°C. The SANS spectra of 2MP – D_2O solutions, measured at 25°C are shown in Figure 5.2.

SANS spectra of the 3MP – D_2O solutions are shown in Figure 5.3, and the results of fitting Equation 6.1 are collected in the Table 5.4. The obtained values of the forward scattering intensity and correlation length in 3MP – D_2O solutions at 25°C are shown in Figure 5.4 as a function of mole fraction of 3MP. Both quantities exhibit a maximum around 8 - 10 mol%, indicating the region with the largest inhomogeneities. The composition 0.084 mole fraction of 3MP in D_2O corresponds to the critical composition of the LCST.

5.1.3. Dimethylpyridine solutions

Heavy water solutions of 2,6-dimethylpyridine have been studied on the SANS instrument Yellow Submarine. This mixture has a very low LCST (28.7°C). We have measured this solution only at 25°C, for which some thermodynamic data are also available. The spectra are shown in Figure 5.5.

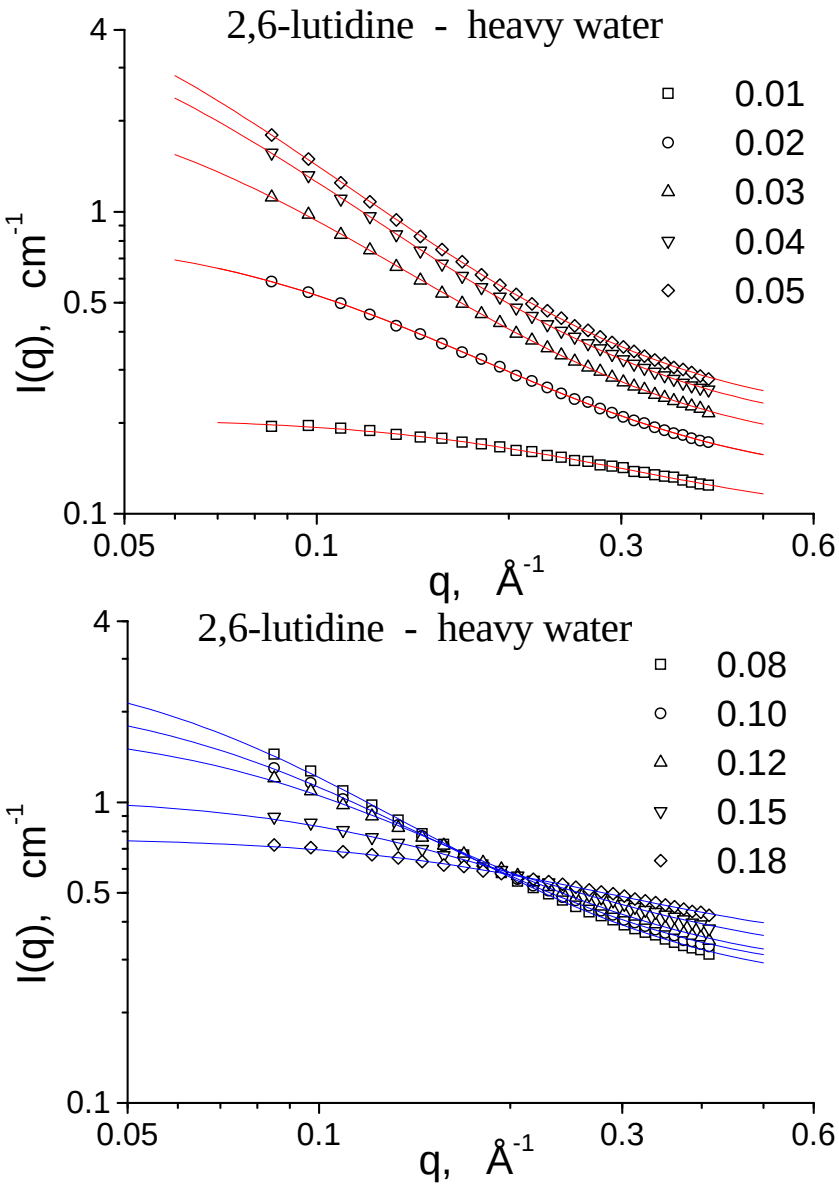

Figure 5.5.: *SANS curves of 2,6-lutidine – D_2O solutions measured on the Yellow Submarine instrument at 25°C. Mole fractions of lutidine in the solution are indicated, and the curves fitted to the Ornstein-Zernike model are plotted.*

5.1.4. Non-aqueous solutions

In order to investigate the effect of different solvents we have made some measurements on mixtures of 3-methylpyridine with other solvents: carbon disulfide and carbon tetrachloride. The chosen concentrations were between 0.05 and 0.30 mole fraction of 3MP, at which the demixing tendencies in the water solutions are the most pronounced. We have not observed any sign of increased small-angle scattering in these solutions.

5.2. Primary analysis of SANS data: Evidence of aggregation in the solution

When looking at the results of the SANS experiments, we can see that for all the aqueous solutions of pyridine and methylpyridines there is an increase of the scattering intensity at low q. Without further analysis, this means that the distribution of the molecules in the liquid is not at all homogeneous. The inhomogeneous scattering length density distribution, responsible for the coherent scattering, is caused by the non-random distribution of the solute molecules in the liquid: the appearance of large domains of different compositions in the liquid corresponds to an effective attractive interaction that is dominant between the similar species. These domains have characteristic sizes of some nanometers, and depend on the concentration and temperature. They are increasing when the temperature-concentration coordinates of the point of the measurement is approaching the phase separation boundary on the phase diagram.

In the solution there is some effective attractive interaction between the methylpyridine molecules, which leads to visible microscopic aggregation, and, presumably, is the driving force of the macroscopic phase separation at higher temperatures.

We recall, that small-angle scattering is a low-resolution method, therefore we cannot expect to obtain detailed structures at near-atomic resolution.

6. Kirkwood-Buff analysis of methylpyridine solutions

6.1. Calculation of the Kirkwood-Buff integrals

Our analysis of the measured small-angle scattering is based on the following assumption: We consider the structure of the solution as being approximated by a continuous variation of the scattering length density. This corresponds to the variation of the local composition, as the two components – heavy water and the perprotiated organic solute have strongly different scattering length densities. The observed small-angle scattering thus corresponds to the fluctuations of the local composition, and allows us to use the Kirkwood-Buff theory, which relates the fluctuations to macroscopic thermodynamic quantities. We use only one measured quantity, the forward scattering intensity, so no real structural information is deduced from the scattering only. This way, no information can be obtained about the different molecular aggregates that might be present in the solution. On the other hand, this approach is a precise way of interpreting SANS data, as it is based on rigorous thermodynamic theory. In the eighties Nishikawa et. al. started to use this method for studying aqueous alcohol solutions by small-angle X-ray scattering technique. We have adapted the formalism proposed by these authors to analyze the neutron scattering data (Section 3.3). We tested the procedure on 1-propanol – heavy water mixtures, and have found sufficiently good agreement between the fluctuations and the Kirkwood-Buff integrals calculated from neutron and X-ray scattering data [57].

The basic relations for computing the Kirkwood-Buff integrals and related quantities have been described in section 3.3. In this chapter we show in more details the practical handling of the neutron and thermodynamic data used for the calculations.

To calculate the fluctuation terms and the KB integrals using small-angle scattering data, the following quantities are needed: the coherent forward scattering intensity, the molar volume of the solution, the partial molar volumes of the components, and the isothermal compressibility. In the next subsections we describe in a detailed way the handling of these scattering and thermodynamic data.

6.1.1. Coherent forward scattering intensity

The scattering at zero angle is most easily obtained by extrapolating the small-angle scattering spectra to $q = 0$. For this purpose we fitted the scattering curves by the following equation (Ornstein-Zernike model):

$$I(q) = \frac{A}{1 + \xi^2 q^2} + Bg \tag{6.1}$$

This model was found to fit perfectly the scattering curves for all concentrations and temperatures studied. The accuracy of the determination of the A parameter was rather good, about 1-2%. Only at the lowest concentrations its uncertainty increased to 20%. This is related to the very small excess of the coherent scattering above the flat background in these solutions.

The coherent forward scattering intensity can be obtained from the fitted parameter A of Eq. 6.1. The forward scattering intensity of a two-component mixture contains a q-independent term arising from the random mixing of the two species [76]. At moderate temperatures the q-dependence of the compressibility term is negligible, therefore its contribution, together with the contribution from the random mixing is flat and is hidden in the background term Bg. Therefore the fitted parameter A does not contain these contributions, and the coherent forward scattering intensity can be obtained by adding these terms to the parameter A:

$$I_{coh}(0) = A + \rho^2 k_B T b^2 \kappa_T + \rho x_1 (1 - x_1)(b_1 - b_2)^2 \tag{6.2}$$

6.1.2. Molar volume and partial molar volumes

The molar volume of the mixture can be determined by measuring its density. In general, the volume of a mixture is not equal to sum of the volumes occupied by the separate components at the same pressure and temperature before mixing. For describing the real volume occupied by a molecule in the mixture, a special quantity, the partial molar volume is defined. It is equal to the increase in volume of the mixture by adding to it an infinitesimal amount of one component. The ratio dV_{mol}/dn_1, where n_1 is the number of moles of the component *1*, is the partial molar volume of species *1* in the mixture. In principle the partial molar volume can be determined by measuring the change of the volume of the mixture when adding a small amount of one component while the amount of the other component is held constant. In practice however the partial molar volumes $\bar{V_1}$ and $\bar{V_2}$ are calculated from the composition dependence of the molar volume using the following equations:

$$\bar{V_1} = V_{mol} - x_2(\partial V_{mol}/\partial x_2); \qquad \bar{V_2} = V_{mol} - x_1(\partial V_{mol}/\partial x_1) \tag{6.3}$$

The differentiation can be performed by various methods, e.g. graphically, or by fitting the concentration dependence of the molar volume by analytical function and calculating its derivatives.

Table 6.1.: *Thermodynamic data used for calculations of the KBIs in pyridine – heavy water solutions at 25°C.*

Mole fraction	V_{water}, cm^3	V_{py}, cm^3	V_{mol}, cm^3	κ_S, $10^{-12} dyn^{-1} cm^{-2}$
0.02	18.07	77.89	19.27	4.34
0.04	18.07	77.93	20.46	4.26
0.06	18.07	77.99	21.66	4.25
0.08	18.07	78.06	22.87	4.26
0.10	18.06	78.14	24.09	4.29
0.12	18.05	78.22	25.27	4.34
0.14	18.04	78.32	26.48	4.37
0.16	18.03	78.42	27.69	4.42
0.20	17.995	78.64	30.12	4.53
0.25	17.93	78.93	33.18	4.65

For approximating the molar volumes with a single equation over the entire concentration range usually the excess volume is fitted by a Redlich - Kister polynomial form. In our case, as we analyzed data only at concentrations below 0.25 solute mole fraction, it was appropriate to fit the molar volume itself by a quadratic polynomial:

$$V_{mol} = a_0 + a_1 x_1 + a_2 x_1^2 \tag{6.4}$$

Then the partial molar volumes of the solute $\bar{V}_1$ and of the water $\bar{V}_2$ can be expressed by the obtained coefficients:

$$\bar{V}_1 = a_0 + a_1 + 2a_2 x_1 - a_2 x_1^2 \tag{6.5}$$

$$\bar{V}_2 = a_0 - a_2 x_1^2 \tag{6.6}$$

In Tables 6.1, 6.2 we give for reference the molar volumes and partial molar volumes of pyridine – heavy water and picoline – heavy water solutions at 25°C.

In 2,6-lutidine – heavy water mixtures the partial molar volumes of the two components are constant over the investigated composition range: $\bar{V}_1 = 116.72$ cm^3, $\bar{V}_2 = 18.04$ cm^3. The molar volume of the mixture changes linearly with composition according to: $V_{mol} = 18.0352 + x_1 * 91.1793$.

6.1.3. Isothermal compressibility

The isothermal compressibility of a liquid can be determined by definition, measuring the volume change with pressure. In these measurements the pressure dependence of

Table 6.2.: *Coefficients of the polynomial equations (Eq. 6.4) fitting the molar volumes of methylpyridine – D_2O solutions in concentration range x_{MP} 0 - 0.3 .*

Temperature	solute	a_0	a_1	a_2
25°C	2MP	18.140	75.102	5.007
	3MP	18.110	76.167	1.285
	4MP	18.127	76.359	2.400
31.1°C	2MP	18.157	75.805	5.143
	3MP	18.137	76.948	0.911
	4MP	18.169	76.508	4.996
51.5°C	2MP	18.311	78.263	4.618
	3MP	18.265	79.598	0.256
	4MP	18.317	79.228	2.318

Table 6.3.: *Sources of thermodynamic data for aqueous solutions of methylpyridines used in our studies. In the analysis of heavy water solutions of pyridine and 2,6-lutidine the corresponding data for light water solutions were used.*

Mixture	Adiabatic compressibility	Density
Pyridine - H_2O	[67]	[36]
Pyridine - D_2O	no data	no data
3MP - H_2O	[41]	[36]
2MP - D_2O	[37]	[37]
3MP - D_2O	[38]	[38]
4MP - D_2O	[39]	[39]
2,6DMP - H_2O	[40]	[40]
2,6DMP - D_2O	no data	no data

the different quantities (compressibility, molar volume) are usually studied. However such studies are relatively rare due to the special equipment needed. It is much easier to determine the compressibility by measuring the speed of ultrasound at normal pressure. The quantity such obtained is the adiabatic compressibility:

$$\kappa_S = \frac{1}{\rho u^2} \tag{6.7}$$

Here ρ is the molecular density of the solution, and u is the speed of ultrasound. The isothermal compressibility κ_T can be calculated from κ_S , the isobaric expansivity α_P and the molar heat capacity C_P:

$$\kappa_T = \kappa_S + VT/\alpha_P^2 C_P \tag{6.8}$$

For our mixtures there were no available data for the expansivities and heat capacities. It is known from literature [58] and it was also checked for our solutions, that at normal conditions the impact of the compressibilities in Equations 3.11, 3.12 is very low (less than 3%), therefore we neglected the difference between isothermal and adiabatic compressibilities.

In Table 6.3 the sources of all data used for calculations of the adiabatic compressibilities and molar volumes of the solutions are listed. For pyridine – heavy water and 2,6-lutidine – heavy water solutions there were no available thermodynamic data, we used instead corresponding data for light water solutions.

6.2. Kirkwood-Buff integrals and related quantities for aqueous solutions of methylpyridines

6.2.1. The Kirkwood-Buff integrals

We calculated Kirkwood-Buff integrals in aqueous solutions of pyridine, all methylpyridines and 2,6-dimethylpyridine using the forward scattering intensities measured by SANS. We have also calculated KBIs for aqueous solutions of pyridine and 3-methylpyridine using thermodynamic data taken from the literature.

The calculations of the KBIs from SANS data were performed using Eqs. 3.8, 3.9, 3.10. Due to the small values of the compressibility in Eq. 3.7, the fluctuation term S_{CC} and the Kirkwood-Buff integrals are roughly proportional to the forward scattering intensity $I_{coh}(0)$. Analyzing the contributions of the various experimental data (volumes and compressibility) it was shown that the uncertainties to the calculated KBIs are mainly determined by the uncertainty in the forward scattering intensity; they are nearly linear with it. Some error can also be introduced due to the lack of appropriate thermodynamic data on mixtures with heavy water. In these cases we used data from light water solutions, supposing that the difference cannot be very large for quantities where the isotope substitution does not produce drastic changes. These quantities are the density and the compressibility. The most critical thermodynamic data – the Gibbs free energy derived from vapor pressure measurements are not needed for calculations of the KBIs when using the values of coherent zero-angle scattering $I_{coh}(0)$.

Therefore we estimated that the uncertainty to the calculated KBIs are caused mainly by the possible errors to the coherent forward scattering. These were calculated taking into account on the error to the fit to Eq. 6.1, and assigning 10% uncertainty to the intensity values related to the absolute normalization.

Due to the availability of thermodynamic data, Kirkwood-Buff integrals could be calculated for all solutions at room temperature, and for three different temperatures in the picoline – water mixtures.

The KBIs at different temperatures in 3MP – heavy water mixtures are shown in Figure 6.1. They exhibit the usual behavior characteristic of mixtures with limited miscibility (e.g. butanol – water mixtures [59]). The most striking feature found in the 3-methylpyridine solutions is the extremely high absolute values of the KB integrals, they are by an order of magnitude larger than those in any earlier reported liquid mixture. The reason for this must be the relative closeness of this mixture to the boundary of the demixing region even at room temperature. With increasing temperature the KBIs increase and tend to infinity when the temperature approaches the demixing line and the mixture becomes partially miscible. This follows from turning into zero of the quantity D in Equations 3.11 and 3.12.

The KBIs at 25°C in the three different picoline – heavy water mixtures are shown in Figure 6.2. It can be seen that in all the three mixtures the tendency to phase

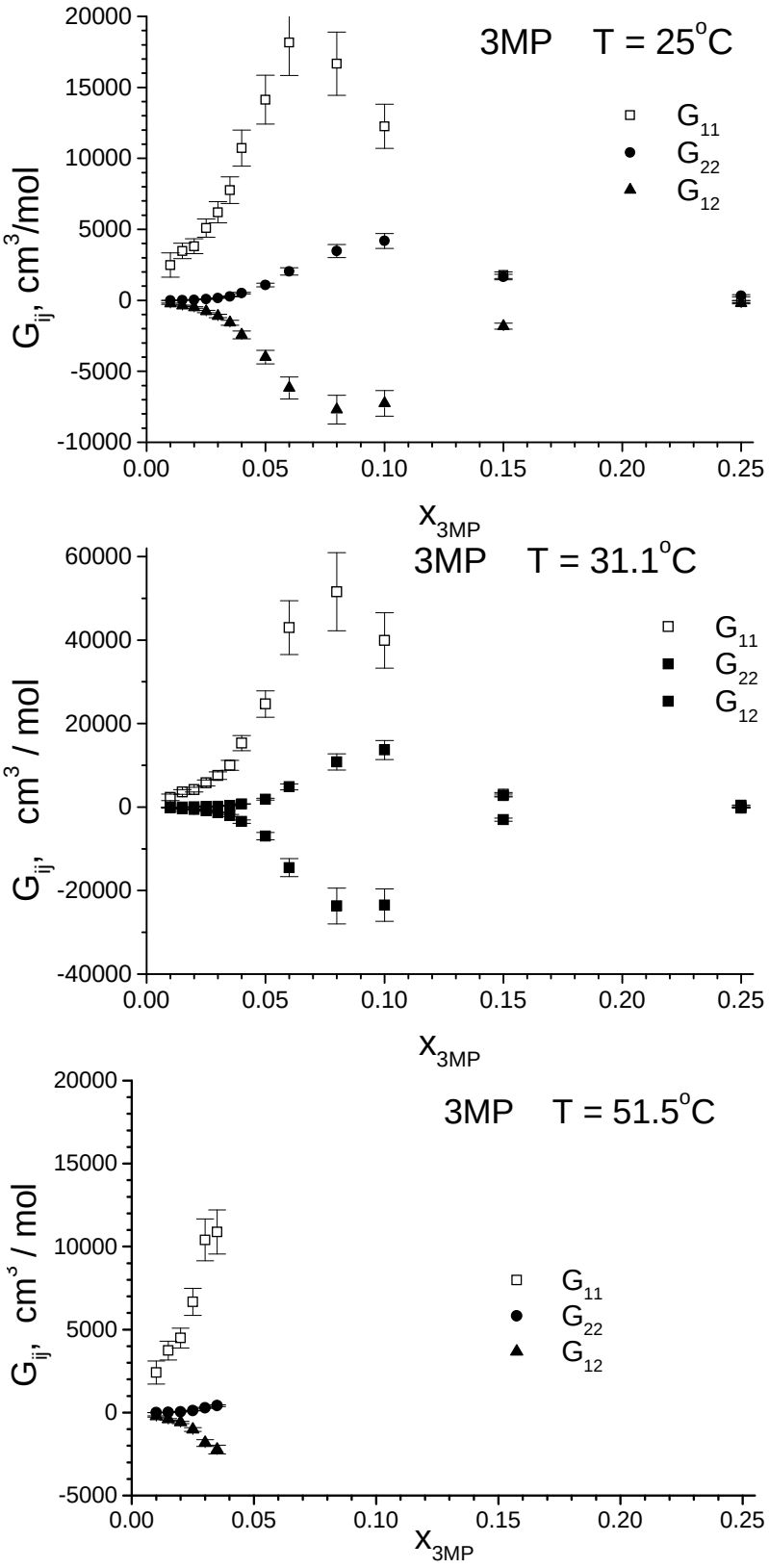

Figure 6.1.: *Kirkwood-Buff integrals for 3MP – D_2O solutions as a function of 3MP concentration X_{3MP} at different temperatures. G_{11} is the solute-solute KB integral, G_{22} is the water-water KB integral, and G_{12} is the solute-water KBI. At 51.5°C the solution demixes above $x_{3MP} = 0.03$.*

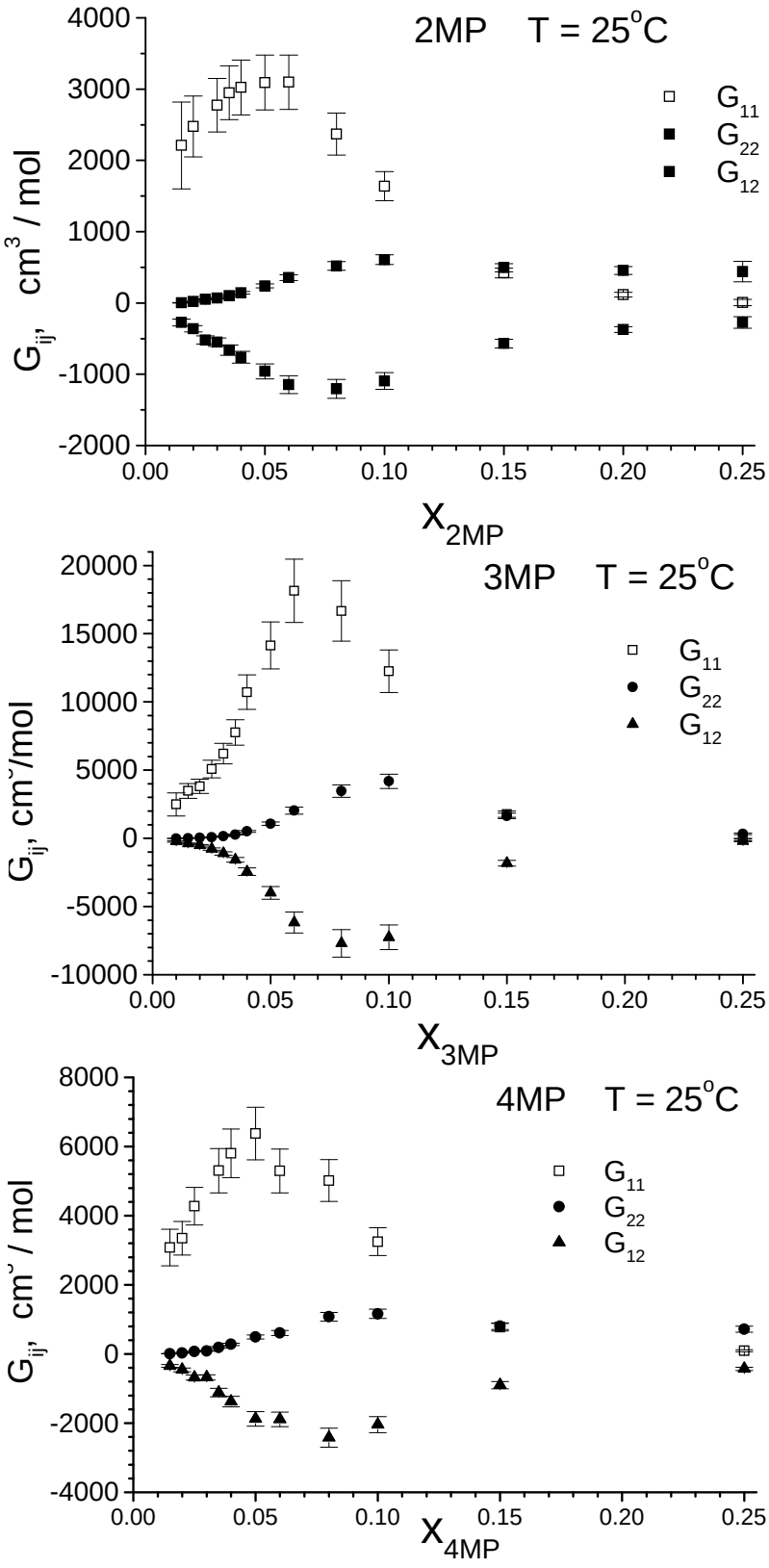

Figure 6.2.: *Kirkwood-Buff integrals for heavy water solutions of the three methylpyridines at 25°C.*

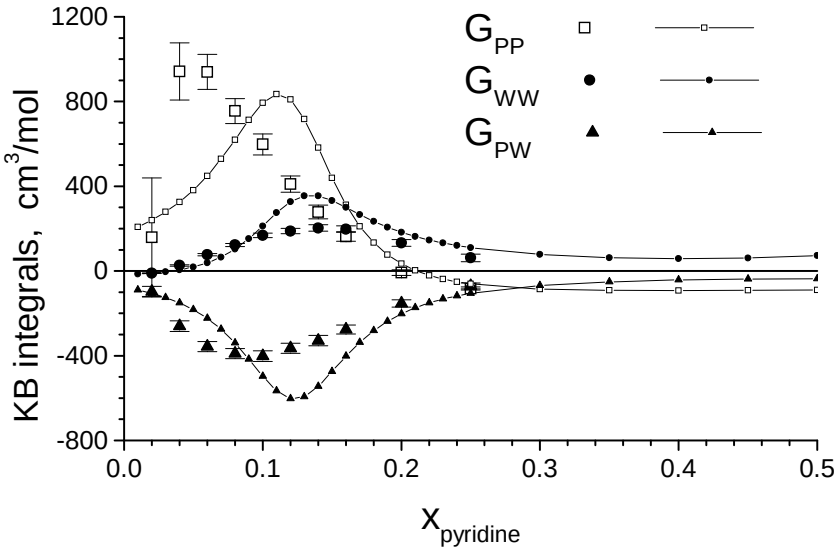

Figure 6.3.: *Kirkwood-Buff integrals for pyridine – water mixtures at 25°C. The symbols with error bars are obtained using SANS data, the lines with points are calculated from thermodynamic data.*

separation increases with rising temperature. In the case of 3MP – heavy water mixture the macroscopic phase separation has taken place before the temperature 51.5°C is reached.

Comparison between KBIs calculated from SANS and thermodynamic data

For three mixtures we compared the Kirkwood-Buff integrals obtained with SANS data (using the experimental $I_{coh}(0)$), and those calculated with the available thermodynamic data. The Kirkwood-Buff integrals for mixtures of pyridine, 3-methylpyridine and 2,6-dimethylpyridine with light water were calculated at 25°C by using Equations 3.11, 3.12, 3.14. The molar volume of the mixture and the partial molar volumes of the components were computed from the molar excess volumes calculated from the densities of the solutions [36]. For the excess Gibbs free energy of mixing the coefficients of the Redlich-Kister type equation were used which had been obtained by fitting the experimental vapor pressure data [36].

The Kirkwood-Buff integrals obtained in both cases for pyridine – water and heavy water mixtures are compared in Figure 6.3. The Kirkwood-Buff integrals for mixtures of 3MP in water calculated from thermodynamic data at 25°C are shown in Figure 6.4.

In Figure 6.4 we can see that near concentrations of 8 mol% and 18 mol% the KBIs diverge, and their signs are changed. The 3MP – H_2O mixture is known to be macroscopically homogeneous over the entire composition range, thus the divergence of the calculated KBIs should be erroneous: it can result from using erroneous thermodynamic

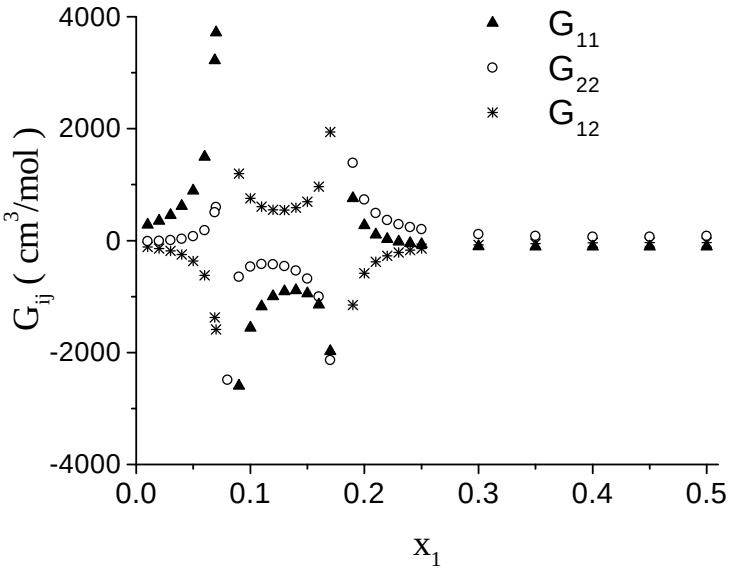

Figure 6.4.: *Kirkwood-Buff integrals for 3MP – H_2O mixtures at 25°C as a function of mole fraction of 3MP (x_1), calculated from thermodynamic data only.*

data. Examining the used equations 3.11, 3.12, 3.14 it can be noticed that the divergence of the calculated KBI values can originate from the incorrect derivatives of the excess Gibbs free energy of mixing. This is not surprising as the free energy is calculated from relatively low precision vapor-liquid equilibrium measurements, and usually only 10 – 20 data points are taken over the whole concentration range. The incorrectness of the calculated second derivatives of the free energy of mixing can be shown by computing the values of the function D defined by Equation 6.9 (same as Eq. 3.14):

$$D = 1 + x_1(1 - x_1)\frac{\partial^2 G^E/RT}{\partial x_1^2} \tag{6.9}$$

The thermodynamic stability condition for solutions is that $D > 0$ [58]. For 3MP – H_2O mixtures, in the concentration range between about 8 mol% and 18 mol% the values of D turned out to be negative, consequently, the thermodynamically inconsistent activity data lead to inaccurate KBI values. Similar result has been obtained when trying to calculate the KBIs for 2,6DMP – H_2O mixtures.

This analysis showed that the precision of the available thermodynamic data is satisfactory for those mixtures, which are far from the demixing (pyridine – water), but they cannot be used for mixtures where the deviation from the ideal behavior is very pronounced (like 3-methylpyridine – water, and dimethylpyridine – water mixtures).

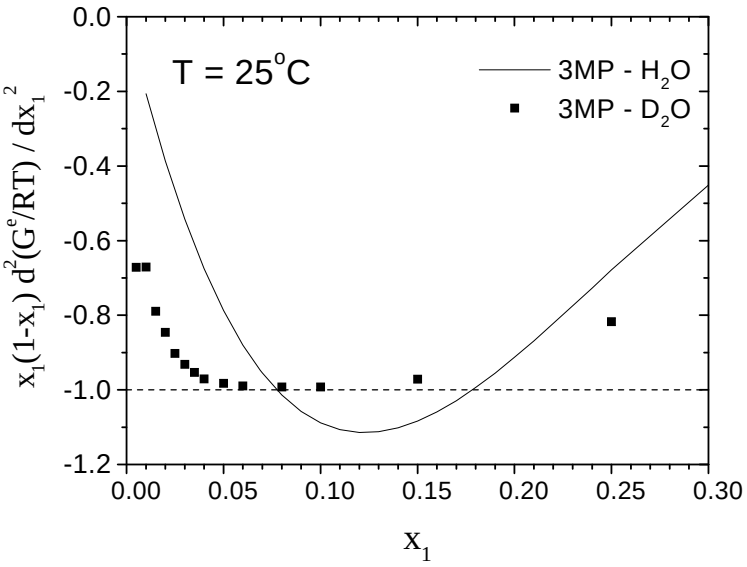

Figure 6.5.: *Closeness to phase separation in 3-picoline solutions at $T = 25°C$. Data points for 3MP – D_2O mixture are calculated using SANS data [filled squares], the full line for 3MP – H_2O mixture is calculated from thermodynamic data only. At this temperature both solutions are miscible over the whole concentration range, the values of the closeness parameter smaller than -1 are attributed to inaccurate thermodynamic data (see the text).*

6.2.2. Closeness to phase separation

The quantity

$$x_1 x_2 \left(\frac{\partial^2 G^E / RT}{\partial x_1^2} \right)_{T,P} \tag{6.10}$$

is often regarded as a parameter characterizing the *closeness to phase separation* of a binary mixture. It is equal to -1 at the critical solution points and within the miscibility gap of a partially miscible mixture while outside the miscibility gap its value should be larger than -1 [79]. It can be expressed also via the concentration fluctuations:

$$\frac{x_1 x_2}{S_{CC}(0)} - 1 \tag{6.11}$$

From this form the natural limit -1 of the quantity is seen: the average value of concentration fluctuations cannot be negative. Approaching the macroscopic phase separation, the concentration fluctuations increase up to infinity. In this case the closeness parameter reaches its limiting value -1.

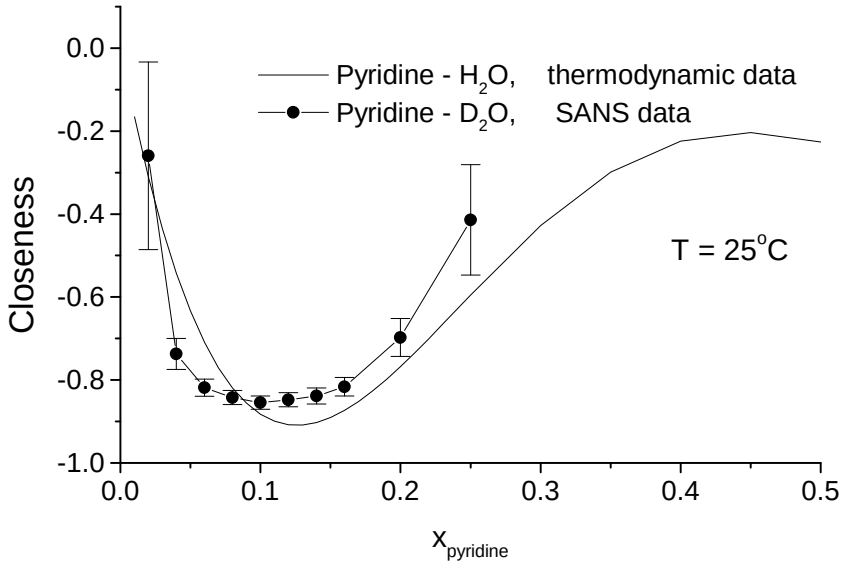

Figure 6.6.: *Closeness to phase separation in aqueous solutions of pyridine at 25°C. Points for pyridine – D_2O are calculated from SANS data [filled circles], the full line for pyridine – H_2O is calculated using thermodynamic data only.*

Figure 6.5 shows the concentration dependence of this parameter in water and heavy water solutions of 3-methylpyridine at 25°C. At this temperature both mixtures are still outside the immiscibility region (see the phase diagram, Figure 2.4). The points obtained using SANS data are seen to approach very closely the limiting value -1, at concentrations of about 8 - 10 mol% of methylpyridine. This illustrates how closely this mixture comes to the formation of two liquid phases. The 3MP – D_2O mixture is extremely close to phase separation already at room temperature, at 12°C below the lower critical solution temperature. The concentration at which the closest approach is observed is the same as the critical concentration 8.4 mol% of the LCST.

In the same figure the line is calculated for 3MP – H_2O solution at 25°C using thermodynamic data only. It can be seen that the line goes below -1, which can be only caused by the use of thermodynamically inconsistent data.

Figure 6.6 shows the concentration dependence of the closeness parameter in water and heavy water solutions of pyridine at 25°C. Comparing to the previous case we see that both the points and the line are above -0.9, such that the pyridine solutions are substantially farther from the phase separation than the 3-methylpyridine solution. The curve calculated from thermodynamic data and the points obtained using SANS data are sufficiently close to each other. Both mixtures are seen to be far enough from the phase separation. at such distance the isotope effect due to the substitution of water by heavy water is not so pronounced, as in the case of methylpyridines, so the fluctuations and the KB integrals both in water and heavy water solutions have similar magnitudes.

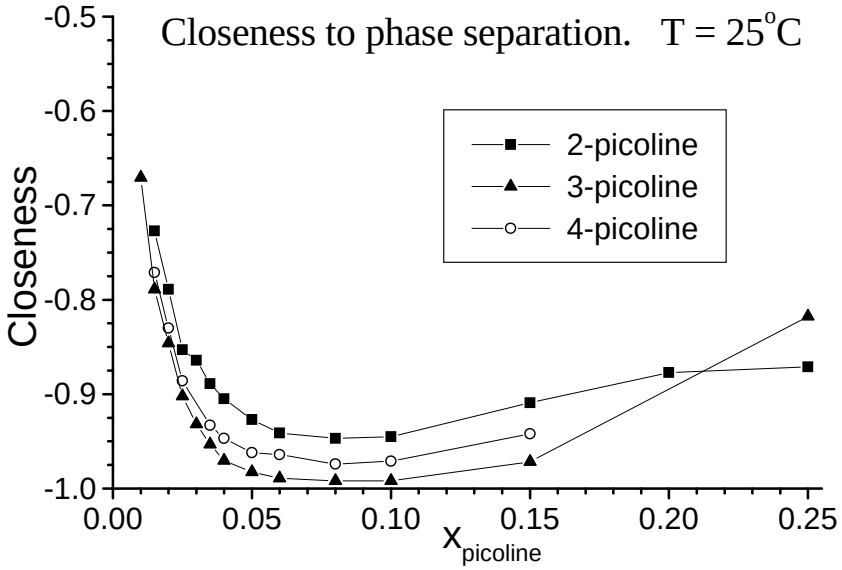

Figure 6.7.: *Closeness to phase separation in methylpyridine – heavy water solutions at $T = 25°C$.*

The corresponding curves for the pyridine – water, pyridine – heavy water mixtures at 70°C, show a minimum of -0.9 at $x_1 = 0.105$ [80]. The comparison with the present values at 25°C (-0.86 at $x_1 = 0.10$) indicates that the position and height of the minimum varies negligibly with temperature, consequently one cannot expect that this mixture undergoes a phase separation at any temperature.

In Figure 6.7 we compare the closeness to phase separation for the three methylpyridine solutions. According to the expectations the line for 3MP approaches most closely the value -1, as this mixture is closer to the phase separation than the other two, according to their phase diagrams (Figure 2.4).

It is surprising that according to the closeness curves the 4MP – heavy water mixture seems to be closer to phase separation than the 2MP – heavy water mixture, despite that 4MP mixes with heavy water in the whole concentration range. This indicates that even though 4MP – water and 4MP – heavy water mixtures are macroscopically homogeneous at all compositions and temperatures under normal conditions, a demixing region might be found by changing pressure, or eventually by deuterating the solute.

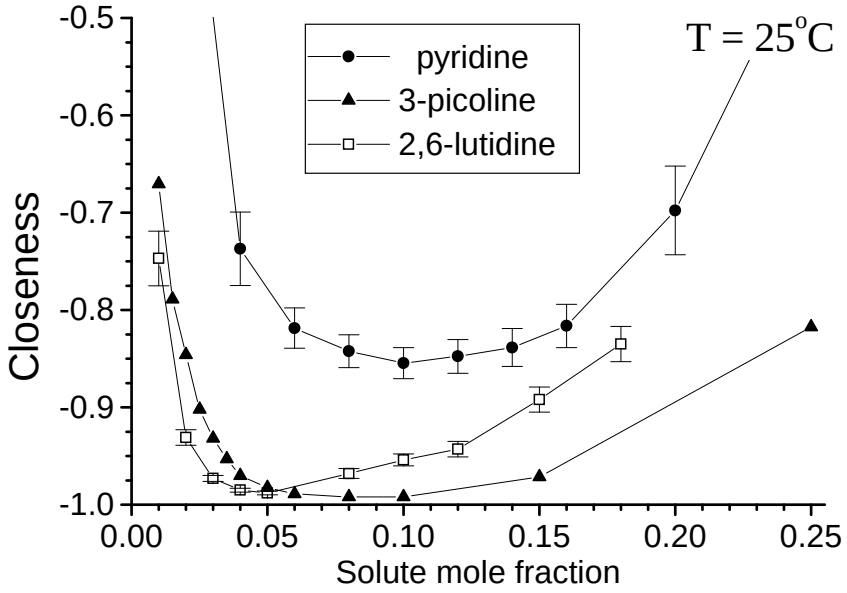

Figure 6.8.: *Closeness to phase separation in the series of pyridine – 3-methylpyridine – 2,6-dimethylpyridine aqueous solutions at $T = 25°C$ in the function of concentration. The 'Closeness' quantity is calculated by expression 6.11.*

In Figure 6.8 the behavior of the representatives of the three groups is compared at 25°C: heavy water solutions of pyridine, 3-methylpyridine and 2,6-dimethylpyridine. The curves for both 3MP and 2,6DMP are very close to the phase separation boundary, due to the closeness of these mixtures to phase separation. (The temperatures of the phase separation are 38.5°C for 3MP and 28.7°C for 2,6DMP). The pyridine – heavy water solution is far away from macroscopic phase separation.

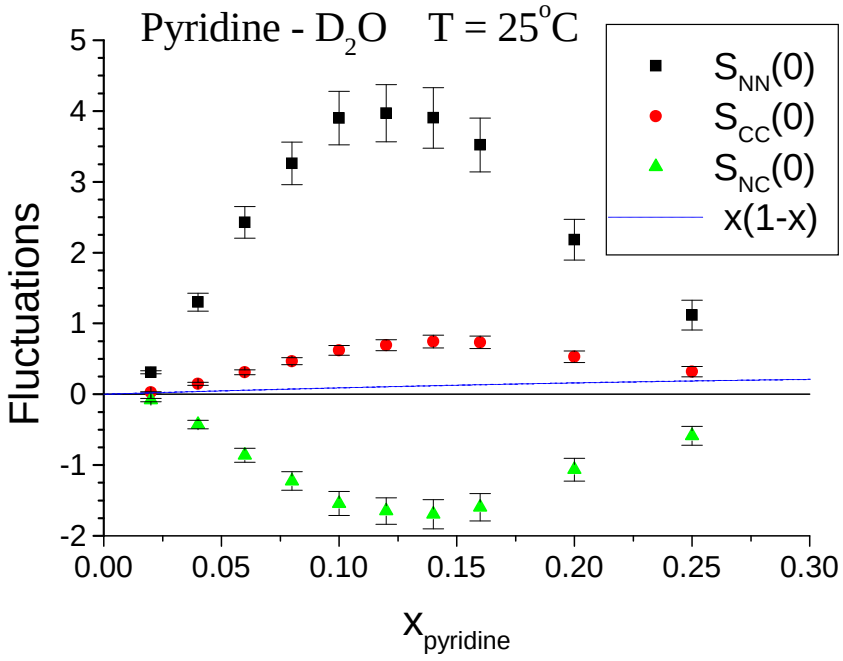

Figure 6.9.: *Fluctuations in pyridine – heavy water solutions at 25°C. The solid line is the concentration fluctuation term in ideal mixture, given by* $x(1-x)$.

6.2.3. Fluctuations

The fluctuation terms $S_{NN}(0)$, $S_{CC}(0)$, $S_{NC}(0)$ in the solutions were calculated using Equations 3.5, 3.6, 3.7.

As we can see from Equations 3.5, 3.6, only one fluctuation term is independent out of the three. The most useful for considerations is the term $S_{CC}(0)$. It is easy to demonstrate why is the concentration fluctuation term $S_{CC}(0)$ related to the particle aggregation in the mixture. The change of the concentration in a hypothetical fixed volume is caused by the random movements of the molecules in and out of the volume. If there are aggregated molecules of the same species, then a molecule, when crossing the boundary of the volume, is followed by the attached molecules. Thus the concentration inside the volume changes by a larger value than if the molecules would move independently. This leads to an increase in the magnitude of the concentration fluctuations. In an ideal mixture, the concentration fluctuation term is given by the equation $S^{id}_{CC}(0) = x(1-x)$, and reaches a maximal value of 0.25 . If the actual magnitude of the concentration fluctuations exceeds this value then there must be some kind of collective motion, or association of the same type of molecules in the mixture.

The fluctuation terms in pyridine – heavy water mixture are plotted in Fig. 6.9. The concentration fluctuation term $S_{CC}(0)$ is seen to be higher than that of ideal solution given by $x(1-x)$. In all the other solutions the behavior of the fluctuation terms is

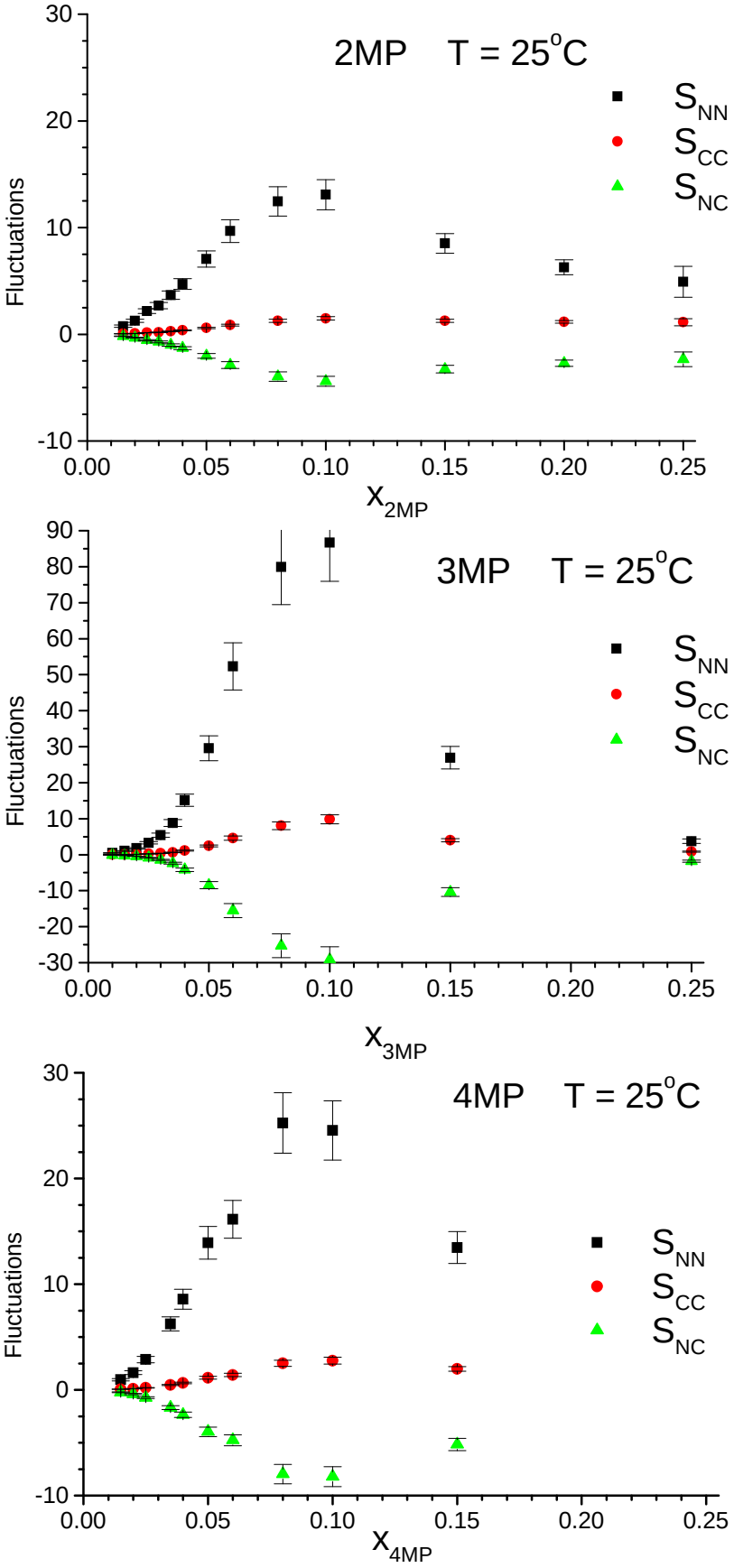

Figure 6.10.: *Fluctuations in heavy water solutions of picolines at 25° C.*

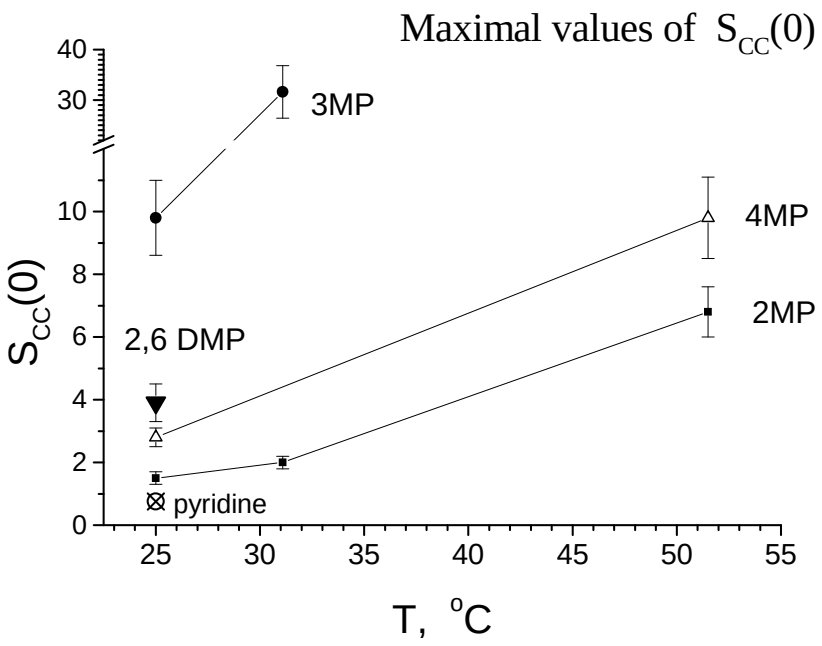

Figure 6.11.: *Maximal values of the concentration fluctuations $S_{CC}(0)$ in heavy water solutions of methyl-substituted pyridines at different temperatures.*

similar, their values are even higher than those in the pyridine solution. In Figure 6.10 they are shown for the three picoline – heavy water solutions at 25°C.

The closeness to the phase separation region is equally well reflected by the values of the concentration fluctuations, see Equation 6.11.

In Figure 6.11 we compare the maximum values of the concentration fluctuation terms $S_{CC}(0)$ in all solutions at different temperatures. It can be seen that at 25°C the fluctuations are the highest ones in the 3MP – D_2O mixture. Their value is even higher than that in the 2,6-lutidine – heavy water mixture, although both mixtures have a phase separation temperature not much above 25°C. Interestingly, according to the phase diagram (Table 5.1) the 2,6-lutidine solution seems to be closer to the phase separation with its LCST 28.7°C than the 3MP – D_2O mixture with LCST = 38.5°C. However, the higher value of the fluctuations in the 3MP – D_2O mixture shows us that the true distance from the phase separation region is actually larger for the 2,6DMP solution. This apparent discrepancy can be explained by looking at the form of the immiscibility region not only in the concentration - temperature coordinate plane, but in the whole phase diagram including also the pressure coordinate. The closeness to the immiscibility domain can be different in two and in three dimensions. Studies of the phase behavior varying the pressure could furnish more complete information about the peculiarities in the mixing behavior of these two-component mixtures.

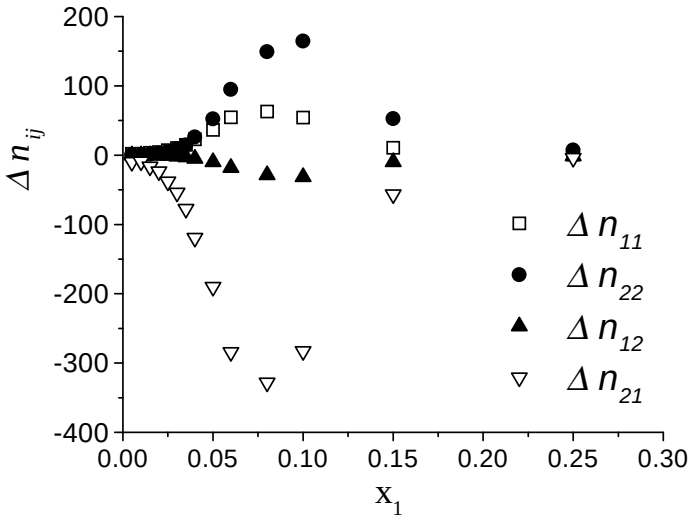

Figure 6.12.: *Excess numbers Δn_{ij} of molecules i around a central molecule j in 3MP – heavy water mixtures at 25°C. Subscript 1 refers to 3MP, 2 refers to D_2O.*

6.2.4. Excess numbers of molecules

Further parameters that characterize the structure can be derived from the Kirkwood-Buff integrals, these are the excess numbers of molecules around a central one. They are calculated using Equation 3.3. The excess numbers of molecules for 3MP – D_2O solutions at room temperature are tabulated in Table 6.4 and shown in Fig. 6.12. As can be seen the local compositions are different from the bulk ones in the concentration range $0.06 < x_1 < 0.15$, which means that in the 3MP – heavy water mixtures clustering of the molecules of the same kind occurs.

The positive Δn_{22} values, exhibiting a maximum at about $x_1 = 0.1$, indicate an enhancement of the mutual interactions of the water molecules. The values of Δn_{11}, which characterize the hydrophobic interactions between the solute molecules are also positive but much smaller than Δn_{22}. The large negative values of Δn_{21} suggest that there is a significant deficit of the water molecules in the vicinity of a methylpyridine molecule.

In all methylpyridine solutions the excess numbers show similar general behavior, as well as the fluctuation terms and the Kirkwood-Buff integrals.

Further quantitative analysis of the excess numbers can be done by comparing Δn_{ij} to the volume, in which this excess number of the molecules are to be found. It is usually called correlation volume. This volume is however not well-defined, different authors use it in different manner: one coordination shell around the central molecule, or two

Table 6.4.: *Excess numbers Δn_{ij} of molecules i around a central molecule j in 3MP – D_2O solutions. Subscript 1 refers to 3MP, 2 refers to D_2O.*

T	3MP mole fraction	Δn_{11}	Δn_{12}	Δn_{22}	Δn_{21}
25°C:	0.005	1.53	-0.040	0.209	-7.98
	0.010	1.41	-0.074	0.38	-7.31
	0.015	2.84	-0.225	1.17	-14.8
	0.020	4.05	-0.430	2.24	-21.1
	0.025	6.55	-0.875	4.56	-34.1
	0.030	9.36	-1.51	7.86	-48.8
	0.035	13.3	-2.52	13.1	-69.5
	0.04	20.5	-4.46	23.3	-107
	0.05	32.6	-8.94	46.6	-170
	0.06	48.4	-16.1	84.1	-252
	0.08	55.6	-25.2	131	-290
	0.10	48.2	-27.9	145	-251
	0.15	9.68	-8.94	46.8	-50.7
	0.25	0.64	-1.13	5.93	-3.38
31.1°C:	0.005	1.69	-0.044	0.23	-8.89
	0.010	1.31	-0.069	0.36	-6.91
	0.015	2.91	-0.23	1.22	-15.3
	0.020	4.40	-0.47	2.4	-23.1
	0.025	7.42	-0.99	5.2	-38.9
	0.030	11.3	-1.83	9.6	-59.3
	0.035	17.1	-3.25	17.1	-89.7
	0.04	29.2	-6.37	33.4	-153
	0.05	56.5	-15.6	81.8	-296
	0.06	114	-38.1	200	-599
	0.08	170	-77.8	408	-894
	0.10	155	-90.5	475	-815
	0.15	16.1	-14.9	78.5	-84.6
	0.25	0.79	-1.39	7.38	-4.19
51.5°C:	0.005	1.69	-0.046	0.245	-9.09
	0.010	1.35	-0.073	0.393	-7.25
	0.015	3.01	-0.25	1.32	-16.1
	0.020	4.69	-0.51	2.75	-25.1
	0.025	8.43	-1.15	6.21	-45.2
	0.030	15.4	-2.54	13.6	-82.2
	0.035	18.4	-3.56	19.1	-98.4

coordination shells [62], or a relatively large volume the size of which is comparable to the size of the inhomogeneity region seen in small-angle scattering experiment [61]. Moreover the volumes in a mixture can be different for the two kind of species, so two characteristic sizes are to be considered in the mixture – one that corresponds to the size of the solute aggregates, and another one is characteristic of the solvent clustering. Unfortunately, though the small-angle scattering is sensitive to the sizes of the inhomogeneities, these two quantities cannot be extracted from one measurement, neither they can be measured separately in two measurements, using contrast variation for example.

In all our measurements we were able to distinguish only one characteristic size: this size corresponds to the loss of the correlation between regions having different compositions. This quantity must be certainly related to the correlation volumes mentioned above, but the relation between the distance and the correlation volume is not known, as the form of solute-rich and solvent-rich regions are not well-defined. Moreover, it is most probably a simplified picture to speak about two different domains, in the real sample the local composition may change continuously, so the "solute-rich" and "solvent-rich" regions will not have sharp boundaries.

In spite of these difficulties, there is a strong temptation to try to determine the local surrounding of the molecules – this can be the main step which helps to relate the macroscopic properties of the solution with the microscopic, structural and energetic parameters of the molecular configuration.

6.2.5. Local concentration and correlation volume

Recently Shulgin and Ruckenstein compared experimental and theoretical results for the characteristic sizes of the solute-rich and the solvent-rich regions in aqueous alcohol solutions [61]. The experimental radii of the inhomogeneity regions were taken from SAXS measurements, the theoretical correlation volumes of the solute rich and solvent rich regions were calculated using the excess numbers (calculated from thermodynamic data) and the local compositions, which can be predicted using the so-called NRTL equations. A remarkable agreement was found for aqueous propanol and buthanol solutions, the calculated sizes of the inhomogeneity regions agreed well (to a factor of two) with the experiments over the whole concentration range. This is so far the only one such study, this way of interpretation of the correlation regions is not yet well-established.

For methylpyridine solutions the parameters needed in these equations are not known, so what we can do is to estimate the local composition in a volume around an arbitrarily chosen central molecule, knowing the excess numbers of molecules inside the volume and taking its size as given by SANS measurements.

The local concentration x_{11} of species 1 around a solute molecule 1 can be written as follows [61, 62]:

$$x_{11} = \frac{n_{11}}{n_{11} + n_{21}} = \frac{\Delta n_{11} + x_1 \rho V_1^{corr}}{\Delta n_{11} + \Delta n_{21} + \rho V_1^{corr}} \tag{6.12}$$

n_{ij} are the total numbers of molecules i in the vicinity of a molecule j. Using this equation the correlation volume V_1^{corr} around a methylpyridine molecule can be calculated from the local composition x_{11}, using the excess numbers Δn_{11}, Δn_{21}, obtained previously (section 6.2.4). This method was used in [61] for calculations of the correlation volumes in alcohol – water mixtures.

Another possibility is to calculate V_1^{corr} for different x_{11}. Then we can follow the variation of the characteristic size of the solute-rich region with the assumed local concentration of the solute in the vicinity of a solute molecule.

In order to compare the calculated cluster size with the experiment, we consider that the correlation length ξ_{exp} measured by SANS is equal to radius of the correlation volume R_{corr} . In Figure 6.13 the radii R_{corr} calculated for different x_{11} local compositions are displayed. They are plotted for all concentration values between 0.01 and 0.25 at which the measurements have been performed. The radii R_{corr} are seen to be higher for higher *local* concentrations of the solute.

The experimental correlation length ξ_{exp} is also plotted. It can be seen that the calculated and measured sizes are close to each other if the local composition in the solute-rich region is of about 0.8 - 0.95 .

Thus we conclude that for the measured system, the experimental forward scattering intensities and the inhomogeneity sizes correspond to such local compositions in the solute-rich domains, which suggest that they should consist mainly of solute (methylpyridine) molecules.

The precision of this calculation depends basically on two assumptions – that the sizes of the solute-rich and the solvent-rich regions are not far from each other and contribute to the measured average parameter – correlation length ξ_{exp}. Rigorously the sizes of these regions are equal only around the critical composition, at which, increasing the temperature, the mixture separates into two phases with equal sizes. Shulgin and Ruckenstein analyzed the local correlation volumes for the solute and the solvent in aqueous alcohol solutions [61] and found that the sizes of the solute-rich and the solvent-rich domains are close to each other, the maximal difference was of a factor of two in favour of the size of the water-rich region.

The second approximation is the correspondence between the ξ_{exp} and the size or the radius of the domains. This equality has been used in several works and is based on the fact that the beginning of the scattering curve corresponds to some characteristic size in the system. The parameters in the different models, – radius of sphere, gyration radius, Debye correlation length, – can be transformed to each other by a multiplicative factor, which is in between 0.5 and 2.

We assume that according to these considerations we have an uncertainty in the size of a factor of two, so the calculated local density can respectively vary within a similar interval. Even allowing for that, we find that in our methylpyridine – water solutions the solute-rich and solvent-rich regions contain predominantly solute and solvent molecules, respectively.

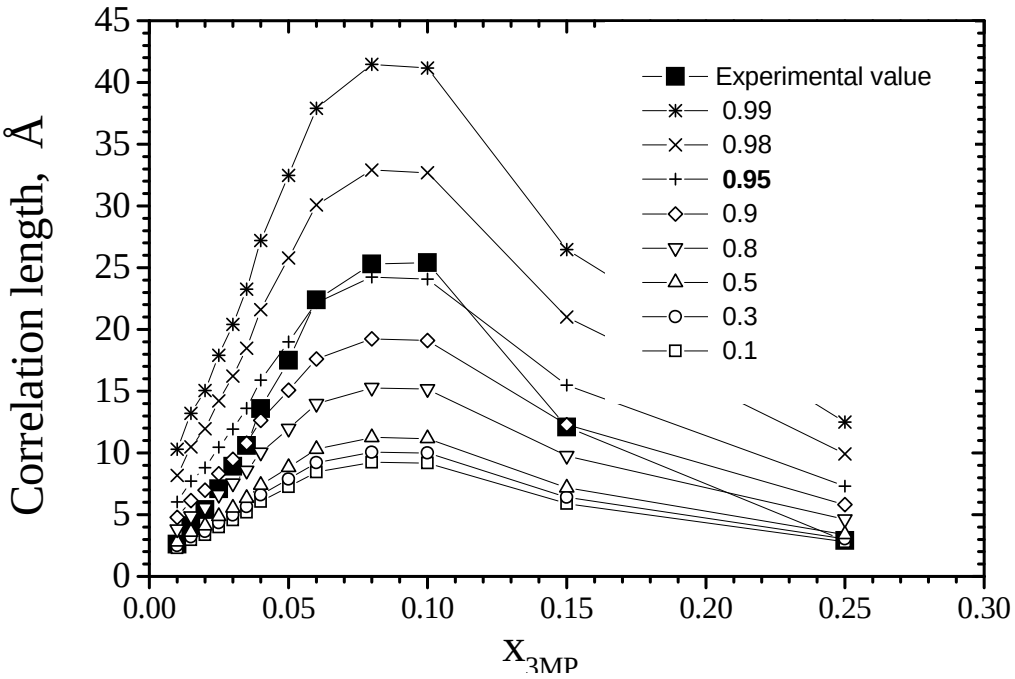

Figure 6.13.: *Size of the correlation volume in the 3MP – heavy water solution at 25°C. The curves with lines and symbols are calculated for different possible local compositions in the solute-rich region. The big symbols are the measured correlation lengths* ξ_{exp}.

This can be suggested also intuitively looking at the high value of the excess numbers of molecules of the same species Δn_{ii}.

7. QENS studies

7.1. Experiments

The quasielastic neutron scattering (QENS) experiments have been performed on the MIBEMOL time-of-flight neutron spectrometer at the reactor Orphée of LLB. The characteristics of this instrument are well suitable for studying dynamic behavior of water and organic molecules in aqueous solutions. To measure the dynamics of various species the energy window of the spectrometer has to be adjusted in order to include the quasielastic broadening due to the motions of the nuclei in the system, taking into account the instrumental resolution necessary for resolving the line broadening caused by the given motion. The energy-window and the q-range covered in a time-of-flight measurement can be varied by changing the incoming wavelength. This is achieved by varying the rotation speeds and adjusting the phases of the choppers. The MIBEMOL spectrometer is optimized for measurements of energy transfers between 0.01 and 10 meV. The characteristic parameters for the most often used configurations of the MIBEMOL spectrometer are collected in Table 7.1.

In our measurements the expected slowest motion was the diffusive motion of the methylpyridine. The high energy resolution of 28 μeV was adequate to measure the methylpyridine diffusion, and it was used also for measuring the diffusive motion of the water in the solution, which is only 2 - 3 times faster than the translational motion of the methylpyridine. Another configuration was necessary when looking at faster motions in the sample, like the rotational motion of the water molecules. This motion leads to energy transfer of the scattered neutron up to one meV, the corresponding energy window is covered by using 6Å neutrons, for which the energy resolution is 96 μeV. For each energy window (and resolution) the accessible momentum transfer range is determined by the angular positions of the detectors, which cover an angular range of 150°. To determine the diffusion coefficients using the most common models like continuous diffusion or jump-diffusion, the appropriate q-range is be safely covered in these configurations.

We used H-D isotopic substitution in order to separate the motion of the two species. This means that fully deuterated 3MP (97% deuteration, Eurisotop, France) was dissolved in distilled water, and normal 3MP was dissolved in 99.9% heavy water.

The samples were filled in cylindrical sample holders made of aluminium. Their thicknesses were chosen so as to reach more than 90% transmission for each sample (as calculated from the density of protons in the liquid). That is why for different solutions

Table 7.1.: *Characteristic parameters for different configurations of the MIBEMOL spectrometer. Mean wavelength λ_0, energy resolution (FWHM), maximal observation time t_{max}, and the accessible momentum transfer range.*

λ_0, Å	Resolution, μeV	t_{max}, ps	q_{min}, Å^{-1}	q_{max}, Å^{-1}
4	446	3	0.693	2.929
6	96	14	0.462	1.953
9	28	47	0.308	1.302
11	8	82	0.149	1.073

different sample thicknesses were used, between 0.2 and 0.6 mm. This choice was made in order to avoid corrections for multiple scattering. The high transmission means also that the measurement is "not efficient" as most of the incoming neutrons just pass the sample without scattering. To achieve sufficient statistics the typical data collection times were not less than 8 hours for each sample at each configuration.

All measurements were performed at temperature T = 25°C, at which the solutions are macroscopically homogeneous over the whole concentration range. We used three characteristic concentrations: 2, 8.4 and 25 mol% 3MP in water. Previous SANS measurements indicated long-range composition fluctuations in the 2 and 8.4 mol% solutions, while the 25 mol% 3MP the solution is nearly homogeneous at microscopic scale also. In the 8.4 mol% solution, the fluctuations have the maximum extension, this is the critical composition of the 3MP – D_2O mixture at the lower phase separation point (see also the phase diagram, Figure 2.4).

7.2. Data analysis

At the medium resolution of 96μeV we can detect contributions from two types of motions: a translational diffusion and a rotational diffusion of the water protons. The scattering function $S^{model}(q,\omega)$ for this case can be written as follows:

$$S^{model}(q,\omega) = e^{-\frac{q^2\langle u^2\rangle}{3}}\left(j_0^2(qa)\frac{1}{\pi}\frac{\Gamma_{trans}}{\omega^2+\Gamma_{trans}^2} + 3j_1^2(qa)\frac{1}{\pi}\frac{\Gamma_{rot}+\Gamma_{trans}}{\omega^2+(\Gamma_{rot}+\Gamma_{trans})^2}\right) \quad (7.1)$$

The first exponential term is the Debye-Waller factor, which stands for the vibrational part of the dynamic structure factor. The $\langle u^2\rangle$ is the mean square amplitude of vibrations of all protons in the sample. The two Lorentzian terms come from the translational and rotational parts of the structure factor, their widths Γ_{trans} and Γ_{rot} are proportional to the translational and rotational diffusion coefficients, respectively. The $j_0(qa)$ and $j_1(qa)$

are spherical Bessel functions; a is the radius of the water molecule, to which the proton motion is confined, interpreted as the O-H distance (0.98Å).

At the high-resolution of 28μeV only the first term is seen, which originates from the translational diffusive motion. The second, more wide Lorentzian cannot be distinguished from the background. We used these model functions for fitting the experimental spectra.

The data analysis was performed using the standard procedures developed at LLB. The intensities measured with the large set of detectors were grouped to points of nearly equal momentum transfer. At each point the time-of-flight spectrum was fitted by one Lorentzian or a sum of two Lorentzian components convoluted with the instrumental resolution function $R(q,\omega)$, and a background term was added to correct for the contribution of inelastic processes:

$$S^{fitting}(q,\omega) = A(q)\left(S^{model}(q,\omega) \otimes R(q,\omega)\right) + B(q,\omega) \tag{7.2}$$

The $A(q)$ term accounts for the Debye-Waller factor and for absolute normalization, from its q-dependence the mean square displacement of the proton vibrations can be derived. The Bessel function prefactors in Eq. 7.1 are replaced by the amplitudes of the Lorentzians. The $B(q,\omega)$ is a background term, linear in the time-of-flight channel numbers. It accounts for the weak inelastic contribution in the quasielastic region of the spectra.

7.3. Results

7.3.1. Motion of the water

High resolution measurements

The line broadening in the deuterated 3MP – H_2O solutions measured at high resolution 28μeV (λ = 9 Å) are shown in Figure 7.2.

The dependence of the Lorentzian linewidth in function of q^2 can be approximated by a straight line only in the small-q part of the momentum transfer range, this indicates that for long distances the water motion is seen as being diffusive. The deviation of the data points from the straight line at higher q values indicate that at shorter distances more subtle effects in the proton motion become visible, this is the result of the influence of interatomic interactions (like hydrogen bonds) between the scattering nuclei. For water and other hydrogen-bonded liquids, these effects are well described as temporary localisation of protons forming hydrogen bonds. We used the conventional jump diffusion model (Eq. 4.19) to obtain the values of the diffusion coefficient D_{trans} and the residence time τ_0 of the protons (Table 7.2).

The diffusion coefficient of water in the solution decreases, when the solute concentration increases.

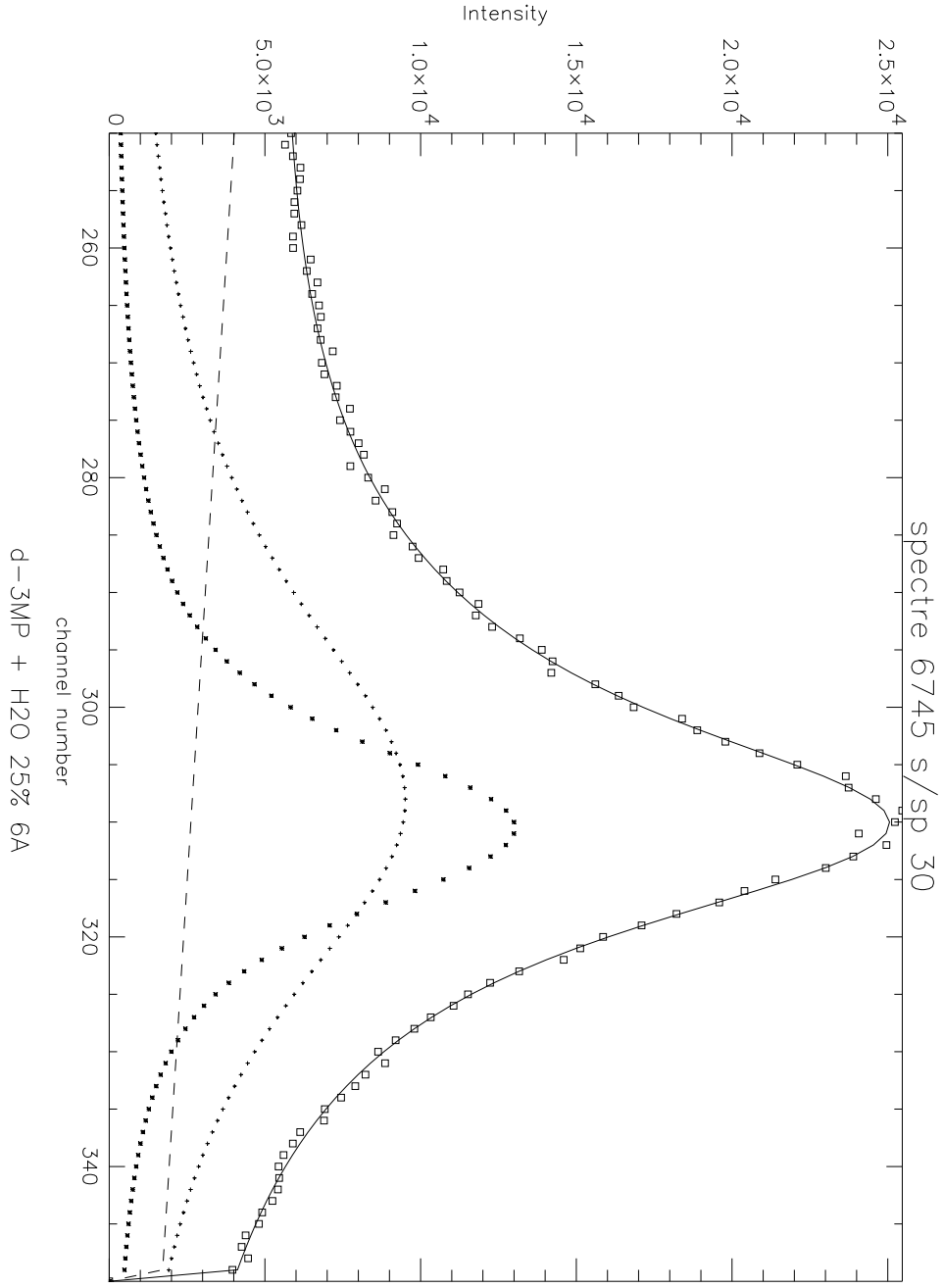

Figure 7.1.: *QENS spectrum of the 25 mol% solution of deuterated 3-methylpyridine in H_2O, measured with 96μeV resolution at $q = 0.46\ ^{-1}$. The full line is the fit to Eq. 7.2, the dotted lines are the components of rotational and translational diffusion. The short dashed line is the background.*

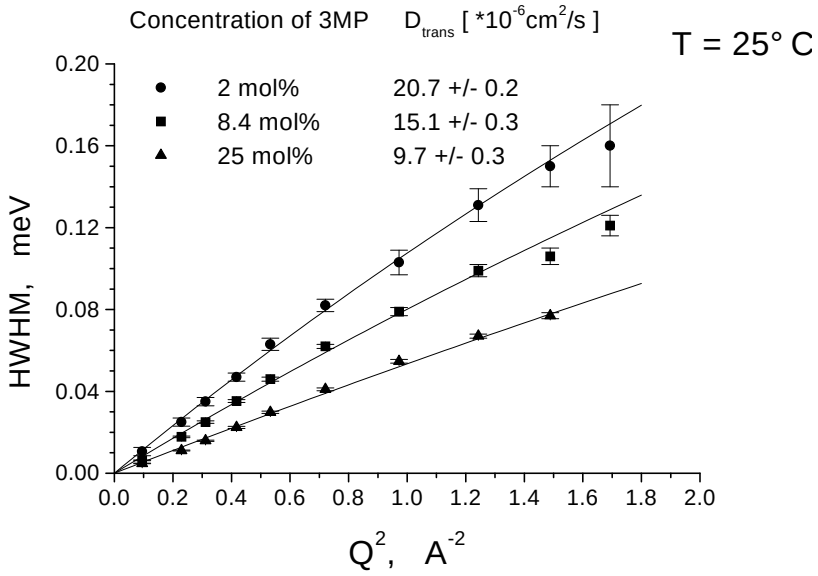

Figure 7.2.: *Quasielastic linewidths obtained from high energy resolution spectra ($\lambda = 9\AA$) in H_2O – C_6D_7N mixtures. The lines are fits using the jump diffusion model.*

Medium resolution measurements

At the medium resolution the wide energy window allows one to detect the relatively fast diffusional motion of the water protons, which is usually interpreted as the rotational motion of the proton in the water molecule. The slower translational diffusive motion of the water is still visible at this resolution, so both types of motions contribute to the quasielastic line broadening. The spectrum measured with $\lambda = 6$ Å at $q = 0.46$ Å^{-1} is shown in Figure 7.1, together with the different components of the fitted model function.

In order to extract the corresponding parameters – the linewidths and the amplitudes of the Lorentzians (Eq. 7.1), one can use several ways to fit the spectra to the model function. When the translational diffusion of the water protons is already known (for example measured at better resolution), then the width of the narrower Lorentzian can be fixed to the previously found values, and only one width parameter is let free in the fitting procedure. This procedure allows one to avoid the interplay between the two Lorentzians, which can sometimes result in erroneous fit if the two linewidths do not differ substantially.

In our measurements we followed a less safe procedure, by letting free all the parameters of the two Lorentzians. Together with the two parameters of the background we fitted six parameters to the measured spectra at each q point. The quality of the data proved to be sufficiently high so the two linewidths could be firmly distinguished by the fitting procedure for all d-3MP – H_2O samples. The broadening of the narrower

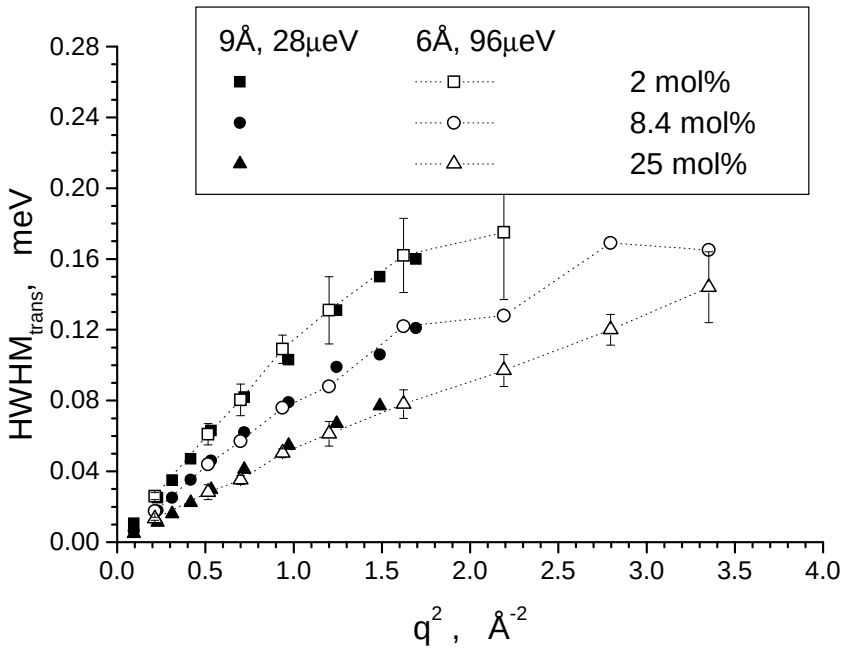

Figure 7.3.: *Linewidths of the water translational component as obtained independently from the high resolution, $\lambda = 6$ Å and the medium resolution, $\lambda = 9$ Å measurements. The filled symbols are obtained by fitting the high resolution spectra with a single translational Lorentzian function. The open symbols with error bars are the results of the fitting of the medium resolution spectra by two Lorentzians.*

Lorentzian, which describes the translational diffusion, was similar to that found in the high resolution measurement. They are shown together in Figure 7.3.

The only exception was for the case of the dilute sample, containing 2 mol% deuterated methylpyridine. In this sample the water diffusion coefficient is not substantially lower than that for pure water. At higher q values the line broadening due to translational diffusion becomes comparable with the rotational broadening, which is usually 0.2-0.3 meV (HWHM) (see also Figure 7.4). Therefore for higher q values the unconstrained fit with two Lorentzians was not possible, so in Figures 7.3, 7.4 there are no data points plotted above 2.5 Å^{-2} for the 2 mol% sample.

The values of the rotational line broadening are shown in Figure 7.4. They are seen to be constant over the measured q-range, but the large error bars do not permit to determine precisely their values. This q-independent linewidth proves the localized character of the motion. A small increase in the linewidth with solute concentration can be inferred if averaging linewidths at all measured q values, however due to the large error bars it is still possible that there is no real change with concentration. The average linewidths are shown in Table 7.2. From the line broadening the rotation relaxation times τ_1 can be

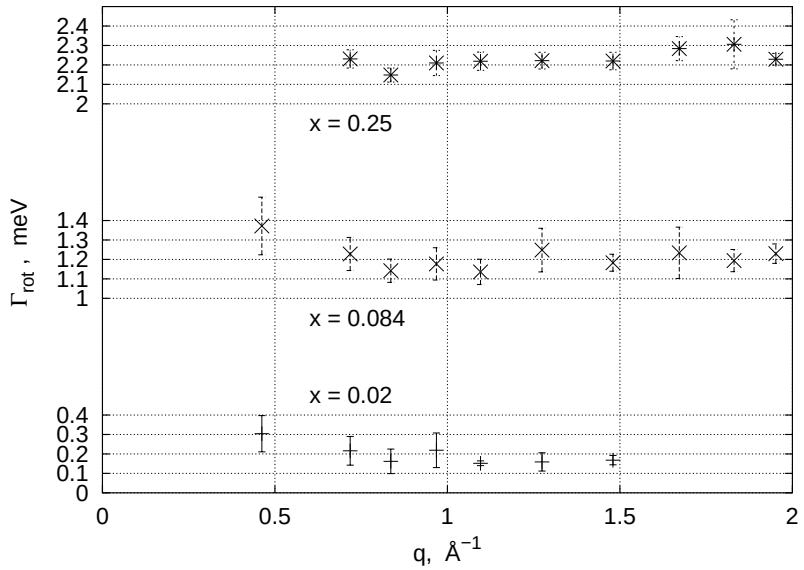

Figure 7.4.: *Linewidths of the water rotational component obtained from the low energy resolution spectra (λ = 6 Å) in H_2O – C_6D_7N mixtures. The mole fractions of 3MP are indicated. The data points for 8.4 mol% and 25 mol% solutions are shifted up by 1 and 2 meV, respectively. The average values of the linewidths are collected in Table 7.2.*

Table 7.2.: *Translational self-diffusion coefficients D_{trans} of water and of 3-methylpyridine as determined from the high resolution measurements. The residence times τ_0 and rotational linewidths Γ_{rot} are obtained from the medium resolution measurements.*

X_{3MP}	D_{trans}^{water} (10^{-6} cm^2/s)	D_{trans}^{3MP} (10^{-6} cm^2/s)	τ_0 (ps)	Γ_{rot} (meV)
0.02	20.7 ± 0.2	11.3	1.1 ± 0.2	0.16
0.084	15.1 ± 0.3	8.6	1.4 ± 0.3	0.19
0.25	9.7 ± 0.3	8.4	1.6 ± 0.3	0.23

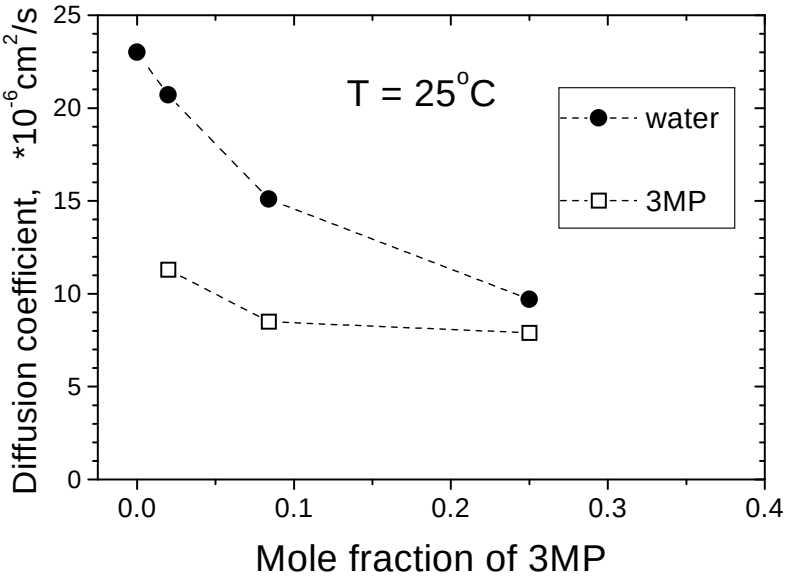

Figure 7.5.: *Self-diffusion coefficients of H_2O and 3MP in the mixtures at room temperature. The value for pure light water is taken from [84].*

obtained, which are usually attributed to the hydrogen-bond lifetime. They are found to be about 1 ps in the methylpyridine solutions.

7.3.2. Motion of the methylpyridine

The line broadening of the high-resolution spectra in the ordinary methylpyridine – heavy water solutions was modeled by Eq. 7.1, with only one Lorentzian corresponding to translational motion. The resulting line broadening was fitted by the simplest diffusion law valid for a continuous diffusion (Eq. 4.16). The resulting diffusion coefficients are shown in Figure 7.5.

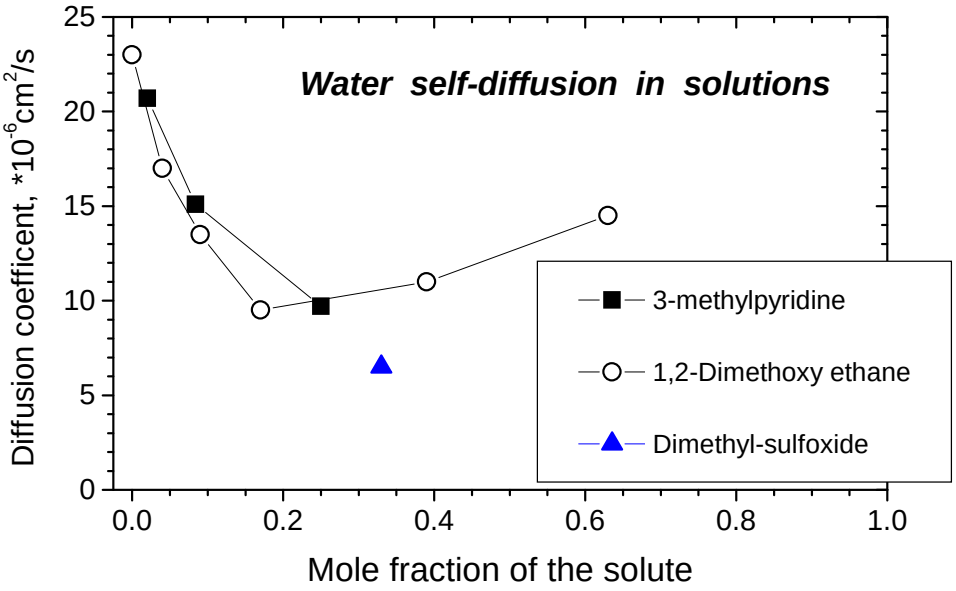

Figure 7.6.: *Self-diffusion coefficients of H_2O in solutions with various organic solutes. Results of QENS measurements on methylpyridine, dimethyl-sulfoxide [82], and 1,2-dimethoxy ethane [84] solutions.*

7.4. Analysis of the water dynamics

In order to have a better understanding of the processes in the mixture, it can be useful to compare the motions of the two species which occur at the same time scale, so that a possible coupling between them can be elucidated. In Figure 7.5 we compare the obtained diffusion coefficients of the solute and of the solvent water in the aqueous solutions of 3MP. It is seen that with increasing the solute concentration the diffusivities of both components decrease.

A remarkable point is that at higher concentrations of methylpyridine the diffusion coefficient of water gets close to that of the solute. We should keep in mind that these self-diffusion coefficients are measured in different solutions (because of the isotope substitution), so we cannot get exactly the diffusivities of both species in the same sample. But assuming that the isotope substitution does not change substantially the behavior at room temperature (far from the phase separation region), we can say that there is a visible tendency of the diffusivities of the two species to become similar at higher concentrations.

Many aqueous solutions of hydrophobic molecules show similar behavior: decrease of the water diffusion coefficient with increasing solute concentration. This is the case for example in aqueous solutions of tetramethylurea [83], of 1,2-dimethoxy ethane [84], or of 1-propanol [85]. In Figure 7.6 we compare the water diffusion coefficients as obtained by QENS in different aqueous solutions of organic molecules.

Table 7.3.: *Results of analysis of the average slowing down of the water motion assuming two populations of water in the 3MP solutions. P is the ratio of the hydration water to the total amount of water, as obtained from Equation 7.3. $N_{hydr.water}/N_{3MP}$ is the ratio of the slow water molecules to the number of the 3MP molecules.*

X_{3MP}	P	$N_{hydr.water}/N_{3MP}$
0	0	–
0.02	0.08	3.9
0.084	0.38	4.1
0.25	1	–

In the more dilute solutions, the observed diffusion coefficients of the water represent an average for all water molecules having different environment: surrounded by water only or attached to the solute molecules with or without hydrogen bonding. The proper way to account for this in the data evaluation would be to describe the water diffusion with more than one Lorentzian function. Attempts to perform non-constrained fitting of the high resolution spectra with two translational relaxation times, without fixing the widths or the ratio of the two Lorentzians were not successful.

A simple way to account for the presence of water molecules having different dynamics is to assume that two populations of water are present in the solution: one part of water behaves like bulk water, the other part is influenced by the solute molecules and has therefore slower dynamics [86, 87]. In this approximation the measured average self-diffusion coefficient consists of the contributions of the slow or hydration water $D^{hydration}$ and the bulk water D^{bulk}, the proportion between them is expressed by a parameter P:

$$\frac{1}{D_s} = (1-P)\frac{1}{D^{bulk}} + P\frac{1}{D^{hydration}} \tag{7.3}$$

where D_s is the measured average self-diffusion coefficient and P is the fraction of the slow water to all water molecules. The slow water molecules are located in the hydration sphere of the solute, thus their diffusion coefficient can be close to the diffusion coefficient of methylpyridine.

The most concentrated solution that we measured contained three water molecules for each methylpyridine molecule. Taking into account the large size of methylpyridine, it is reasonable to assume that there is no free water in this solution, i. e. all water is in contact with solute. Thus the water diffusion coefficient measured in the 25 mol% solution can be regarded to be similar to the diffusivity of the hydration water in the more dilute samples. Substituting into Equation 7.3 the diffusion coefficients of pure water ($23 * 10^{-6} cm^2/s$) and that found in the concentrated mixture ($9.7 * 10^{-6} cm^2/s$) we

obtain the fractions of the hydration water in the 2 mol% and in the 8.4 mol% solutions: they are 0.08 and 0.38, respectively. The resulting numbers are shown in Table 7.3.

The apparent increase of the bound water fraction with increasing solute concentration is the consequence of the mathematical form of the Equation 7.3. A more interesting quantity is the ratio of the bound water molecules to the number of the solute molecules. In the 2 mol% solution this ratio equals to 3.9, in the 8.4% solution – to 4.1 (Table 7.3).

It is remarkable that they are similar to each other. If the situation is the same in the even more dilute solutions, than this number can be interpreted as the average number of water molecules that are somehow bonded to a single methylpyridine molecule, they can be attached for example by the strong H-bond to the nitrogen atom of the ring.

We know that the methylpyridine solutions are not homogeneous, but there exist zones rich in water and rich in solute. As most of the solute molecules are accumulated in the solute-rich zones, the obtained quantity $N_{hydr.water}/N_{3MP}$ shows the composition of the solute-rich zone: this is an aggregate consisting of several methylpyridine molecules, and four times more water molecules.

We can notice the difference in the composition of the solute-rich clusters, as seen by small-angle scattering and by quasielastic neutron scattering. It can be understood taking into account, that the SANS measurement gives the size and the composition of the cluster, in which the composition (the contrast) differs from that of the surrounding solution. If the cluster is compact, then those water molecules, which are on the outer surface of the cluster are not visible by SANS, while dynamically they still can be attached to the solute-rich clusters.

8. NMR studies

8.1. Experiments

^{1}H NMR experiments on aqueous solutions of 3-methylpyridine have been performed in collaboration with M. Bokor at the KFKI, Budapest. The concentrations used were the same as those for the QENS experiments: 2, 8.4 and 25 mol% methylpyridine in water and in heavy water. The measurements were performed over a temperature range 250 - 350 K. The proton spin-lattice relaxation rates ^{1}H R_1 were measured on a Bruker SXP 4-100 spectrometer at $\nu_0 = 86.68$ MHz by using inversion recovery method. The stability of the frequency and magnetic field was better than $\pm 1 \times 10^{-6}$. The temperature was controlled with precision better than 1 K by using nitrogen gas flow.

For all samples and at all temperatures the recovery of magnetization was found to exhibit a single exponential behavior, and the relaxation rate was determined by least squares fitting.

8.2. Results

The relaxation rates R_1 measured in the liquid phase of the six samples are shown in Figure 8.1. Above 310 K all solutions show an Arrhenius type behavior, with the possible exception of the data for the 8.4 mol% 3MP – D_2O sample, for which the points scatter around the straight line. Activation energies in the solutions were determined by applying the Arrhenius law (Table 8.1).

Table 8.1.: *Activation energies of the methyl group rotation (E_a) in 3MP – H_2O and D_2O solutions, obtained from ^{1}H spin-lattice relaxation rate data at $T > 310$K.*

X_{3MP}	E_a (kJ/mol)	
	3MP–H_2O	3MP–D_2O
0.02	17.8 ± 0.2	18.3 ± 0.4
0.084	18.3 ± 0.6	20.0 ± 1.2
0.25	19.1 ± 0.5	18.7 ± 0.2

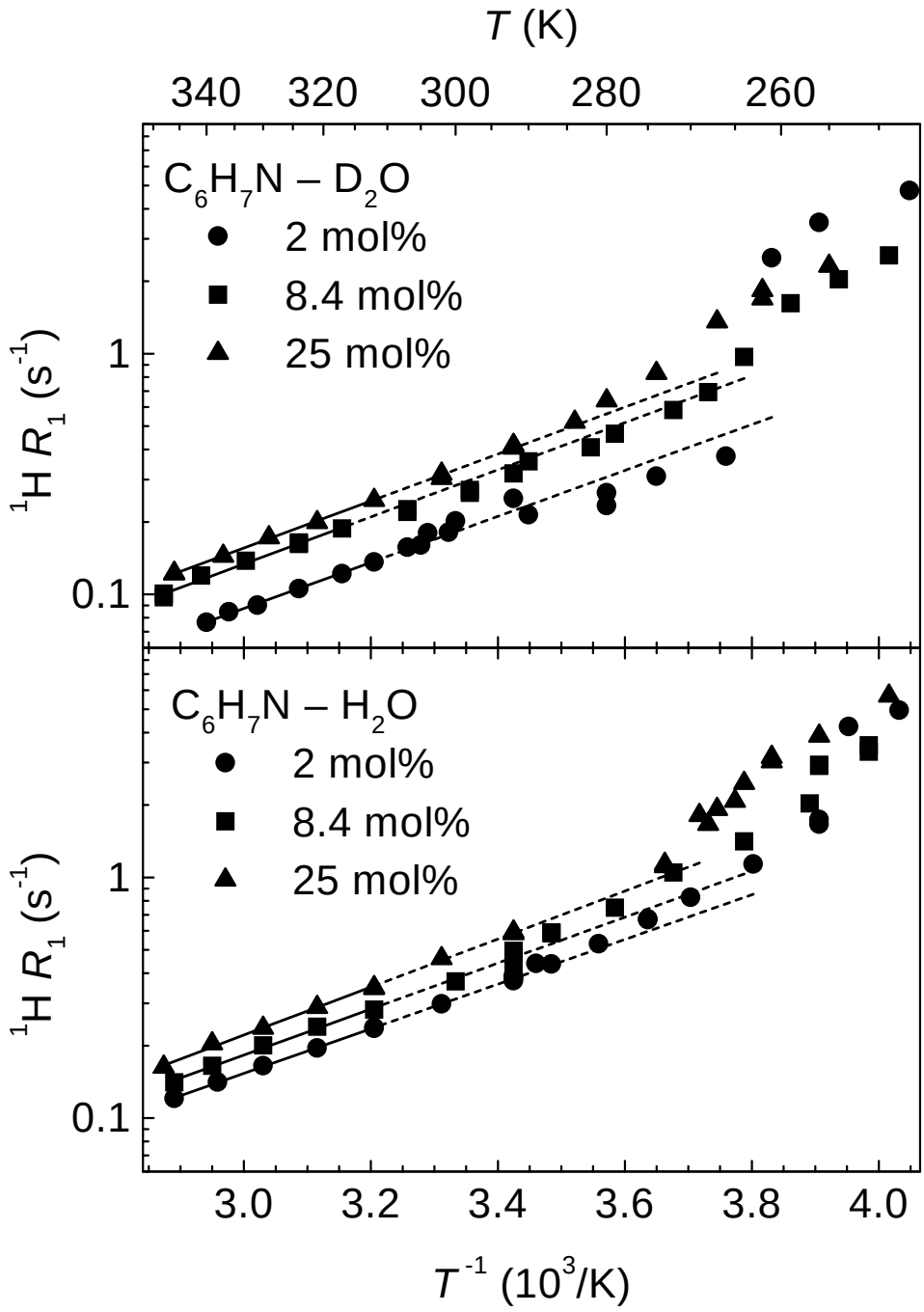

Figure 8.1.: *^1H spin-lattice relaxation rates in 3MP – D_2O (upper graph) and 3MP – H_2O (lower graph) solutions. Size of symbols are of about the measurement error. Solid lines are fits used for activation energy determination using data at $T > 310K$; dashed lines are extrapolation to lower temperature.*

In the heavy water solution there are two types of hydrogen atoms which can contribute to the NMR signal: the protons of the pyridine ring and the protons of the methyl group. It is possible to distinguish their contribution to the observed NMR signal. The motions of the ring protons are substantially slower than the rotational motions of the methyl group protons. Hence the observed activation energy can be attributed to the methyl group rotation in the picoline.

In the light water solutions both the reorientational motions of the methyl group and the mobility of the hydrogen of water contribute to the measured relaxation. As the spectra did not show the presence of two relaxation processes having different times, it is more difficult to attribute the observed relaxation to one of the two species. Most probably both water and the methyl group show nearly similar relaxation rate, which becomes lower with increasing the picoline concentration (Figure 8.1, lower part).

The activation energies (E_a) observed in light and heavy water solutions containing 2 and 25 mol% picoline are found to be equal within the errors of measurement. Thus the activation energies obtained both in the light water and heavy water solutions can be considered as being characteristic of the reorientational behavior of the methyl group of 3MP molecules. It is worth noting that the activation energy of pure water, equal to 18.3 kJ/mol at 25°C [90], is very close to the observed activation energies of the methyl group reorientation in the solution.

The $x_1 = 8.4$ mol% solution of 3MP in heavy water undergoes a phase separation in the measured temperature range (above 38.5°C, [27]) so the fitted E_a can represent only an average for the motions in the two phases. This can be seen on the high uncertainty of the calculated activation energy E_a, as well as on the larger deviations of the $R_1(1/T)$ data from linear behavior (see Fig. 8.1).

The activation energies (Table 8.1) are similar at different concentrations, however a slightly increasing trend with increasing 3MP concentration cannot be excluded. The precision of the present NMR data are not sufficient to prove such behavior, though the possible hindering of the methyl group rotation can be related to the slowing down of all motions in the more concentrated solutions.

Part IV.

Summary and perspectives

9. Summary of the results

We carried out experimental structural and dynamic studies of aqueous solutions of methyl-substituted pyridines. The work has been stimulated by the increasing demand to understand the behavior of liquid mixtures in general, the relations between the mixing behavior and the structure of the components and the structure of the mixture at atomic or molecular level.

The aqueous solutions of methylpyridines are a particular class of aqueous solutions of small organic molecules having both hydrophilic and hydrophobic parts. Among such solutions a non-ideal mixing behavior composition inhomogeneity can often be observed, and it is expected that these processes can be understood on the same basis for the aqueous solutions of different organic molecules. We have chosen methylpyridine solutions because they have been studied by thermodynamic and by quantum chemistry methods. We compared the aggregation behavior of several members of this group in order to find some correlation between the strength of aggregation and some characteristic parameters of the solute molecules, like their geometry or electronic configurations.

The results of our investigations have been presented in papers [23, 57, 91, 92, 93, 94], they are summarized below.

We used **small-angle neutron scattering** to look for the local order in the solutions, and analyzed the experimental data by using the Kirkwood-Buff theory. Some information has been obtained on the structural arrangements of the molecules in the solution. As the small-angle scattering is a low-resolution technique, we did not have the possibility to investigate the structure at the molecular level, so the geometry of the pairwise intermolecular interaction remains uncovered. The main numerical results concern the various parameters that characterize the clustering, which is present in the solutions. They can be divided into two classes:

The first is a length parameter, which characterizes the extension of the clustering in a direct way, that is the correlation length of the concentration fluctuations. We found that in all the studied systems the inhomogeneous distribution of the two components extends to sizes of some nanometers, and the closer is the mixture to the phase separation in the composition-temperature phase diagram, the larger is the extension of the inhomogeneities. This is in accordance to the existing theories describing the phase separation as a phase transition, in which the characteristic parameters (length and amplitude of the fluctuations) increase up to infinity approaching the phase separation.

The second class of parameters obtained with the help of the small-angle scattering are

parameters related to the zero-angle limit of the scattering intensity, that is proportional to the integral of the pair correlation function over the whole space. These parameters give quantitative information about the number of molecules of one species in the vicinity of an arbitrarily chosen molecule of the same or different species. These quantities are related to the thermodynamic state of the mixture, they can characterize the degree of the non-ideality, and the closeness of the given state of the mixture to the macroscopic phase separation.

In the following we list some questions which have been investigated and partially answered by the use of small-angle scattering data.

1. In aqueous solutions of methyl-substituted pyridines we observed very high values of the parameters related to the non-ideality of the mixture: In effect, the fluctuation terms and the Kirkwood-Buff integrals are by an order of magnitude higher in the methylpyridine and dimethylpyridine solutions, than those in any other earlier reported mixture. These numbers, together with the difference between the local concentrations for the solute-rich and the solvent-rich regions show that these solutions are highly structured in terms of thermodynamic equilibrium between the two types of different domains that are rich in solute and rich in solvent.

The presence of relatively large domains with different composition contradicts to the hypothetical clathrate-like structure suggested in these solutions based on the temperature behavior of the compressibilities [37, 38]. The increase of the inhomogeneities raising the temperature is neither consistent with the supposed stable structure of the solutions having 0.04 mole fractions of methylpyridine.

2. We calculated Kirkwood-Buff integrals for several solutions by two methods: 1. using only thermodynamic data (compressibility, partial molar volumes, molar volume, Gibbs free energy of mixing), and 2. using zero-angle neutron scattering intensities instead of the Gibbs free energy data. We observed that in many cases, for those systems which are far from ideal mixing, calculations using the Gibbs free energy data derived from vapor pressure measurements failed. We did not analyze the sources of the errors at the origin of the inconsistency of the free energy data reported in the literature. However it can be suggested that the precision of these data are limited mainly by the accuracy of the standard experimental techniques. We used thermodynamic data for different solutions, published by Abe, Nakanishi et. al. [36], and found that for those systems in which the degree of non-ideality is moderate (water – pyridine in our case), the agreement between the KBIs calculated by the two methods was rather good. For systems with pronounced deviations from ideal mixing, the vapor pressures measured by the same authors using the same technique (probably with same precision) lead to erroneous excess free energy values that could not be used further. So for such systems it is preferable to use the experimental values of zero-angle scattering intensity instead of the excess free energies calculated from vapor pressure measurements.

A similar analysis has been recently published [59], comparing the KB integrals in water – alcohol mixtures obtained by using thermodynamic data and X-ray scattering data. For these systems, which deviate much less from the ideal mixing, the two methods gave identical results.

These findings suggest that the scattering techniques are well adapted for studying the mixing behavior in strongly non-ideal mixtures. Small-angle neutron scattering (SANS) is in particular a useful tool, as it allows one to vary the contrast between the components by isotopic substitution. Thus, for aqueous solutions of organic molecules one can use heavy water as solvent, in order to increase the contrast between the two species. For multicomponent mixtures, the protiated and deuterated molecules of one of the components can be mixed so as to obtain similar scattering length density with the second species, thus only the distribution of the third one will be seen in the SANS measurement. Additionally, the scattering techniques give also information about the spatial distribution of the inhomogeneities in the mixtures, which cannot be obtained from thermodynamic data only.

3. The analysis of the excess numbers of molecules in the vicinity of a central one gave evidence, that in all studied solutions of methyl-substituted pyridines strong clustering of the same species occurs. These findings can be interpreted in the following way. Two mechanisms of hydrophobic interaction are usually considered in the literature:

According to the first one, in the so-called "solvent-separated" interactions the solute molecules are separated from each other by a layer of water molecules. The origin of these repulsive forces is probably the stable hydrogen-bonded layer which surrounds a hydrophobic solute molecule. When another water-coated solute molecule comes close, the water layer prevents the direct contact between them. This type of solution structure has its analog in the crystalline phase. Many aqueous solutions of organic molecules freeze forming crystal hydrates, in which the solute molecules are placed in large cages consisting of 20 to 40 water molecules.

The second possibility are the attractive contact-pair solute-solute interactions, which can be due to direct attraction or by the simple hydrophobic effect, when the hydrophobic solute is pushed out from the hydrogen-bonded water network. This mechanism leads to the appearance of more or less compact solute aggregates, and of solute-free water regions.

The large values of the excess numbers found in the methylpyridine - water solutions are in favour of this second picture.

4. The results of the SANS investigations showed the general trend of the mixing behavior in these solutions: The degree of non-ideality is similar to the tendency to phase separate, it increases as more methyl groups are attached to the pyridine ring. Comparing the degrees of non-ideality in solutions of the three mono-methylsubstituted pyridines no clear relation could be found between the miscibility behavior and the strength of the hydrogen bond between a water and a methylpyridine molecule, neither between the miscibility behavior and the closeness to phase separation of the mixture.

The mechanism of the hydrophobic interaction still remains to be not fully understood at the level of molecular interactions.

5. The absence of aggregation of methylpyridine in non-polar and no hydrogen-bonding CCl_4 and CS_2 solvents indicates the essential role of the water in enforcing the aggregation of the solute molecules and inducing the macroscopic phase separation in some cases. It is interesting to note that in a similar SANS study of tetramethylurea (TMU) dissolved in CS_2 [95] the aggregation of the TMU was seen to be as strong as in aqueous solution, but did not show any temperature dependence. No tendency to macroscopic phase separation is known for that mixture.

Another aim of the SANS studies was to measure the pairwise solute-solute interaction, which can in principle be detected in experiments with very low solute concentrations. However the limitations of the technique – the low signal-to-noise ratio and the limited structural resolution prevented us to obtain valuable information on this level.

Quasielastic neutron scattering (QENS) studies on aqueous solutions of 3-methylpyridine showed that with increasing solute concentration the diffusional motions of both components slow down, and at the highest solute concentration studied the diffusion coefficients of both components become similar. We attributed this effect to the strong coupling between the dynamics of the two species.

We interpreted the decrease of the average mobility of the water by assuming the presence of two kinds of water in the mixture: one which behaves like bulk water, and a second one, which is coupled to the solute molecules. The proportion between the "free" and "bound" water suggests that the bound (less mobile) water molecules can be attached to the outer part of the clusters consisting mainly of methylpyridine molecules, at least for less then 50 picoseconds, the time scale of the QENS measurements.

This picture is consistent with the results of SANS measurements, according to which the clusters are composed mainly by methylpyridine molecules, and are surrounded by bulk water or a very dilute MP solution. A similar character of the distribution of water molecules was suggested in a recent simulation study on propanol aggregation in aqueous solution, based on results of small-angle neutron scattering measurements [96].

By **NMR technique** we investigated the dynamics of 3MP solutions in the liquid state. In all solutions the relaxation mechanism showed a single exponential behavior, independently of the solute concentration. This means that the relaxation times of the water proton motions and that of the methyl group rotation are equal or at least very close to each other. The values of the activation energy obtained for methyl group reorientation are very close to the activation energy for self-diffusion in pure water. This can mean that the dynamical behavior of the water and that of the solute are correlated, the rotation of the methyl group can take place only by disturbing or rearranging the surrounding water shell.

The increase of the activation energy of the methyl group motion with the solute concentration can be related with two effects:

1. In the dilute solutions most of the MP molecules are surrounded by a water shell. The sharp hindrance of the water motion with increasing solute concentration must also slow down the methyl reorientation.
2. In the concentrated solutions a part of the MP molecules are in contact with neighboring MP molecules. This certainly causes some slowing of the dynamics of some of the methyl groups present in the solution. Eventually there can exist a hydrogen bonding type interaction between the methyl protons and some sites of the neighboring methylpyridine molecule, as it seems to be the case in the crystalline states of the pure 2-methylpyridine and 3-methylpyridine.

The most important observation made by NMR is that the dynamics of the water and the methyl group are strongly connected. It suggests that the mixing behavior in the methylpyridine solutions has mainly hydrophobic character, and the anomalous mixing of the aqueous solutions of picolines could be partly related to the dynamics of the water hydrate shell surrounding the hydrophobic part of the solute molecule.

How can our findings for these particular systems be generalized to other aqueous solutions?

One of the main questions about the behavior of aqueous solutions of hydrophobic molecules is the question whether the interaction between the solute molecules is direct or induced by the solvent.

We found that in the case of aqueous solutions of methylpyridine the solute aggregation is very strong, while in other solvents we found no signs of aggregation. The increase of temperature promotes the methylpyridine aggregation in the aqueous solution, it can be suggested that the interaction is related to the mobility of the water molecules. On the other hand, in the case of aqueous and non-aqueous solutions of tetramethylurea studied earlier, the behavior is similar in water and in an apolar solvent such as carbon disulfide – the TMU molecules do aggregate. The role of the solvent is not fully clear in the aggregation: in aqueous solutions the interaction increases with the rise of the temperature, while in carbon disulfide the aggregation was found to be temperature-independent in the studied temperature range. The different temperature behavior in the two solvents can be explained by the role of the mobility of the solvent molecules in facilitating the solute – solute interactions.

According to the old theory of Hirschfelder [3], the demixing in a binary mixture by elevating the temperature is caused by the presence of stable, directional pair interactions between the two types of molecules. Such an interaction in our case is the hydrogen bonding between the nitrogen atom of the pyridine ring and the water molecule. Accordingly, the highly non-ideal behavior of aqueous methylpyridine solutions is seen to be dominated by the presence of this hydrogen bond: dissolving methylpyridine in carbon disulfide or carbon tetrachloride such directional bonds between the solute and the solvent are absent, correspondingly there is no sign of phase separation.

In the case of tetramethylurea the situation is different: the demixing tendency can be observed both in aqueous and non-aqueous solutions, and no strong hydrogen bonds can form between the two components. Therefore the interaction responsible for the aggregation of TMU can be the usual hydrophobic attraction in the aqueous solutions, and a similar type of direct or solvent-induced attractive interactions between the TMU molecules in the carbon disulfide solutions.

There are few experimental studies of solutions in the literature which deal with the solute – solute or solute – solvent interaction by direct methods like scattering techniques (e. g. [95, 97, 98]), there is not enough knowledge gathered so far to explain fully the behavior in liquid mixtures. We hope that the present work can contribute in some extent to the development of this obviously important field of the science.

10. Perspectives

The work carried out showed us some directions in which further research can be continued. We try to describe some possibilities.

A relatively large number of aqueous solutions has been investigated by means of the Kirkwood-Buff approach based on thermodynamic data [58, 62], the deviations from the ideal mixing behavior were expressed through the behavior of the fluctuation terms and the Kirkwood-Buff integrals. Information concerning the concrete mechanism that can be responsible for the pronounced deviations from the ideality, seems to be absent in the KB integrals. The reason for that is simple – the KBIs reflect only the average structure of the solution and do not depend explicitly on the pairwise interactions.

We feel however that some progress can be achieved in extracting more information from the Kirkwood-Buff integrals. It is known that the KBIs are reduced to the second virial coefficients of the solute molecules at high dilution. By measuring the KBIs at very low solute or solvent concentration we can calculate parameters that characterise the pairwise interaction between two solute or two solvent molecules. The difficulties are mainly of experimental character: for most of mixtures, at very low concentrations, it is practically impossible to obtain the derivatives of the free energy, or to measure the small-angle scattering signal. One should search therefore for such liquid mixtures, in which the small-angle scattering can be measured with sufficient precision. The criteria are the following: the two species must have high contrast for neutrons or X-rays; the solute molecules must be sufficiently large so that the scattering by one molecule or an aggregate can be seen and distinguished; and the association tendency has to be strong and has to set up at very low concentrations, at which the small-angle scattering is free from the interference caused by the presence of neighboring solute particles or aggregates.

In this way the Kirkwood-Buff integrals can furnish information about the intermolecular interactions as well: at the infinite dilution limit the KBIs reduce to the second virial coefficients, so from their exrapolated values the effective pairwise interactions can be determined.

It is suggested by some authors [46, 99, 100], that the mixing behavior of binary aqueous solutions can be described by different mixing schemes which are characteristic for different composition intervals. These schemes switch on and off at some characteristic concentrations. There are so far only indirect indications for the presence of such behavior: the sudden changes in the concentration dependence of the second and higher

order derivatives of the thermodynamic quantities suggest the change of the mechanism of the mixing. In order to obtain more information about the different mixing schemes it can be useful to perform small-angle scattering measurements with substantially smaller steps in concentration. It would allow one to follow the structural changes by scattering techniques, and eventually show the structures of the aggregates formed in the mixture.

Some further progress can be made extending the power of small-angle neutron scattering to provide information on the structure of the mixtures. In our analysis, we did not fully use all the information given in the amplitude of the small-angle scattering intensity and the correlation length. The difficulty was the unknown structural model of the solution, which has to correspond to the measured intensity distribution. It should be possible to construct such a model using an analytical form of the scattering length distribution, which is in agreement with the given sample composition and contains several adjustable parameters. In this way the structure can be obtained by fitting the experimental data to the model equation.

Alternatively, it is possible to construct a real-space model of the mixture by distributing molecules of the two species in a very large simulation box, large enough to be used for comparison with the small-angle scattering measurement. It is not possible to handle such big simulation boxes with the usual computer simulation methods, therefore some tricks, some simplification must be used for matching the measurement with the modeled scattering intensity. For example, the simulations could be performed in lattice space, or a change of positions of two distant (nonsimilar) molecules can be allowed as well, it can lead to a much faster development of inhomogeneous structure in the simulation box. The resulting molecular configurations can hopefully give some idea about the distribution of the two species in the real mixture. Such an attempt has been recently presented by Misawa [96].

Bibliography

[1] T. Narayanan and A. Kumar: *Reentrant phase-transitions in multicomponent liquid mixtures.* Physics Reports **249** 135-218 (1994)

[2] B. Jönsson, B. Lindman, K. Holmberg, B. Kronberg: *Surfactants and Polymers in Aqueous Solution* (John Wiley & Sons 1999)

[3] J. Hirschfelder, D. Stevenson, H. Eyring: *A theory of liquid structure.* J. Chem. Phys. **5** 896-912 (1937)

[4] I. Pápai, G. Jancsó: *Hydrogen bonding in methyl-substituted pyridine – water complexes: a theoretical study.* J. Phys. Chem. A **104** 2132 (2000)

[5] I. V. Brovchenko, A. V. Oleinikova: *Structural changes of the molecular complexes of pyridines with water and demixing phenomena in aqueous solution.* J. Chem. Phys. **106** 7756 (1997)

[6] A. L. L. Sinoti, J. R. S. Politi, L. C. G. Freitas: *Monte Carlo simulation of water – pyridine mixtures.* J. Braz. Chem. Soc. **7** 133 (1996)

[7] F. Sokolic, A. Idrissi, A. Perera: *Concentrated urea solutions: A molecular dynamics study of different models.* J. Chem. Phys. **116** 1636 (2002)

[8] I. V. Brovchenko, A. V. Oleinikova: *Role of hydrogen bonds in demixing phenomena in aqueous solutions.* High Temp. – High Press. **30** 229 (1998)

[9] P. A. Egelstaff: *An introduction to the liquid state* (Clarendon Press, Oxford 1992)

[10] H. Bertagnolli, T. Engelhardt, P. Chieux: *Study of dipolar interaction in liquid pyridine by X-ray and neutron diffraction.* Ber. Bunsenges. Phys. Chem. **90** 512 (1986)

[11] I. Bakó, T. Radnai, G. Pálinkás: *Investigation of the structure of liquid pyridine: A molecular dynamics simulation, an RISM, and an X-ray diffraction study.* Z. Naturforsch. A **51** 859 (1996)

[12] Y. Danten, B. Guillot, Y. Guissani: *Investigation of charge-transfer complexes by computer-simulation. 2. Iodine in pyridine solution.* J. Chem. Phys. **96** 3795 (1992)

[13] E. Megiel, T. Kasprzycka-Guttman, A. Jagielska, L. Wroblewska: *A theoretical and experimenatl ^{14}N NMR study of association of pyridine.* J. Mol. Struct. **569** 111 (2001)

[14] A. D. Bond, J. E. Davies: *2-Picoline.* Acta Cryst. **E57** o1089-o1090 (2001)

[15] A. D. Bond, J. E. Davies: *3-Picoline.* Acta Cryst. **E57** o1087-o1088 (2001)

[16] A. D. Bond, J. E. Davies: *2,5-Lutidine.* Acta Cryst. **E58** o326-o327 (2002)

[17] A. D. Bond, J. E. Davies, A. J. Kirby: *2,6-Lutidine.*
Acta Cryst. **E57** o1242-o1244 (2001)

[18] A. D. Bond, J. E. Davies: *3,4-Lutidine.* Acta Cryst. **E58** o328-o330 (2002)

[19] A. D. Bond, J. E. Davies: *3,5-Lutidine.* Acta Cryst. **E58** o5-o7 (2002)

[20] D. Mootz, H.-G. Wussow: *Crystal structures of pyridine and pyridine trihydrate.* J. Chem. Phys. **75** 1517 (1981)

[21] M. Born, D. Mootz, S. Schaefgen: *Tautomeric water layers – formation and structure of low-melting trihydrates of triethylamine and 4-methylpyridine.*
Z. Naturforsch. B **50** 101 (1995)

[22] W. Müller-Warmuth, R. Schüler, M. Prager, A. Kollmar: *Rotational tunnelling in methylpyridines as studied by NMR relaxation and inelastic neutron scattering.*
J. Chem. Phys. **69** 2382 (1978)

[23] I.I. Vorontsov, L. Almásy, Yu.M. Antipin: *Low-temperature crystallization and X-ray structure determination of 2-methylpyridine at 153K.* J. Mol. Struct. **610** 271 (2002)

[24] A. Cousson, *private communication*

[25] Z. Ciunik, S. Berski, Z. Latajka, J. Leszczynski: *New aspects of weak C-H $\cdots$ π bonds: intermolecular interactions between alicyclic and aromatic rings in crystals of small compounds, peptides and proteines.* J. Mol. Struct. **442** 125 (1998)

[26] F. Franks *Water Science Rev.* **1** 171 (1985)

[27] J. D. Cox: *Phase relationships in the pyridine series. Part II. The miscibility of some pyridine homologues with deuterium oxide.*
J. Chem. Soc. (London) pp. 4606-4608 (1952)

[28] R. J. L. Andon, J. D. Cox: *Phase relationships in the pyridine series. Part I. The miscibility of some pyridine homologues with water.*
J. Chem. Soc. (London) 4601-4606 (1952)

[29] J. D. Cox: *Phase relationships in the pyridine series. Part IV. The miscibility of ethylpyridines and dimethylpyridines with water.* J. Chem. Soc. p. 3183 (1954)

[30] R. J. L. Andon, J. D. Cox, E. F. G. Herington: *Phase relationships in the pyridine series. Part 6. The thermodynamic properties of mixtures of pyridine, and of three of its homologues, with water.* Trans. Faraday Soc. **53** 410 (1957)

[31] J. Szydlowski: *Influence of deuterium substitution on miscibility of water with methyl derivatives of pyridine.* Nukleonika **43** 423 (1998)

[32] L. I. Lysniansky, M. F. Vuks: *Concentration fluctuations and stability of solutions. Their influence on the light scattering and other phenomena.* Vestnik Leningrad Univ. p. 67 (1962)

[33] J. Jacob, A. Kumar, S. Asokan, D. Sen, R. Chitra, S. Mazumder: *Evidence of clustering in an aqueous electrolyte solution: a small-angle X-ray scattering study.* Chem. Phys. Lett. **304** 180 (1999)

[34] I. K. Yushkova, I. G. Belavina, G. D. Kharlampovich: *Dependence of thermodynamic properties of system 3-methylpyridine – water on concentration and temperature. 2.* Zh. Prikl. Khimii (Leningrad) **47** 2313 (1974) (*in Russian*)

[35] I. K. Yushkova, I. G. Belavina, G. D. Kharlampovich: *Thermodynamic properties of system 4-methylpyridine – water and 2,6-dimethylpyridine – water.* Zh. Prikl. Khimii (Leningrad) **48** 1067 (1975) (*in Russian*)

[36] J. I. Abe, K. Nakanishi, H. Touhara: *Thermodynamic properties of aqueous solutions of hydrophilic compounds. 1. Pyridine and methylpyridines.* J. Chem. Thermodyn. **10** 483 (1978)

[37] W. Marczak: *Speed of ultrasound, density, and adiabatic compressibility for 2-methylpyridine plus heavy water in the temperature range 293 K to 313 K.* J. Chem. Eng. Data **44** 621-625 (1999)

[38] W. Marczak: *Speed of ultrasound, density, and adiabatic compressibility for 3-methylpyridine plus heavy water in the temperature range 293-313 K.* J. Chem. Eng. Data **41** 1462-1465 (1996)

[39] W. Marczak: *Speed of ultrasound, density, and adiabatic compressibility for 4-methylpyridine + heavy water in the temperature range 293 K to 313 K.* J. Chem. Eng. Data **44** 936-940 (1999)

[40] S. Ernst, W. Marczak, D. Kmiotek: *Ultrasonic velocity, density, and adiabatic compressibility for 2,6-dimethylpyridine plus water in the temperature range 293-318K.* J. Chem. Eng. Data **41** 128 (1996)

[41] W. Marczak, S. Ernst: *Effects of hydrophobic and hydrophilic hydration on the compressibility, volume and viscosity of mixtures of water with beta-picoline.* Bull. Pol. Acad. Sci. – Chem. **46** 375-395 (1998)

[42] S. Ernst, W. Marczak: *Hydrophobic and hydrophilic interactions in binary mixtures of α-picoline with water.* Bull. Polish Acad. Sci. – Chem. **43** 259-278 (1995)

[43] A. B. Bhatia and T. E. Thornton: *Structural aspects of the electrical resistivity of binary alloys.* Phys. Rev. **B 2** 3004 (1970)

[44] J. G. Kirkwood and F. P. Buff: *The statistical mechanical theory of solutions. I.* J. Chem. Phys. **19** 774 (1951)

[45] K. Nishikawa: *Simple relationship between the Kirkwood-Buff parameters and the fluctuations in the particle number and concentration obtained by small-angle X-ray scattering – application to tert-butyl alcohol and water mixtures.* Chem. Phys. Lett. **132** 50 (1986)

[46] K. Nishikawa, H. Hayashi, T. Iijima: *Temperature-dependence of the concentration fluctuation, the Kirkwood-Buff parameters, and the correlation length of tert-butyl alcohol and water mixtures studied by small-angle X-ray scattering.* J. Phys. Chem. **93** 6559 (1989)

[47] H. Hayashi, K. Nishikawa, T. Iijima: *Small-angle X-ray scattering study of fluctuations in 1-propanol – water and 2-propanol – water systems.* *J. Phys. Chem.* **94** 8334 (1990)

[48] G. D'Arrigo, J. Teixeira: *Small-angle neutron scattering study of D_2O - alcohol solutions.* J. Chem. Soc. Faraday Trans. **86** 1503 (1990)

[49] G. D'Arrigo, J. Teixeira, R. Giordano, F. Mallamace: *A small-angle neutron scattering study of 2-butoxyethanol/D_2O solutions.* J. Chem. Phys. **95** 2732 (1991)

[50] L. Cser, T. Grósz, Yu. M. Ostanevich: *Intermolecular interaction in tetramethylurea solutions.* J. de Physique IV, Colloque **C8** 229 (1993)

[51] S. Borbély, L. Cser, T. Grósz, G. Jancsó: *Neutron-scattering on dense solutions of tetramethylurea.* Physica B **213** 513 (1995)

[52] E. Matteoli and L. Lepori: *Kirkwood-Buff integrals and preferential solvation in ternary mixtures.* J. Chem. Soc. Faraday Trans. **91** 431 (1995)

[53] R. Chitra, P. E. Smith: *Properties of 2,2,2-trifluoroethanol and water mixtures.* J. Chem. Phys. **114** 426 (2001)

[54] M. C. A. Donkersloot: *Concentration dependence of the zero-angle X-ray scattering from liquid mixtures of water and methanol.* J. Solut. Chem. **8** 293 (1979)

[55] M. Misawa, K. Yoshida: *Concentration fluctuation and salt-induced percolation in 1-propanol aqueous solution.* J. Phys. Soc. Japan **69** 3308 (2000)

[56] Y. Kataoka: *A Monte Carlo study of concentration fluctuations in a 2D aqueous solution.* J. Chem. Phys. **80** 4470 (1984)

[57] L. Almásy, G. Jancsó, L. Cser: *Application of SANS for the determination of Kirkwood-Buff integrals in liquid mixtures.* Appl. Phys. A, **74**[Suppl] S1376 (2002)

[58] E. Matteoli and L. Lepori: *Solute-solute interactions in water. 2. An analysis through the Kirkwood-Buff integrals for 14 organic solutes.*
J. Chem. Phys. **80** 2856 (1984)

[59] I. Shulgin and E. Ruckenstein: *Kirkwood-Buff integrals in aqueous alcohol systems: Comparison between thermodynamic calculations and X-ray scattering experiments.* J. Phys. Chem. B **103** 2496 (1999)

[60] Y. Marcus: *Preferential solvation in mixed solvents. 5. Binary mixtures of water and organic solvents.* J. Chem. Soc. Faraday Trans. **86** 2215 (1990)

[61] I. Shulgin and E. Ruckenstein: *Kirkwood-Buff integrals in aqueous alcohol systems: Aggregation, correlation volume, and local composition.*
J. Phys. Chem. B **103** 872 (1999)

[62] Y. Marcus: *Preferential solvation in mixed solvents X. Completely miscible aqueous co-solvent binary mixtures at 298.15K.* Monatshefte für Chemie **132** 1387 (2001)

[63] Y. G. Wu, M. Tabata, T. Takamuku: *A Rayleigh light scattering study on mixing states of 2-propanol – water binary mixtures widely used as mobile phase in separation.*
Talanta **54** 69 (2001)

[64] Y. G. Wu, M. Tabata, T. Takamuku: *A local solvent structure study on 1,4-dioxane – water binary mixtures by total isotropic Rayleigh light scattering method.*
J. Mol. Liq. **94** 273 (2001)

[65] K. Nishikawa, Y. Kasahara, T. Ichioka: *Inhomogeneity of mixing in acetonitrile aqueous solution studied by small-angle X-ray scattering.*
J. Phys. Chem. B **106** 693 (2002)

[66] S. V. Zenin: *Complexation of acetonitrile and methanol with water.*
Zh. Fiz. Khim. **73** 835 (1999)

[67] N. Manohara Murthy, S. V. Subrahmanyam: *Excess thermodynamic functions of water + pyridine system.* Indian J. Chem. A **19** 724 (1980)

[68] L. van Hove: *Correlations in space and time and Born approximation of scattering in systems of interacting particles.* Phys. Rev. **95** 249 (1954)

[69] H. E. Stanley: *Introduction to phase transitions and critical phenomena* (Clarendon Press, Oxford 1971)

[70] G. T. Chudley and R. Elliott, J. Proc. Phys. Soc. **77** 353 (1961)

[71] J. P. Hansen and I. R. McDonald: *Theory of simple liquids*

[72] J. Teixeira, M.-C. Bellissent-Funel, S. H. Chen, A. J. Dianoux: *Experimental determination of the nature of diffusive motions of water molecules at low temperatures.* Phys. Rev. **A31**, 1913 (1985)

[73] K. S. Singwi, A. Sjölander: *Diffusive motions in water and cold neutron scattering.* Phys. Rev. **119** 863 (1960)

[74] `http:\\www-llb.cea.fr`

[75] `http:\\www.bnc.hu`

[76] J. P. Cotton, in: *Neutron, X-ray and Light Scattering*, ed. P. Lindner and Th. Zemb, (North-Holland, Amsterdam 1991.)

[77] B. Jacrot: *Study of biological structures by neutron-scattering from solution.* Rep. Prog. Phys. **39** 911 (1976)

[78] R. E. Ghosh, A. R. Rennie: *Assessment of detector calibration for SANS experiments.* J. Appl. Cryst. **32** 1157 (1999)

[79] I. Prigogine and R. Defay: *Chemical Thermodynamics* (Longmans Green and Co, London, 1954)

[80] T. C. Chan, W. A. Van Hook: *Vapour pressure isotope effects in aqueous systems. Part 7. – The system* $^1H_5$*Pyridine +* $^2H_5$*Pyridine +* H_2O*.*
J. Chem. Soc. Faraday Trans. **72** 583 (1976)

[81] J. T. Cabral, A. Luzar, J. Teixeira, M.-C. Bellissent-Funel: *Water dynamics in DMSO-water mixture.* Physica B **276-278** 508 (2000)

[82] J. T. Cabral, A. Luzar, J. Teixeira, M.-C. Bellissent-Funel: *Single-particle dynamics in dimethyl–sulfoxide/water eutectic mixture by neutron scattering.*
J. Chem. Phys. **113** 8736 (2000)

[83] L. Cser, T. Grósz, G. Jancsó, G. Káli: *The nature of the interaction of tetramethylurea in various solvents.* Physica B **234-236** 349 (1997)

[84] D. Bedrov, O. Borodin, G. D. Smith, F. Trouw, C. Mayne: Simulation and QENS studies of molecular dynamics in aqueous solutions of 1,2-dimethoxyethane. *J. Phys. Chem. B* **104** 5151 (2000)

[85] M. Misawa, K. Yoshida, K. Maruyama, H. Munemura, Y. Hosokawa: *Salt-induced phase separation in aqueous solution.* J. Phys. Chem. of Solids **60** 1301 (1999)

[86] M. Mayele, M. Holz: *NMR studies of hydrophobic interactions in solution - Part 5. Effect of urea on the hydrophobic self-association of tert-butanol in water at different temperatures.* Phys. Chem. Chem. Phys. **2** 2429-2434 (2000)

[87] H. G. Hertz, in: *Water, A Comprehensive Treatise*, ed. F. Franks, (Plenum, New York, 1973, vol. 3, ch. 7)

[88] A. G. Novikov, M. N. Rodnikova, V. V. Savostin: *Diffusion processes in an aqueous solution of tetramethylammonium chloride according to inelastic neutron scattering.* Zh. Fiz. Khim. **70** 1086 (1996)

[89] K. Yoshida *et. al.*, ... Appl. Phys. A **74**[Suppl.] (2002)

[90] H. Weingärtner: *Self-diffusion in liquid water – a reassessment.* Z. Phys. Chem. NF **132** 129 (1982)

[91] L. Almásy, L. Cser, G. Jancsó: *Small-angle neutron scattering study on 3-methylpyridine – heavy water solutions.* Physica B **276-278** 446 (2000)

[92] L. Almásy, P. Bánki, M.-C. Bellissent-Funel, M. Bokor, L. Cser, G. Jancsó, K. Tompa, J. M. Zanotti: *QENS and NMR studies of 3-picoline – water solutions.* Appl. Phys. A **74**[Suppl.] (2002)

[93] L. Almásy, L. Cser, G. Jancsó: *Kirkwood-Buff integrals in aqueous solutions of 3-methylpyridine.* J. Mol. Liq. **101** 89 (2002)

[94] L. Almásy, G. Jancsó: *Small-angle neutron scattering and Kirkwood-Buff integral study of aqueous solutions of pyridine.* J. Mol. Liq. (2003)

[95] L. Cser, G. Jancsó, P. Jóvári, G. Káli: *Temperature dependence of small-angle neutron scattering of tetramethylurea in carbon disulfide solution.* J. Phys. Chem. B **102** 2313 (1998)

[96] M. Misawa: *Mesoscale structure and fractal nature of 1-propanol aqueous solution: A reverse Monte Carlo analysis of small-angle neutron scattering intensity.* J. Chem. Phys. **116** 8463 (2002)

[97] S. Ansell, L. Cser, T. Grósz, G. Jancsó, P. Jóvári, A. K. Soper: *Solute-solute correlation in aqueous solutions of tetramethylurea.* Physica B **234** 347 (1997)

[98] N. G. Polydorou, J. D. Wicks, J. Z. Turner: *Hydrophobic interaction of tetrapropylammonium ions in water: A neutron diffraction and reverse Monte Carlo study.* J. Chem. Phys. **107** 197 (1997)

[99] Y. Koga: *Excess partial molar free energies and entropies in aqueous tert-butyl alcohol solutions at 25°C.* J. Phys. Chem. **94** 7700 (1990)

[100] Y. Koga: *Vapor pressures of aqueous 2-butoxyethanol solutions at 25°C: Transitions in mixing scheme.* J. Phys. Chem. **95** 4119 (1990)